ESA/ESOC Contract to ISTI/CNR
"Analysis of Mitigation Measures based on the Semi-Deterministic Model"
Contract No. 18423/04/D/HK

Long-Term Simulation of Objects in High-Earth Orbits

Work Package No. 2
Progress Report No. 1

Prepared by

Luciano Anselmo

6 December 2005

Space Flight Dynamics Laboratory
Istituto di Scienza e Tecnologie dell'Informazione "A. Faedo"
CNR – Area della Ricerca di Pisa
Via G. Moruzzi 1, 56124 Pisa, Italy

TABLE OF CONTENTS

ABSTRACT

This report presents the activity carried out to identify suitable long-term orbit propagators for inclusion in SDM 4.0. The analysis was basically focused on the MEO and GEO orbital regimes, comparing the results with a special perturbations approach, in order to find reasonable and generally applicable compromises of accuracy and computational speed.

After having simulated GEO, GPS, Molniya and GTO orbits for one century, also including the main non-gravitational perturbations on objects with very high area-to-mass ratios, and having investigated the maximum computational speed attainable within certain accuracy constraints (in GEO, MEO and LEO), the influence of the disposal orbit eccentricity vector on the long-term preservation of the GEO protected region (IADC AI 22.1) has been evaluated.

1. INTRODUCTION

1.1 Task Description

The final goal of this work package is to address the long-term (200 years) orbital evolution of objects in MEO (e.g. Molniya, GPS, Galileo, etc…) and GEO. In particular, the following investigations are foreseen [1]:

- Analysis of the orbital lifetime of objects in Molniya orbits as a function of initial conditions;
- Study of the long-term evolution of objects disposed of in GEO graveyard orbits as a function of the initial orbital elements, in particular the eccentricity vector, in order to identify the possible return of such objects in the GEO protected region, due to the effects of the orbital perturbations;
- A similar analysis for the objects placed in the graveyard orbits used or proposed for the navigation satellites in MEO, like GPS, GLONASS and, in particular, Galileo;
- Identification of candidate debris sources to explain the geosynchronous objects with high eccentricity discovered by the ESA 1 m telescope in Tenerife.

These study objectives can be fulfilled using only a subset of the new SDM functionalities, in particular the orbit propagators for the MEO and GEO orbital regimes.

During the first phase of the activity, extensive analyses were carried out for testing purposes, comparing different approaches and available models, in order to assist Work Package 1 in the development of the upgraded SDM software. This Progress Report presents the tests executed and the results obtained during this preliminary phase, with the aim of identifying and implementing appropriate trajectory propagators and model options to study the long-term trajectory evolution of objects in MEO and GEO.

1.2 Orbit Propagators

For the tests described in this report, three trajectory propagators were employed: a modified (2005) version of LOP, LEGO and SATRAP.

LOP [2] is a long-term orbit predictor on which is based the approach used by FOP to integrate the Lagrange's planetary equations used to describe the satellite motion. FOP [3][4][5] is the three-dimensional, multi-object, orbit propagator implemented in SDM. Both LOP and FOP use the variation of parameters method in the formulation of the equations of motion. The perturbations taken into account are: the Earth's geopotential, the third body attraction of the Moon and the Sun, the air drag (when applicable) and the solar radiation pressure, including the eclipses. To expedite the computations, the terms including the mean anomaly (fast variable) are removed in the Earth's and third-body potentials before numerical integration (singly averaged method). On the other hand, when resonances occur between the orbital period and the Earth rotation, the terms containing the mean anomaly in the tesseral harmonics of the geopotential are retained, giving rise to resonant effects.

To average the potential due to solar radiation pressure and air drag, a standard 8^{th} order Gaussian quadrature method is used. The resulting averaged equations are integrated numerically using a multi-step, variable step-size and variable order method. The computation time is maintained under control, without compromising the accuracy, due to the elimination of the fast variable and the possibility to use large step sizes (days).

LEGO is a very fast ESOC software tool based on the analytic theory developed by J.C. Van Der Ha [6]. It includes the main terms of the geopotential, luni-solar effects and solar radiation pressure. However, it is only applicable to the geosynchronous and near-geosynchronous orbital regimes.

SATRAP [7], a special perturbations propagator using a high accuracy numerical integrator, has been used as a benchmark with which to compare and evaluate the results obtained with LOP (FOP) and LEGO. Derived from ASAP [8], the force model includes the zonal and tesseral harmonics of the Earth's gravity potential, the luni-solar gravitational perturbation, the solar radiation pressure, with eclipses, and several thermospheric density models for air drag computation, in particular for reentry predictions.

For the aims of the present study, the value 1.2 was used for the solar radiation pressure coefficient, while a simple exponential atmospheric density model, with the parameters shown in Table 1.1, was adopted both for SATRAP and LOP.

Table 1.1

Parameters of the Exponential Atmospheric Density Model and Drag Perturbation

Termospheric Density Model	Jacchia-71
Exospheric Temperature	1000 K
Reference Altitude for Air Density	400 km
Scale Height of Air Density	55.92 km
Air Density at Reference Altitude	3.11×10^{-3} kg/km^3
Maximum Altitude to Include Drag	1000 km
Drag Coefficient	2.2

Concerning the geopotential, gravity harmonics up to the 8^{th} order and degree were included, but LOP considered only the resonant tesserals and the resonance effects.

2. THE GEOSYNCHRONOUS REGIME

2.1 Long-Term Evolution of Objects Abandoned in GEO

The aim of the analysis was to compare the long-term trajectory evolution predicted by LOP[1], LEGO and SATRAP for objects abandoned in geostationary orbit. The reference orbit adopted as initial conditions for the runs is given in Table 2.1. The time span of the simulations was 100 years and area-to-mass ratios (A/M) of 0.05, 1, 10, 20, 30 and 40 m^2/kg were considered, in order to include both large telecommunications satellites (A/M ≅ 0.05 m^2/kg) and high A/M fragments.

Table 2.1

Reference Geostationary Orbit (Initial Conditions)

Epoch	2005.05.01 00:00 UTC
Orbital Elements	Mean Keplerian
Earth Centered Reference Frame	True of Date
Semimajor Axis	42164.465 km
Eccentricity	0.0001
Inclination	0.097 deg
Right Ascension of Ascending Node	52.087 deg
Argument of Perigee	171.191 deg
Mean Anomaly	287.842 deg

The results of the propagations are summarized in the following figures. For A/M = 0.05 m^2/kg, LOP and SATRAP provide practically the same results. LEGO displays a good agreement as far as the semimajor axis (Figure 2.1) and the orbital plane evolution (Figures 2.3 and 2.4) are concerned. However, the eccentricity vector evolution is not modeled so well, with differences, in both magnitude (Figure 2.2) and phase (Figure 2.5), resulting into a maximum error in the perigee/apogee height of less than 120 km. The same applies for A/M = 1 m^2/kg (Figures 2.6-2.11), where the long-term evolution is very similar; the difference in the eccentricity vector translates into a maximum error on the perigee/apogee height of less than 4% (Figure 2.11).

For A/M = 10 m^2/kg, or higher, LEGO is not appropriate anymore to describe the long-term trajectory evolution: the orbital plane and eccentricity vector behaviors are markedly different from those predicted by LOP and SATRAP. Moreover, for A/M = 20 m^2/kg, or higher, LEGO predicts a much shorter orbital lifetime (Figures 2.17, 2.23 and 2.26), due to a rapid and

[1] In the LOP runs described in this section, ABSERR = RELERR = 10^{-8}.

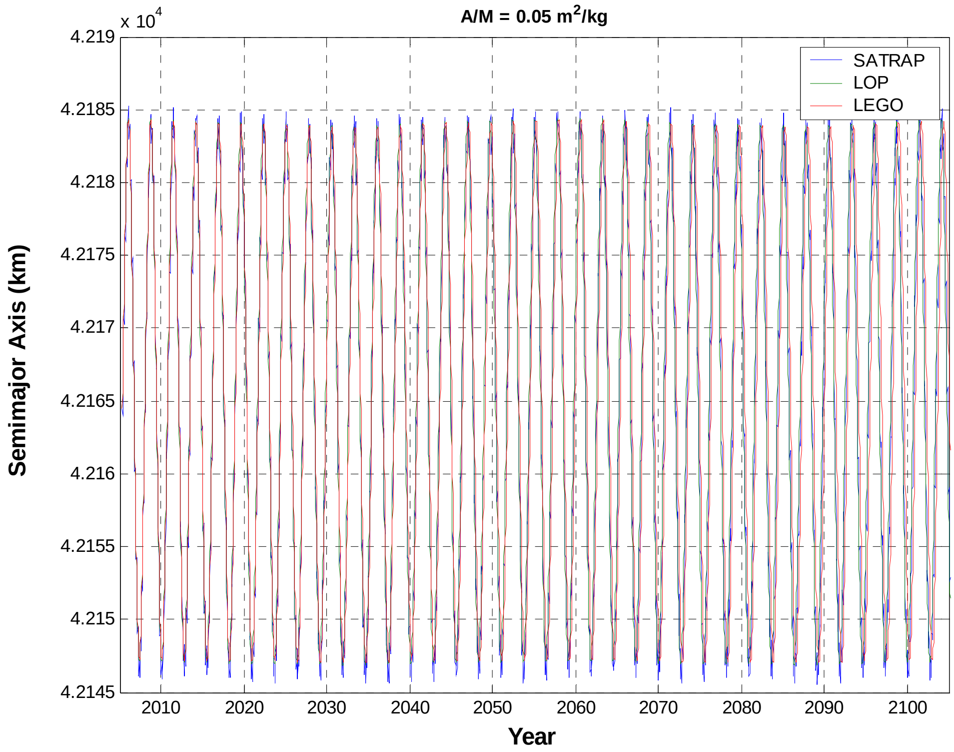
A/M = 0.05 m2/kg
x 10^4
4.219
4.2185
4.218
4.2175
4.217
4.2165
4.216
4.2155
4.215
4.2145
Semimajor Axis (km)
SATRAP
LOP
LEGO
2010
2020
2030
2040
2050
2060
2070
2080
2090
2100
Year

Fig. 2.1

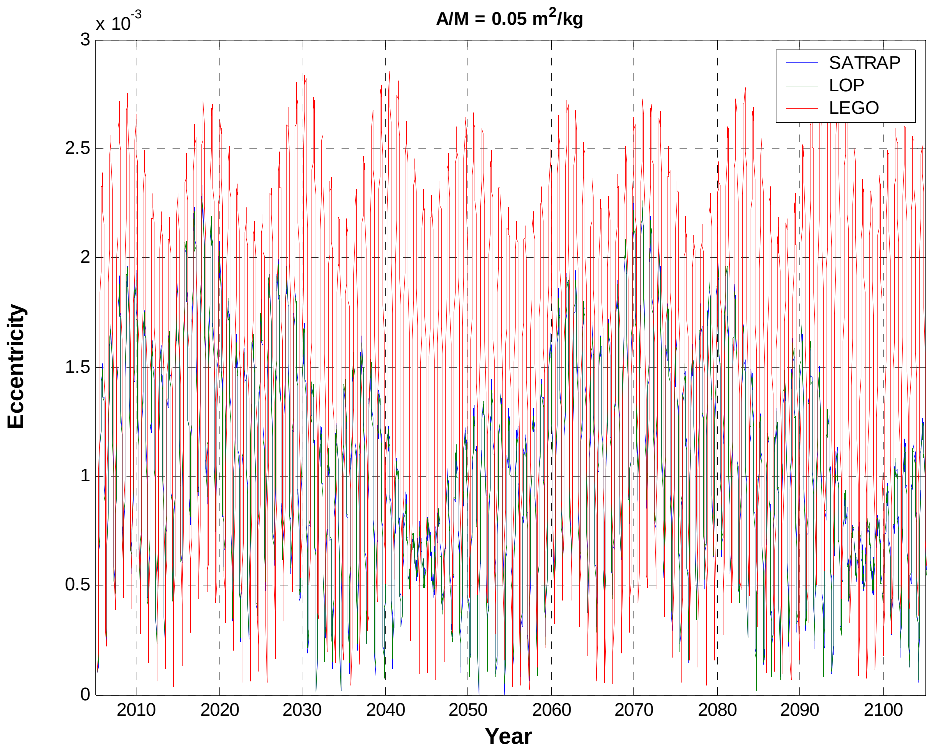
A/M = 0.05 m2/kg
x 10^-3
3
2.5
2
1.5
1
0.5
0
Eccentricity
SATRAP
LOP
LEGO
2010
2020
2030
2040
2050
2060
2070
2080
2090
2100
Year

Fig. 2.2

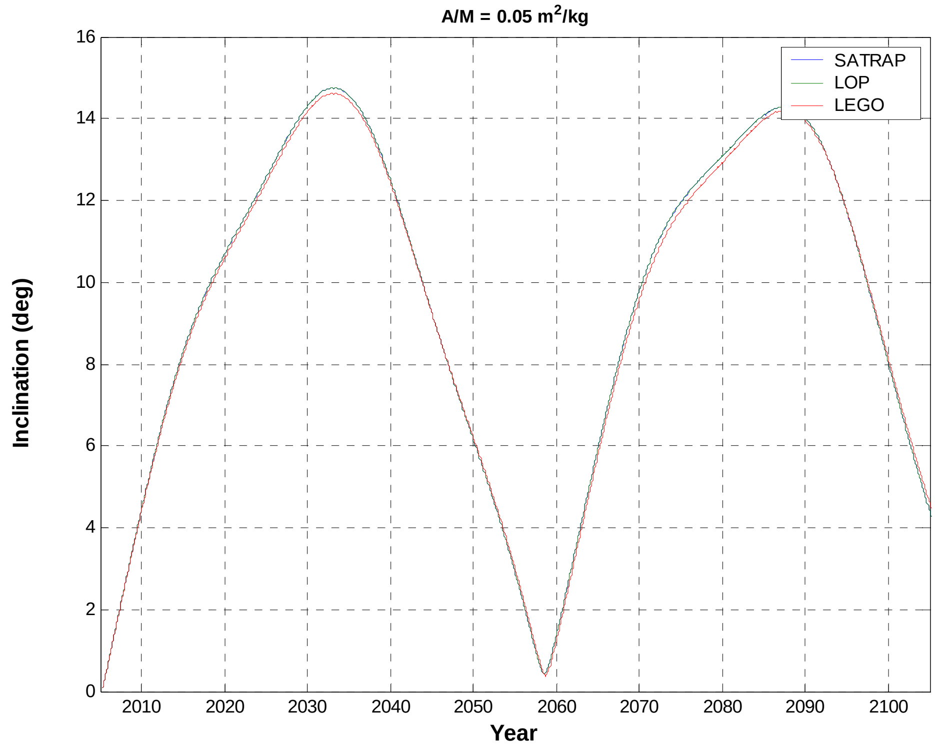
A/M = 0.05 m²/kg
SATRAP
LOP
LEGO
Inclination (deg)
Year
0
2
4
6
8
10
12
14
16
2010
2020
2030
2040
2050
2060
2070
2080
2090
2100

Fig. 2.3

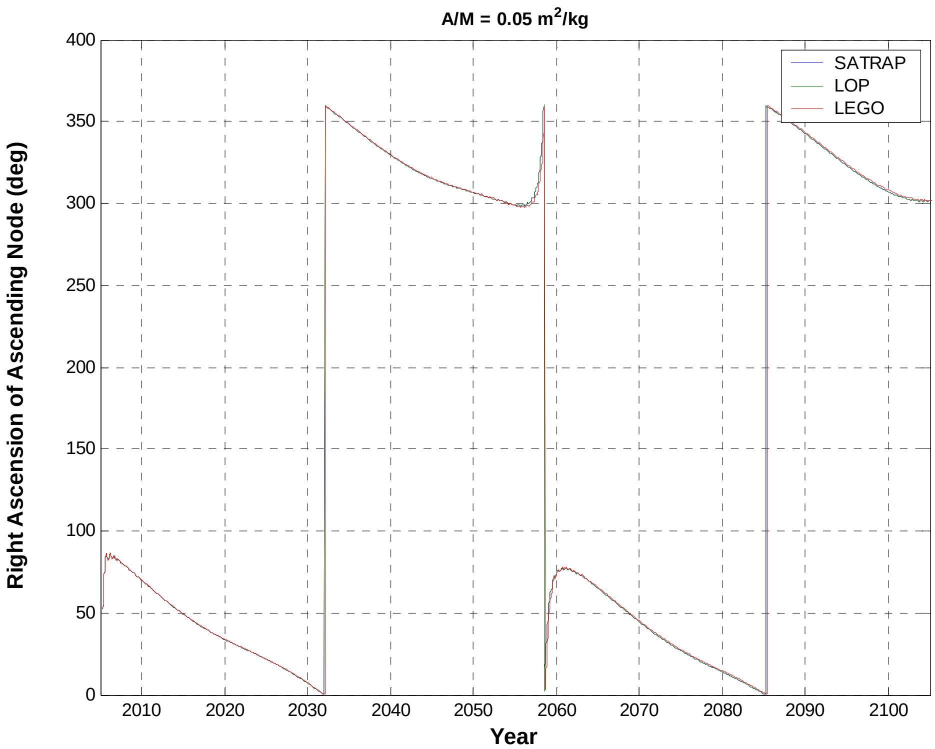
A/M = 0.05 m²/kg
SATRAP
LOP
LEGO
Right Ascension of Ascending Node (deg)
Year
0
50
100
150
200
250
300
350
400
2010
2020
2030
2040
2050
2060
2070
2080
2090
2100

Fig. 2.4

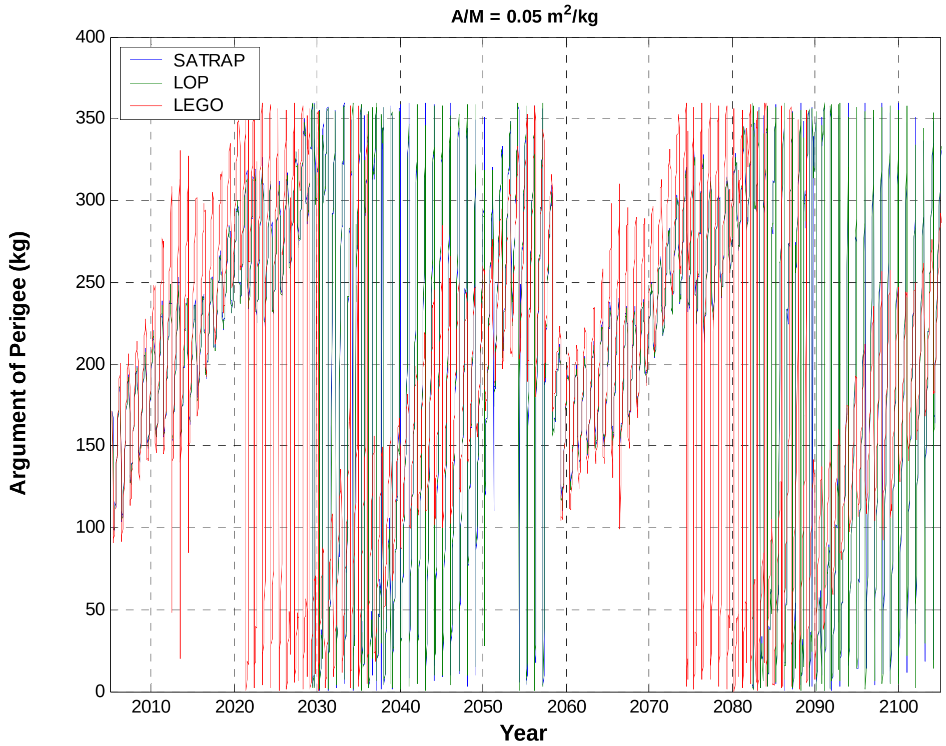
A/M = 0.05 m2/kg
SATRAP
LOP
LEGO
Argument of Perigee (kg)
Year
0
50
100
150
200
250
300
350
400
2010
2020
2030
2040
2050
2060
2070
2080
2090
2100

Fig. 2.5

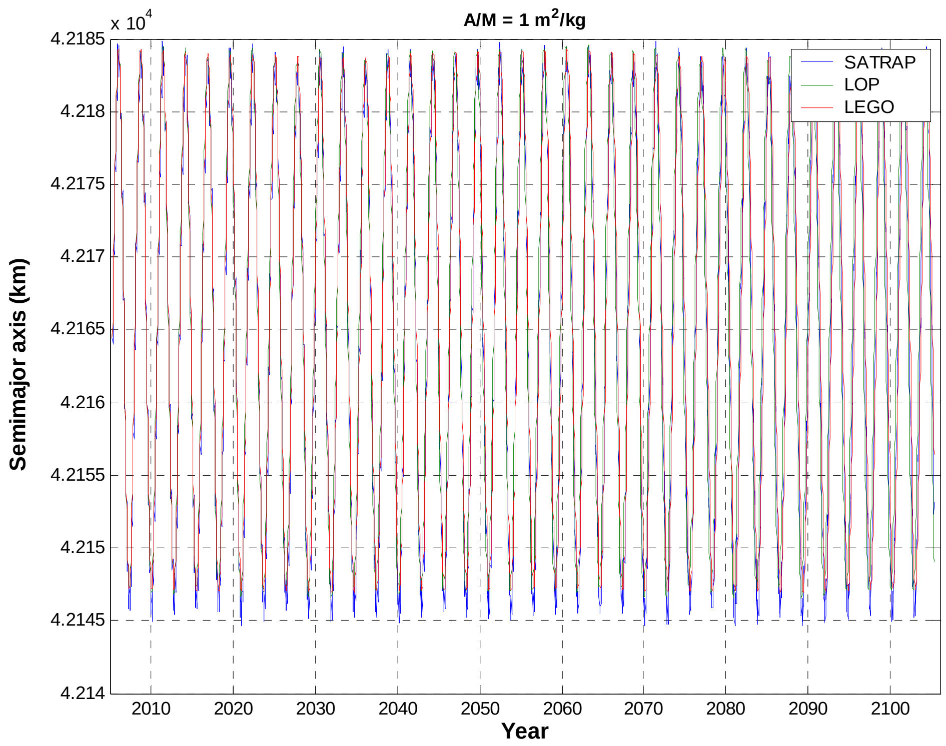
A/M = 1 m2/kg
x 10^4
SATRAP
LOP
LEGO
Semimajor axis (km)
Year
4.214
4.2145
4.215
4.2155
4.216
4.2165
4.217
4.2175
4.218
4.2185
2010
2020
2030
2040
2050
2060
2070
2080
2090
2100

Fig. 2.6

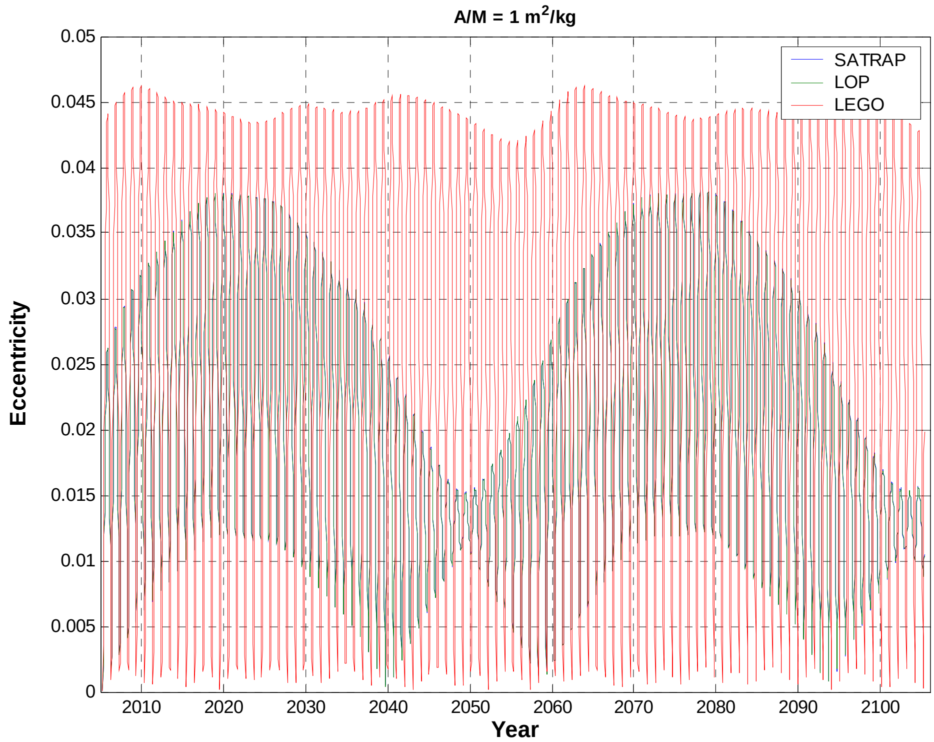
A/M = 1 m²/kg
SATRAP
LOP
LEGO
Eccentricity
Year
0.05
0.045
0.04
0.035
0.03
0.025
0.02
0.015
0.01
0.005
0
2010
2020
2030
2040
2050
2060
2070
2080
2090
2100

Fig. 2.7

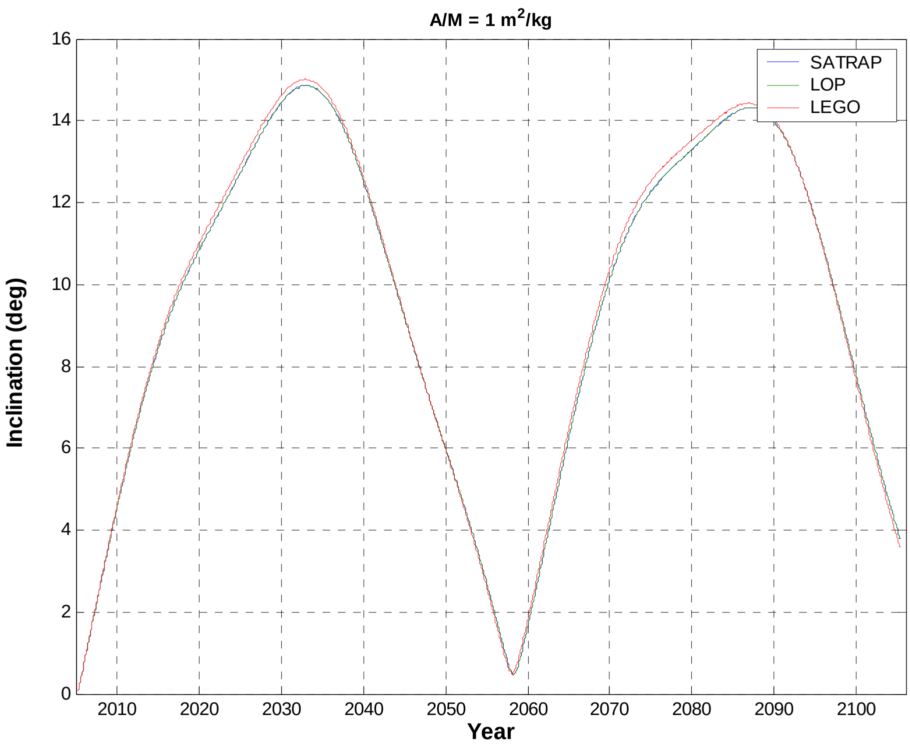
A/M = 1 m²/kg
SATRAP
LOP
LEGO
Inclination (deg)
Year
16
14
12
10
8
6
4
2
0
2010
2020
2030
2040
2050
2060
2070
2080
2090
2100

Fig. 2.8

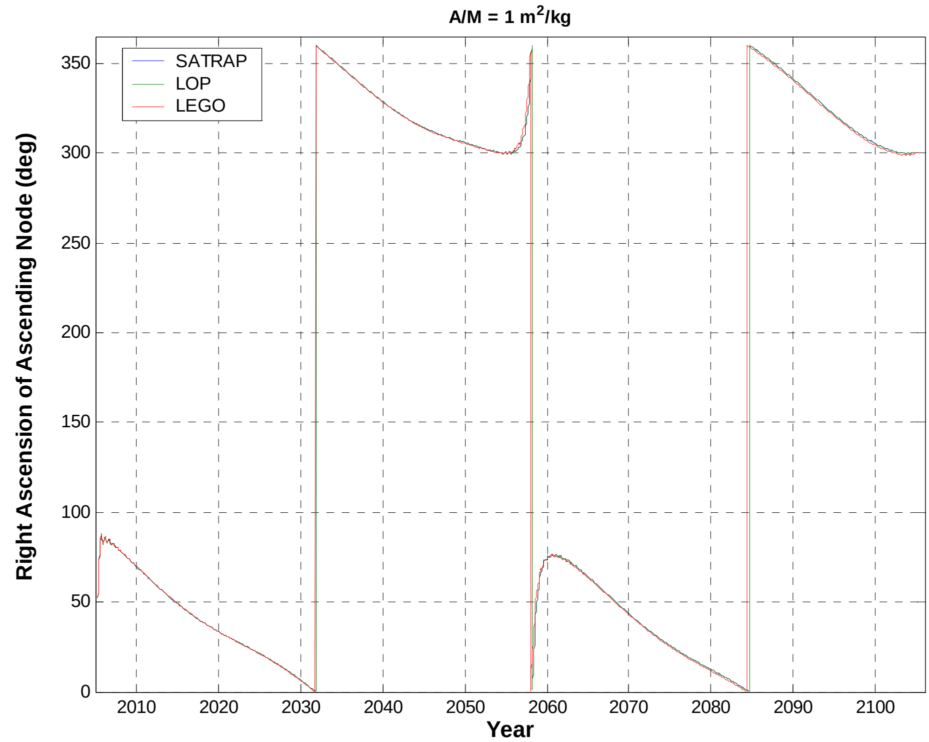

Fig. 2.9

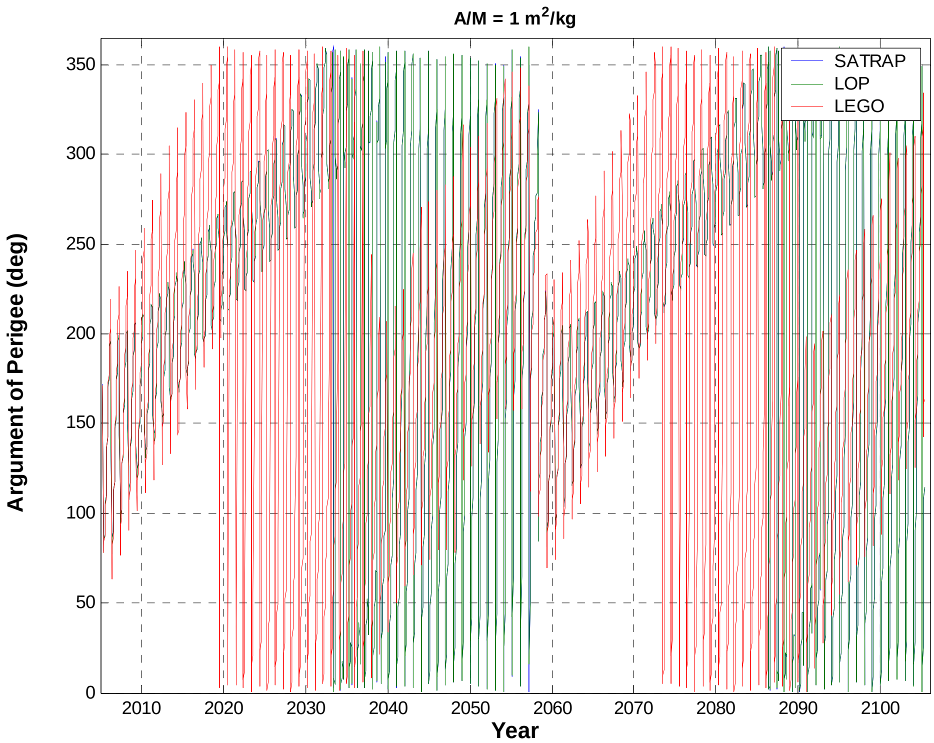

Fig. 2.10

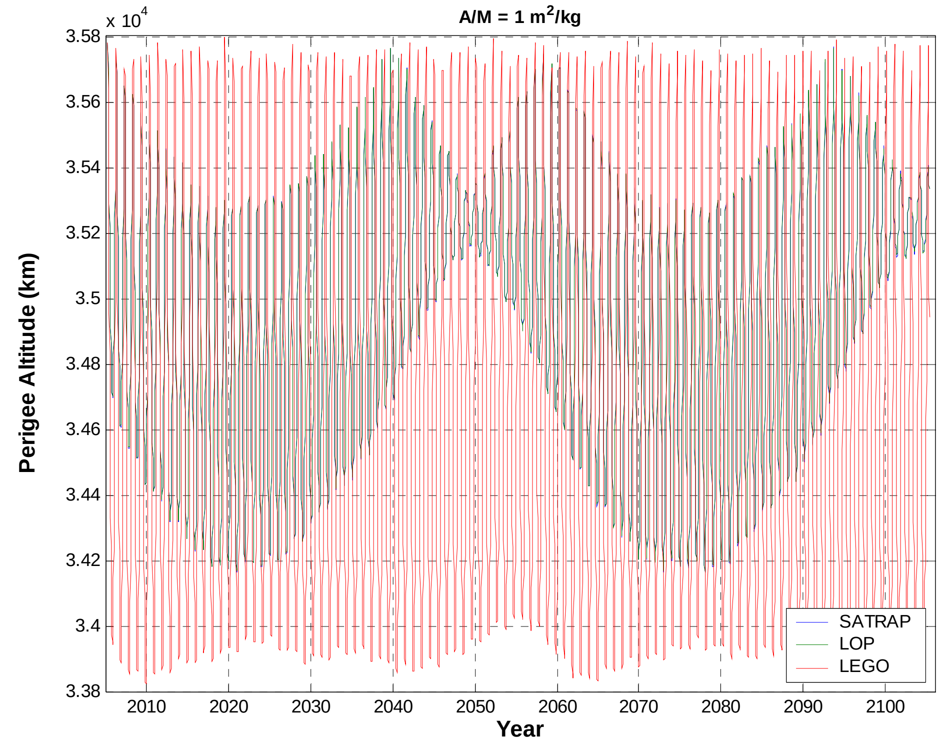

Fig. 2.11

Fig. 2.12

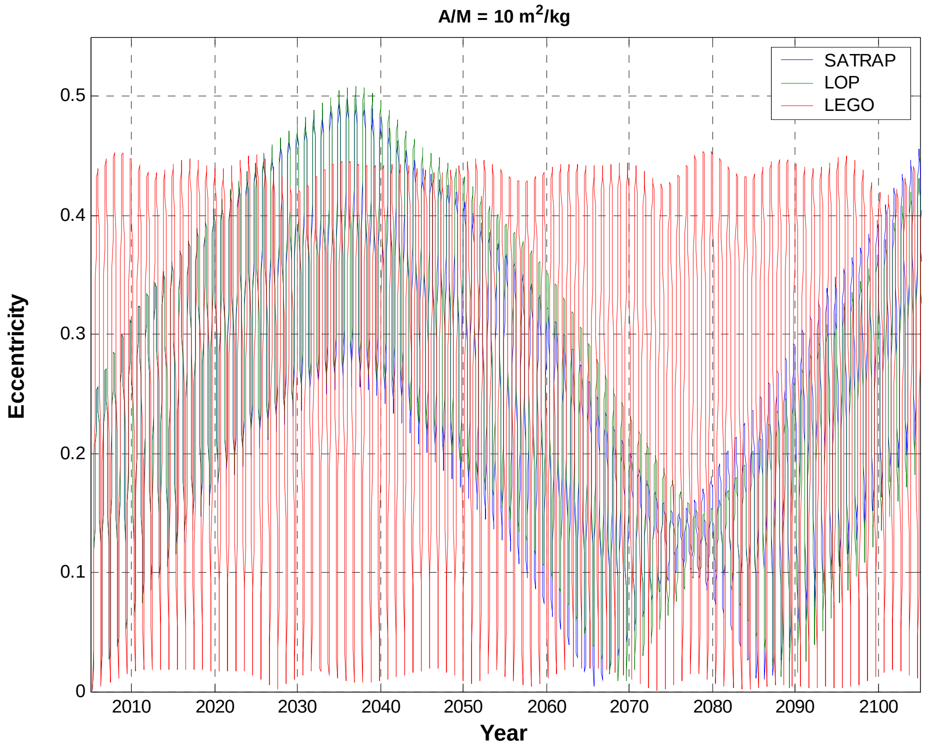

Fig. 2.13

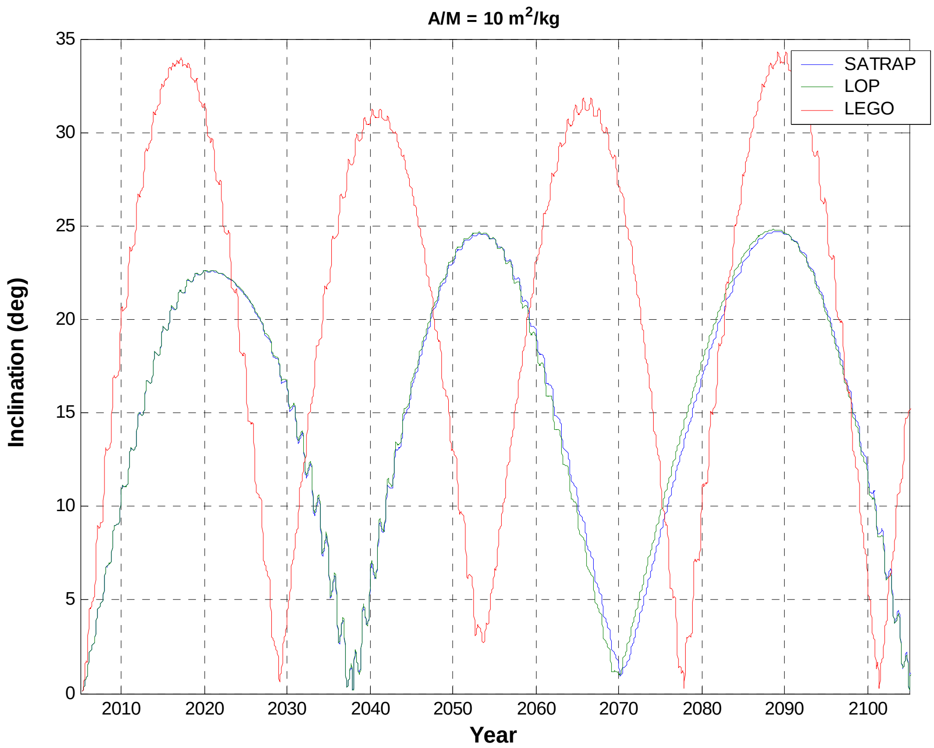

Fig. 2.14

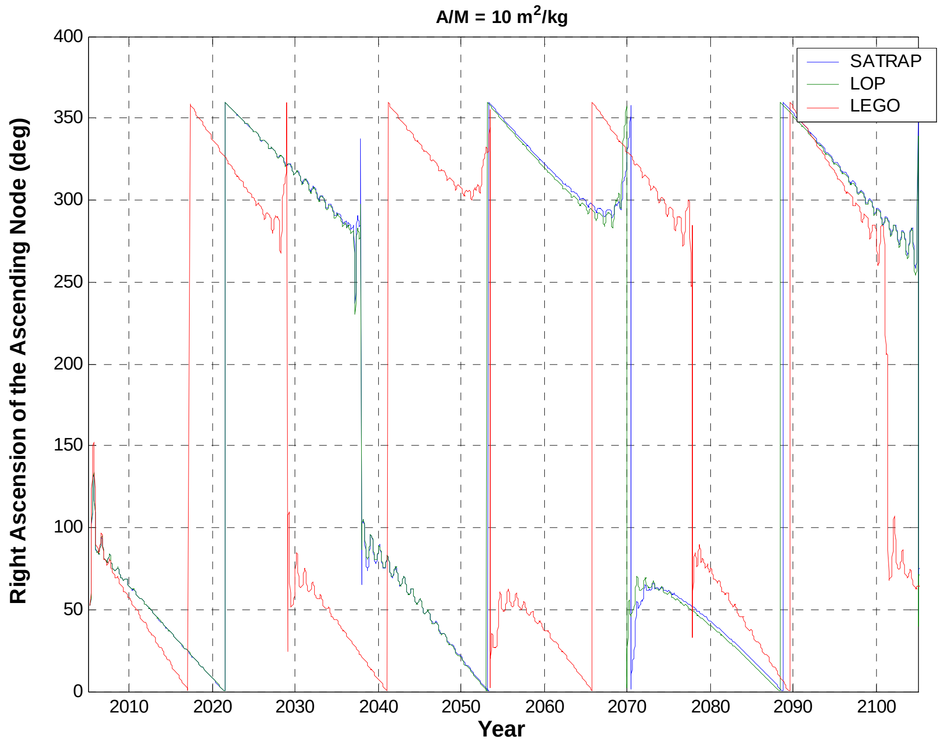

Fig. 2.15

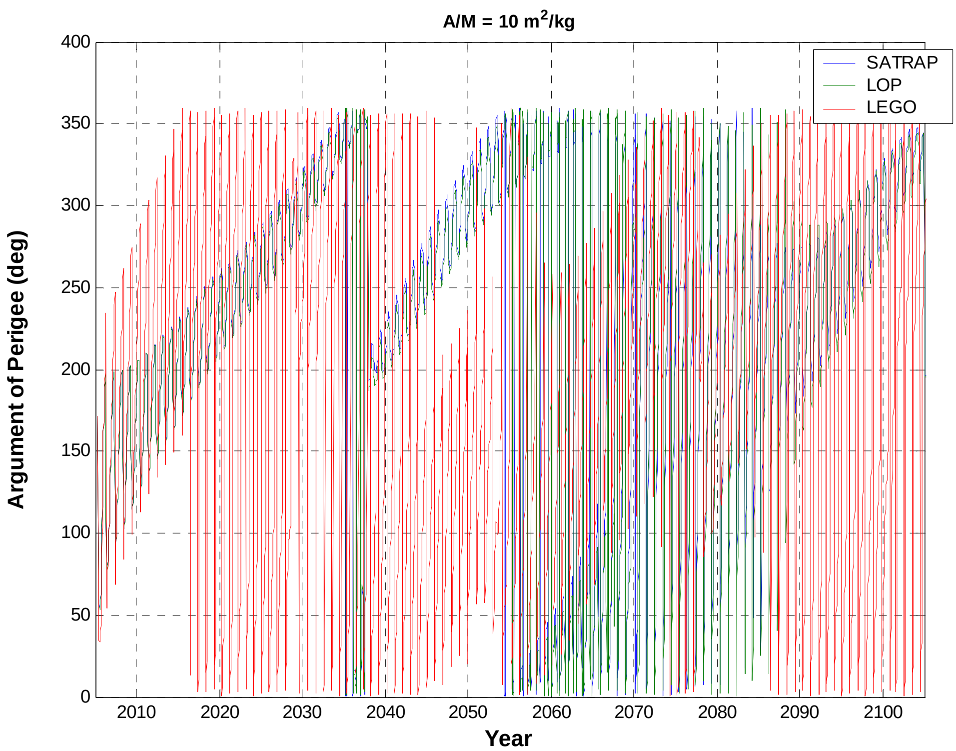

Fig. 2.16

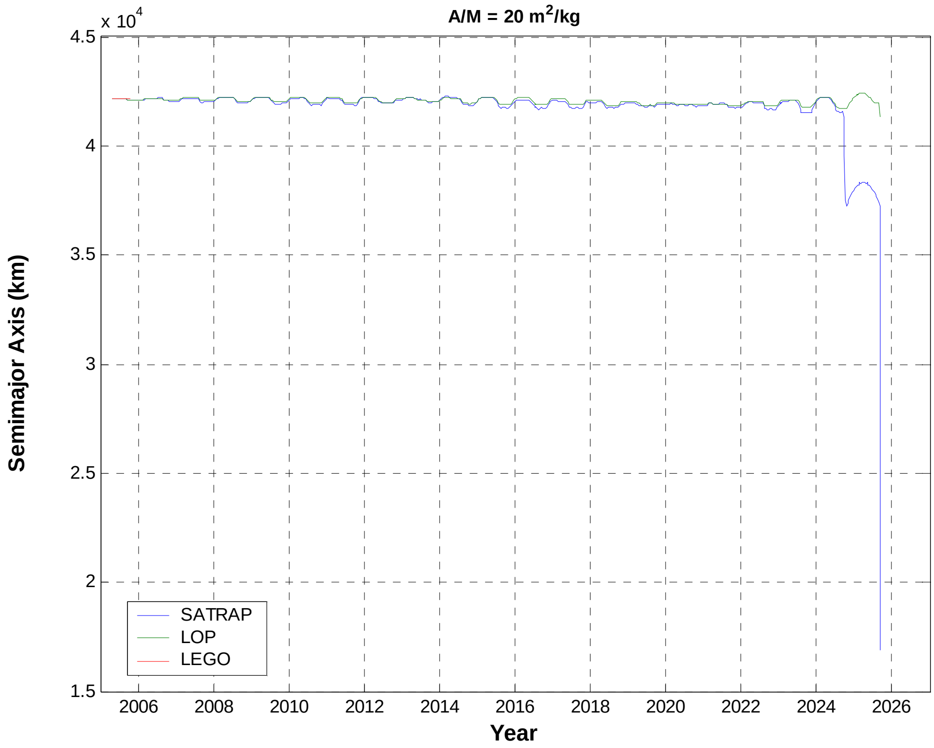

Fig. 2.17

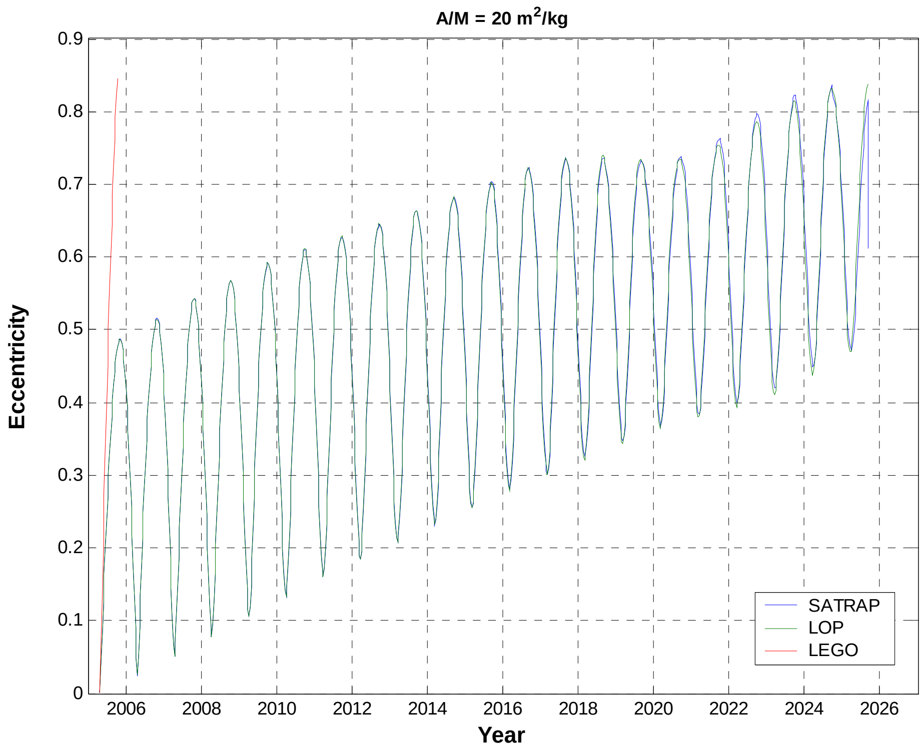

Fig. 2.18

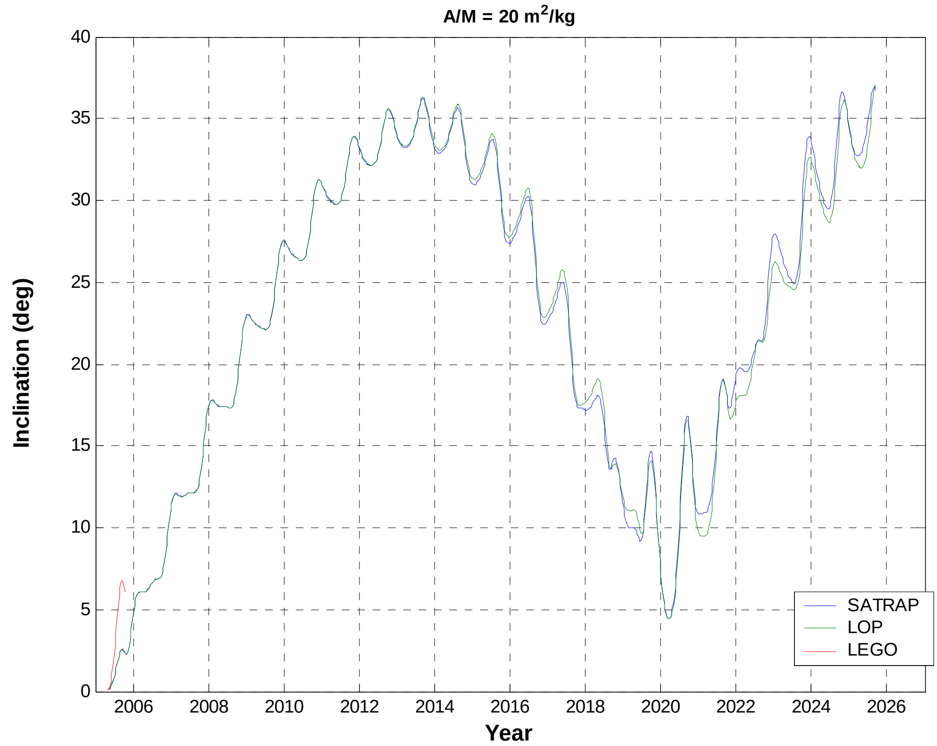

Fig. 2.19

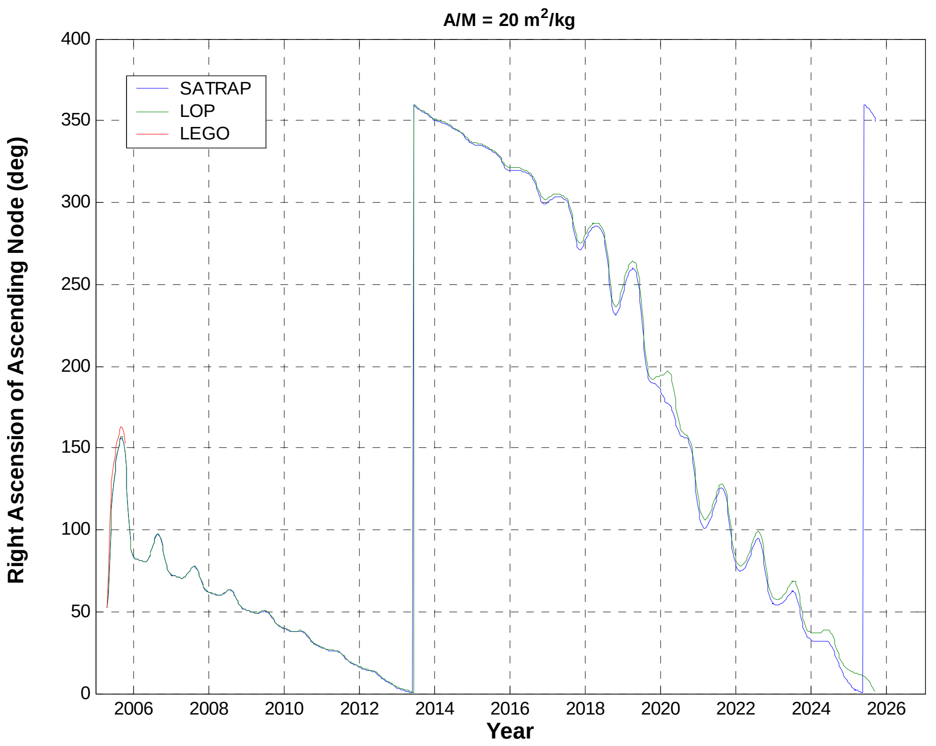

Fig. 2.20

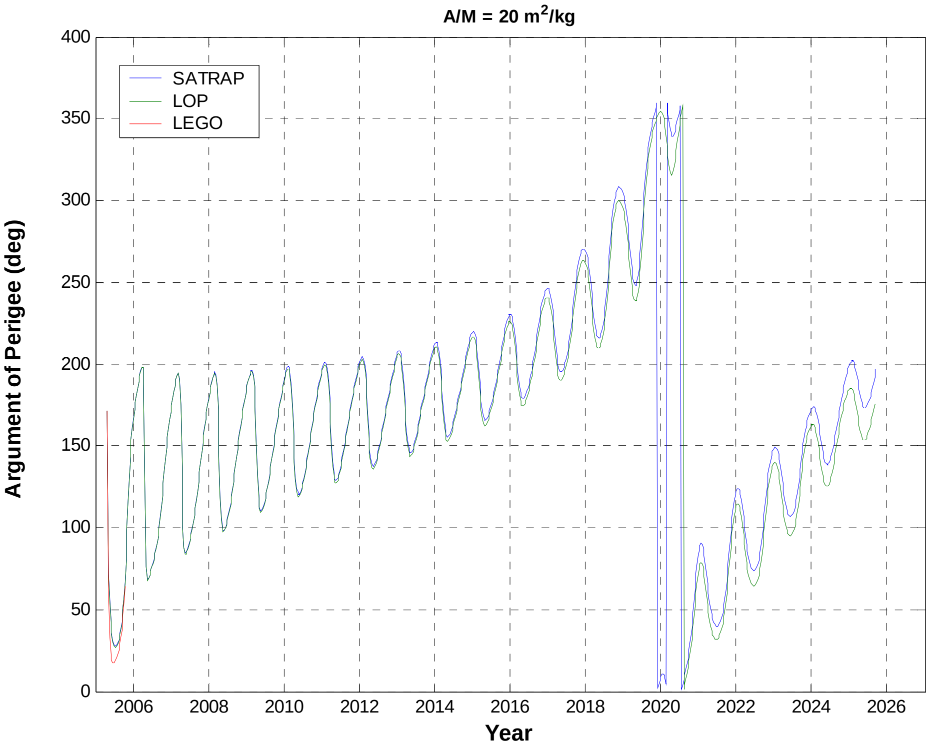

Fig. 2.21

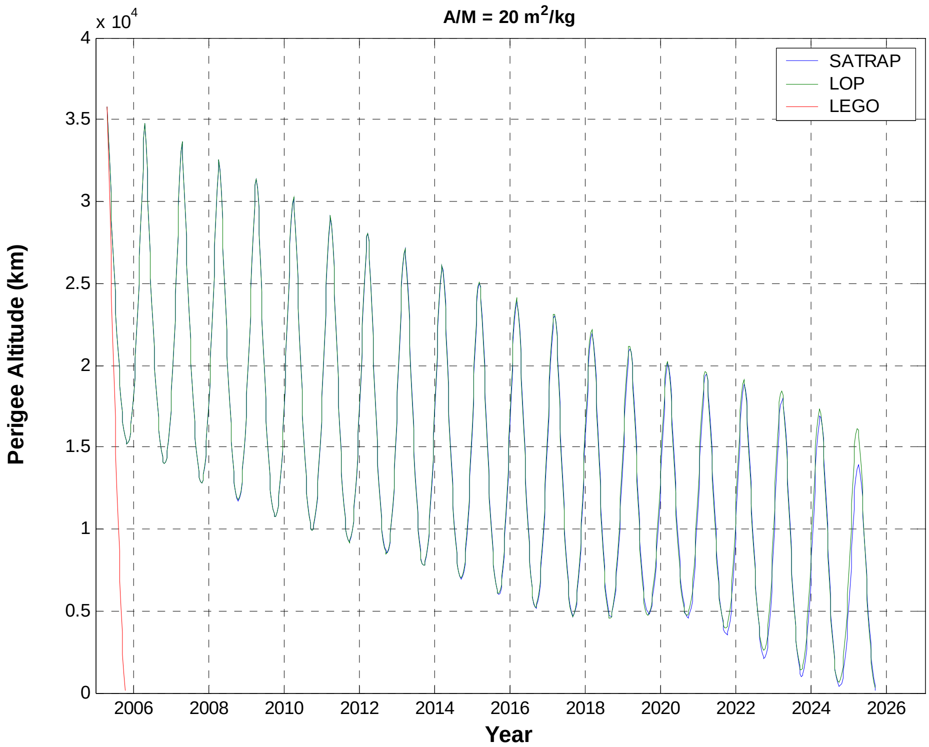

Fig. 2.22

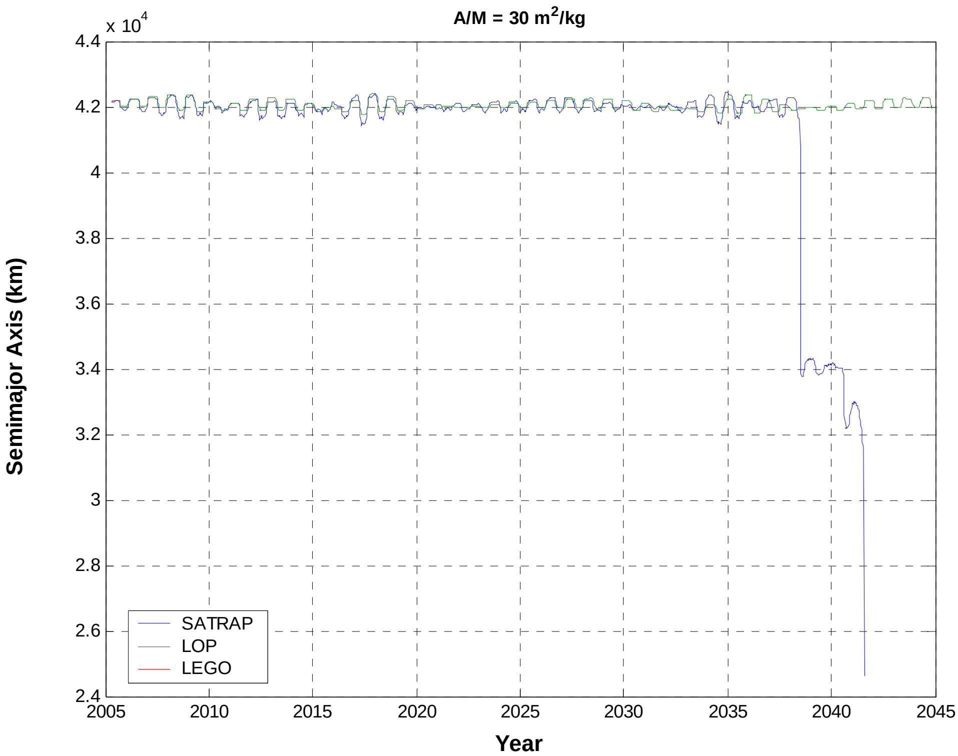

Fig. 2.23

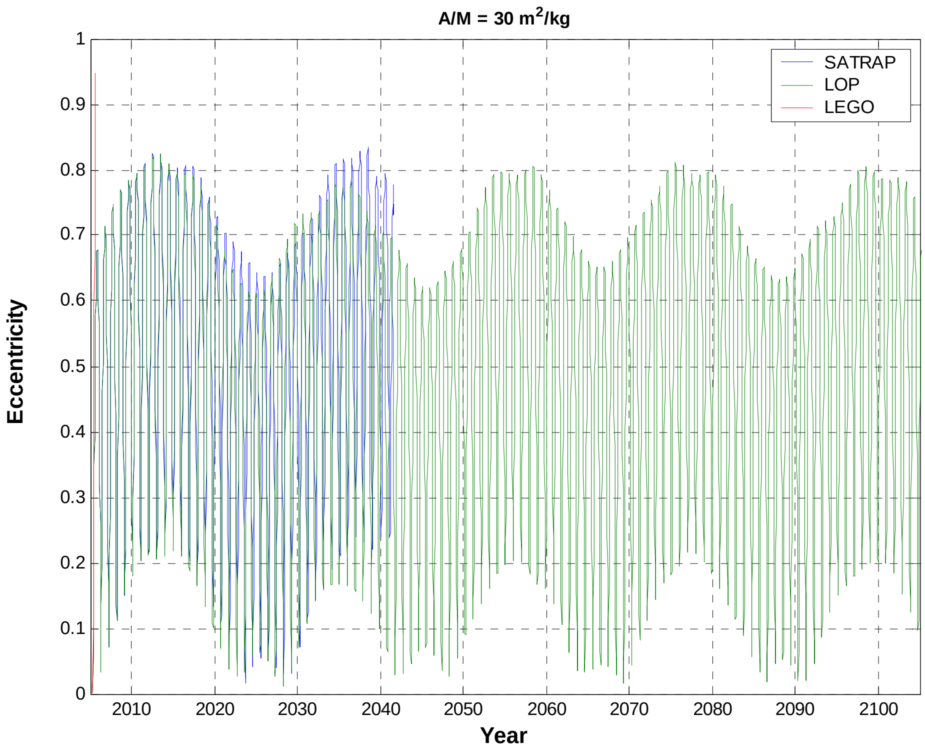

Fig. 2.24

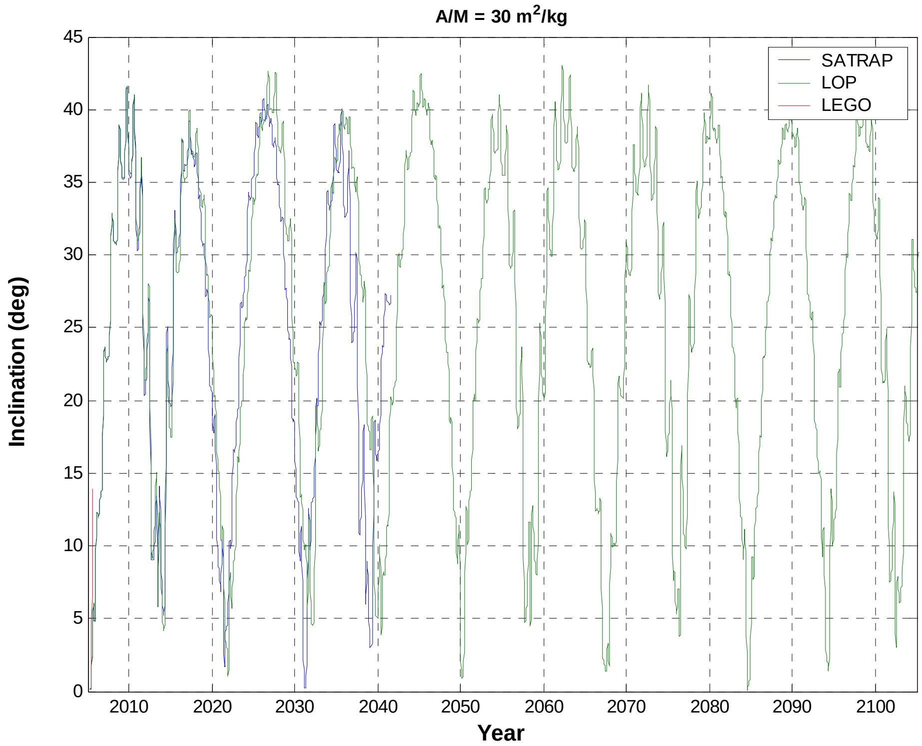

Fig. 2.25

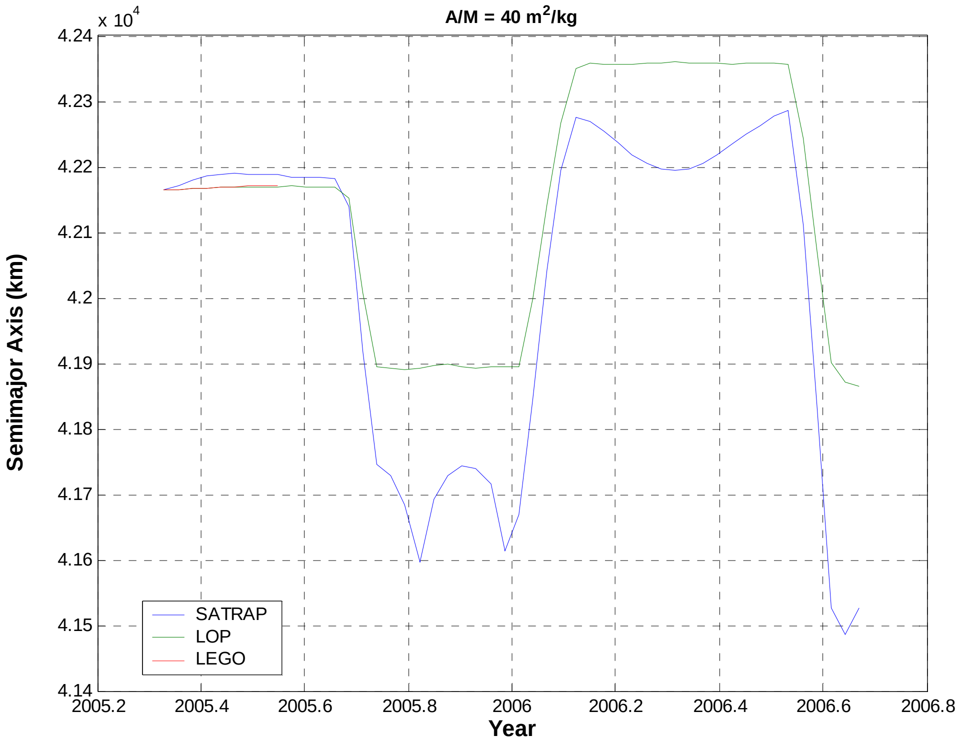

Fig. 2.26

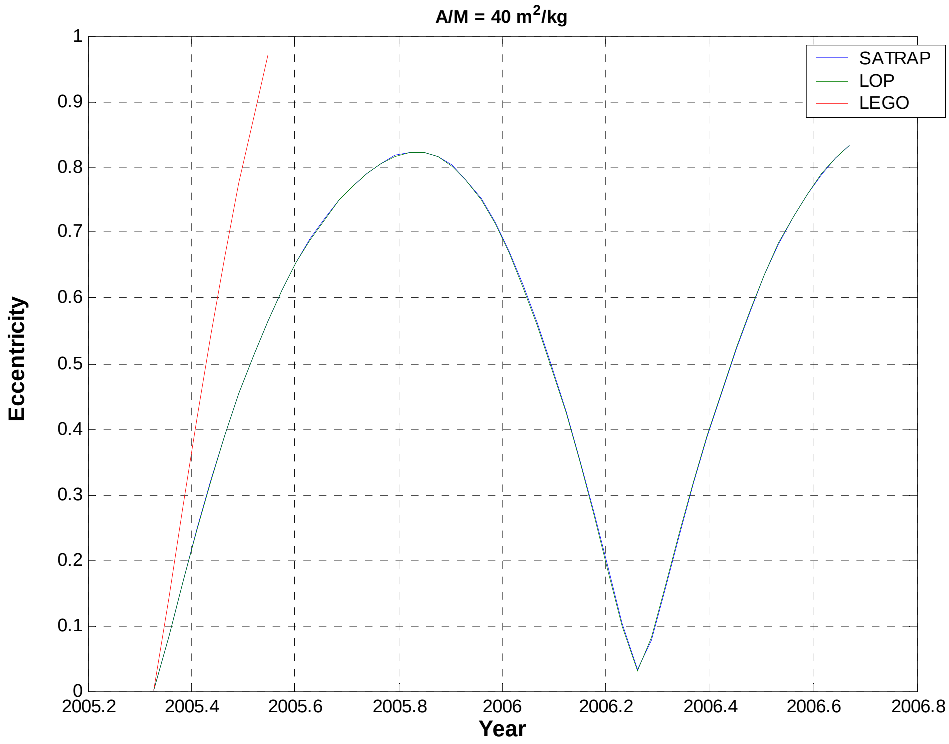

Fig. 2.27

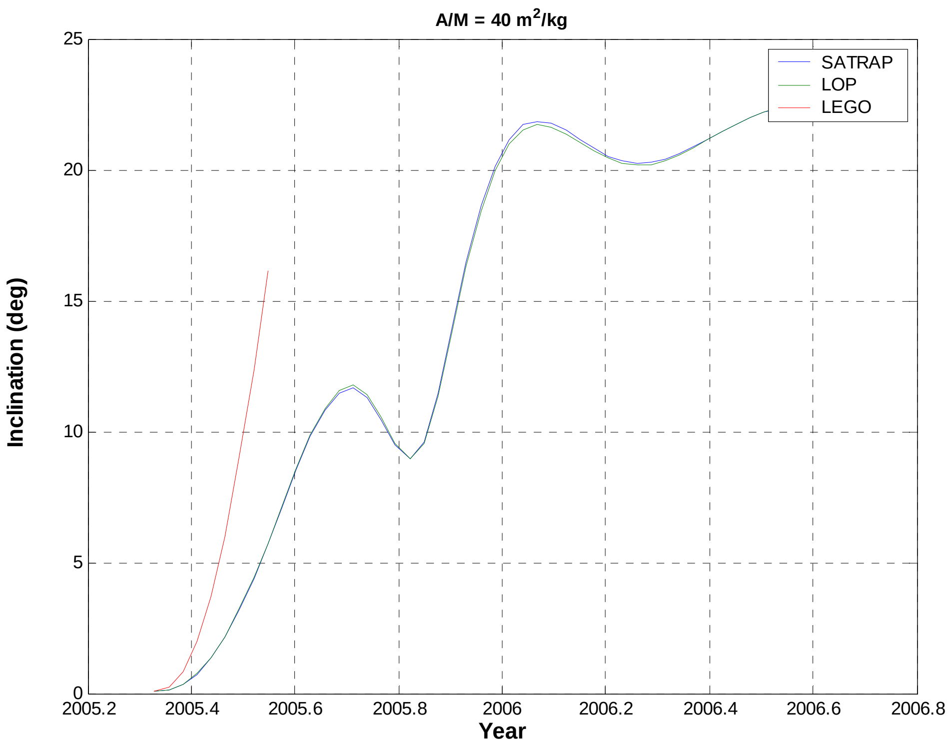

Fig. 2.28

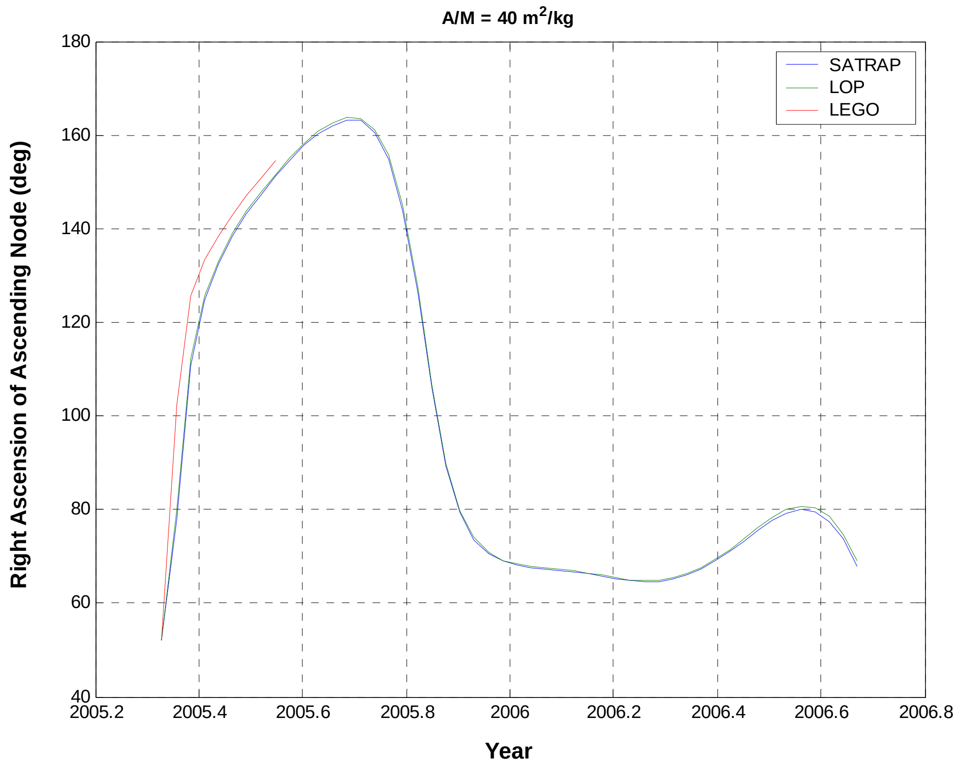

Fig. 2.29

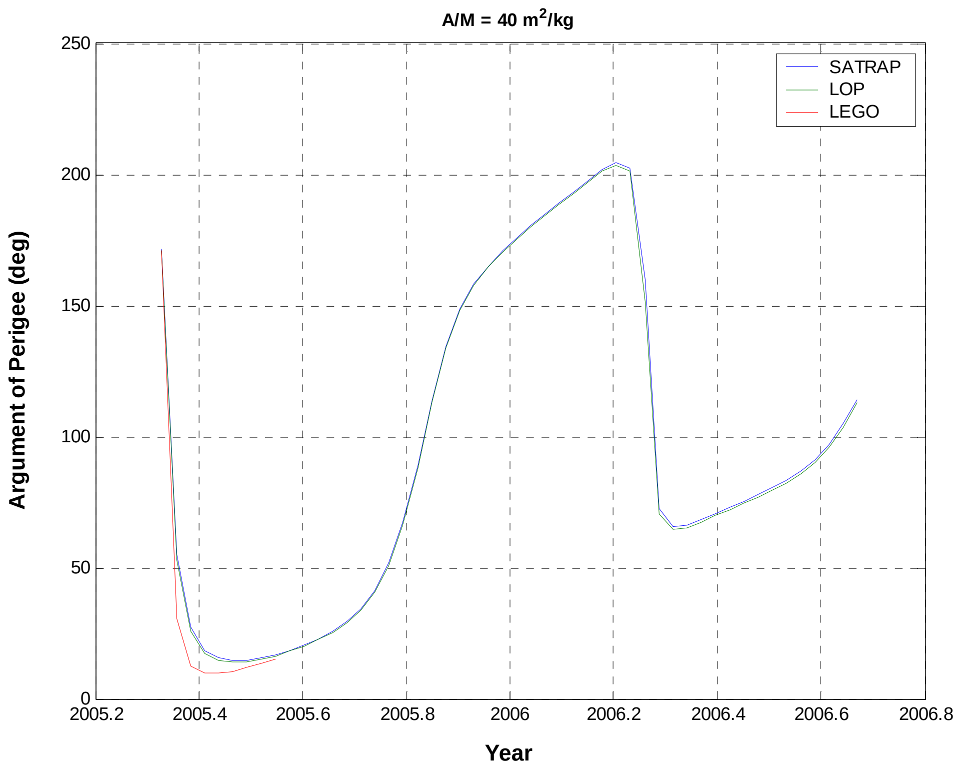

Fig. 2.30

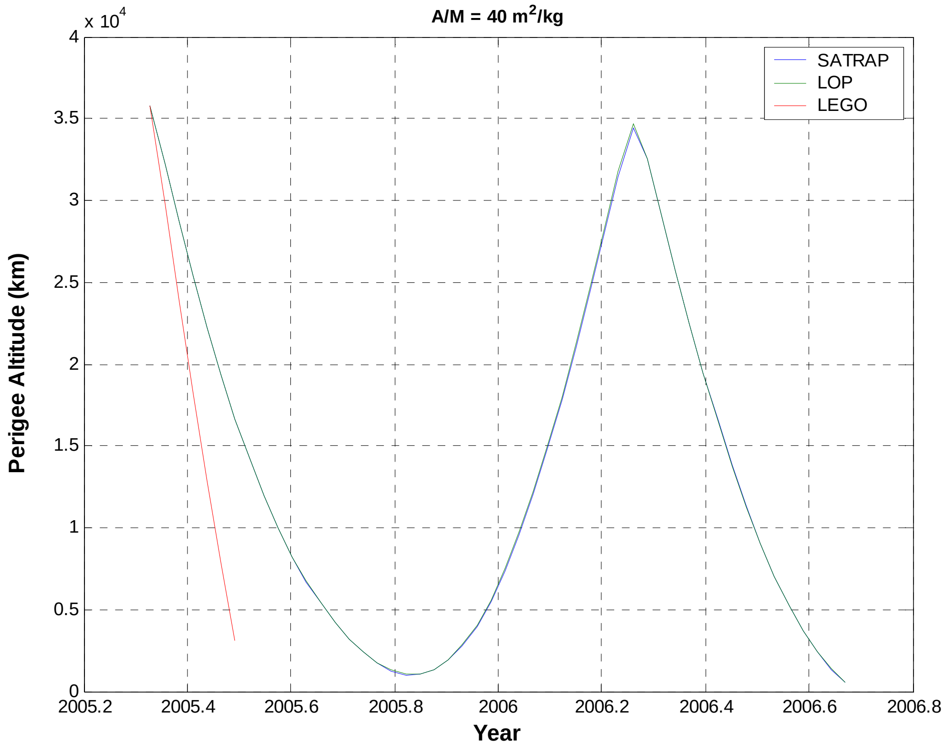

Fig. 2.31

uncontrollable increase of the eccentricity (Figures 2.18, 2.24 and 2.27) and the corresponding decrease of the perigee altitude (Figures 2.22 and 2.31).

Concerning LOP, the agreement with the numerical propagator SATRAP is very good up to A/M = 20 m^2/kg (Figures 2.1-2.22), and acceptably good up to A/M = 40 m^2/kg (Figures 2.23-2.31). For A/M = 30 m^2/kg (Figures 2.23-2.25), the agreement is quite good until the earlier decay of the object propagated with SATRAP. This macroscopic effect is, however, the result of a relatively small drift of the eccentricity and perigee altitude, subjected to a large long-period oscillation: after approximately 35 years, during an eccentricity peak (Figure 2.24), this small difference is sufficient, in fact, to induce the observed decay.

In conclusion, due to its extraordinary computational speed, the use of LEGO can be recommended, in SDM 4.0, to propagate uncontrolled GEO trajectories of objects with A/M ≤ 1 m^2/kg. For A/M > 1 m^2/kg, a LOP derivative, like FOP, can guarantee in most cases accuracies comparable to those provided by special perturbations approaches, as in SATRAP.

2.2 Eccentric Geosynchronous Orbits

The comparison was extended to eccentric geosynchronous orbits. A satellite with A/M = 0.05 m^2/kg was propagated for 100 years with the initial conditions detailed in Table 2.1, apart from the eccentricity, for which initial values in between 0.01 and 0.8 were considered.

The results obtained are qualitatively summarized in Table 2.2 for LEGO and in Table 2.3 for LOP[2]. LEGO provides a satisfactory agreement with SATRAP up to eccentricities of 0.2, while the use of a LOP derived propagator (FOP) is recommended for higher eccentricities.

Table 2.2

Eccentric Geosynchronous Orbit Evolution (A/M = 0.05 m^2/kg): LEGO vs. SATRAP

Orbital Elements	Initial Eccentricity								
	0.01	0.1	0.2	0.3	0.4	0.5	0.6	0.7	0.8
SMA	=	≈	≈	≈	≈	~	≠	≠	~
ECC	~	≈	≈	~	≠	≠	≠	≠	≠
INC	≈	≈	≈	~	≠	≠	≠	≠	≠
RAAN	≈	≈	≈	~	≠	≠	≠	≠	≠
AP	≈	≈	≈	~	≠	≠	≠	≠	≠

= Excellent agreement
≈ Satisfactory agreement
~ Approximate agreement
≠ Disagreement

Table 2.3

Eccentric Geosynchronous Orbit Evolution (A/M = 0.05 m^2/kg): LOP vs. SATRAP

Orbital Elements	Initial Eccentricity								
	0.01	0.1	0.2	0.3	0.4	0.5	0.6	0.7	0.8
SMA	=	=	=	=	=	=	≈	~	~
ECC	=	=	=	≈	≈	≈	≈	≈	~
INC	=	=	=	=	≈	≈	≈	≈	≈
RAAN	=	=	=	=	≈	≈	≈	≈	≈
AP	=	=	=	=	≈	≈	≈	≈	≈

= Excellent agreement
≈ Satisfactory agreement
~ Approximate agreement
≠ Disagreement

2.3 Circular Orbits Above and Below GEO

The performances of the propagators were also tested for circular orbits above and below the GEO altitude. Taking the initial conditions given in Table 2.1, the semimajor axis was increased, or decreased, by 1000, 5000 and 10000 km, studying the evolution over one century of a satellite with A/M = 0.05 m^2/kg. For GEO ± 1000 km, LEGO, LOP and SATRAP show a good agreement in semimajor axis, inclination and right ascension of the ascending node. Less good is the agreement of LEGO in eccentricity (see, for instance, Figure 2.32), but the corresponding maximum error in the altitude of perigee (or apogee) is less than

[2] In the LOP runs described in Sections 2.2 and 2.3, ABSERR = RELERR = 10^{-4}.

150 km. LOP displays a peculiar behavior of the semimajor axis (Figure 2.33), however the effect is quite small, less than 4 km in 100 years.

For GEO + 5000 km, there is a good agreement in semimajor axis between the three propagators. The LEGO divergence is of the order of 1 km in one century. Regarding the orbital plane precession, LEGO predicts the same amplitude of the others, but the oscillation period is longer by 5.6 years, i.e. less than 10% (Figure 2.34), while the eccentricity behavior is qualitatively and quantitatively similar to that encountered for GEO ± 1000 km.

For GEO – 5000 km, the trends are substantially similar, even though the differences are more pronounced. The semimajor axis drift of LEGO is 15 km after one century (Figure 2.35), while the maximum difference in inclination is just a little bit more than one degree (Figure 2.36).

For GEO ± 10000 km, the semimajor axis and eccentricity evolution repeat the pattern observed, respectively, for GEO ± 5000 km. Therefore, LEGO exhibits a behavior qualitatively different from those of LOP and SATRAP, even though the quantitative discrepancies remain modest. Significant deviations emerge, however, in the evolution of the orbital plane (see Figures 2.37 and 2.38). The agreement between LOP and SATRAP, on the other hand, remains very good.

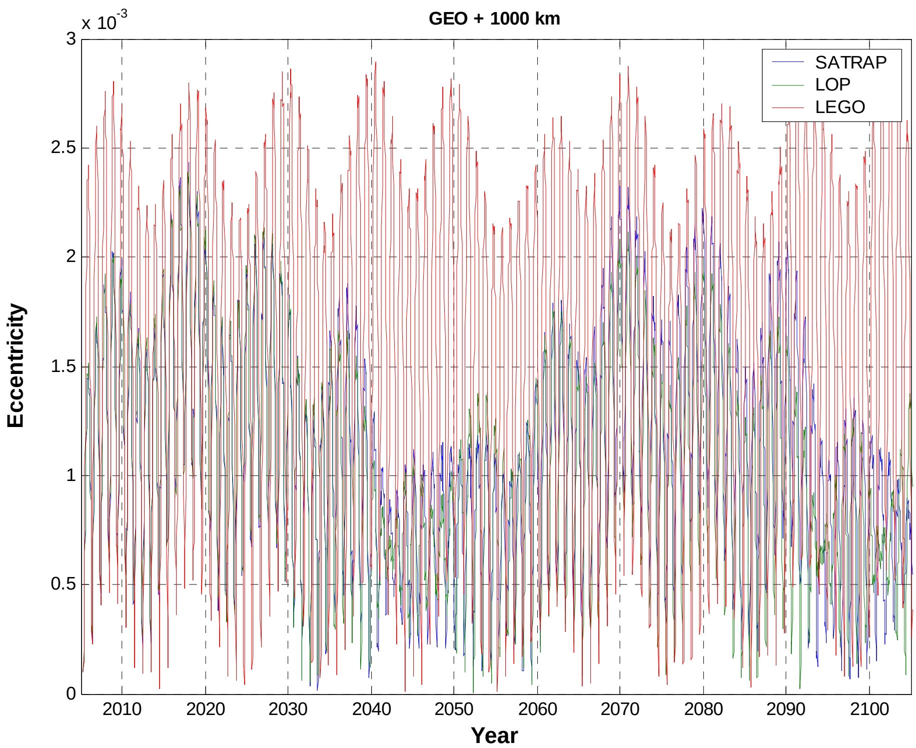

Fig. 2.32

Fig. 2.33

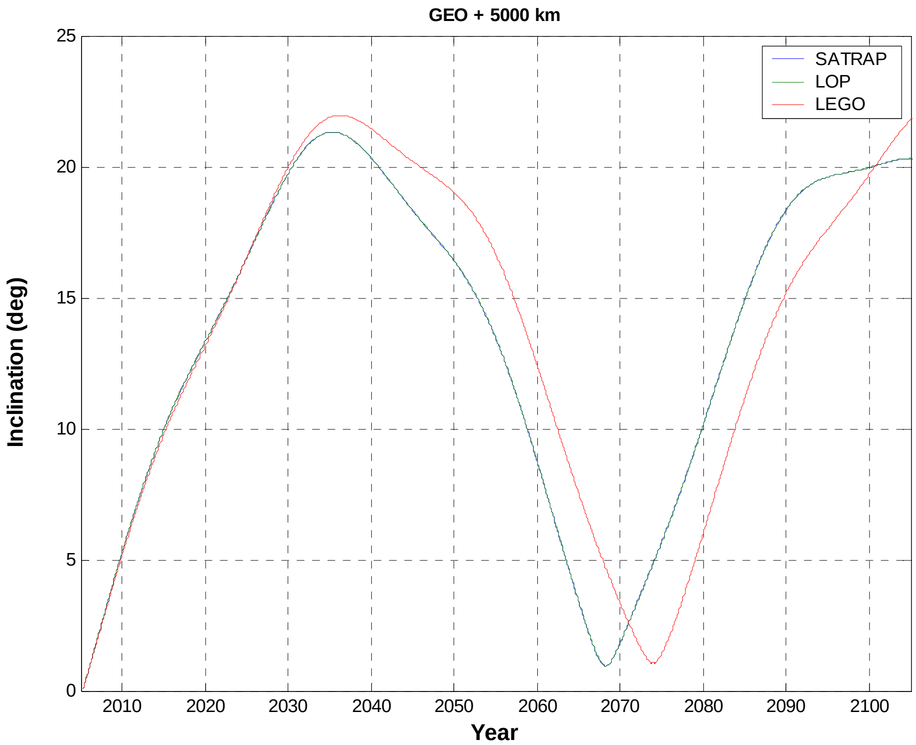

Fig. 2.34

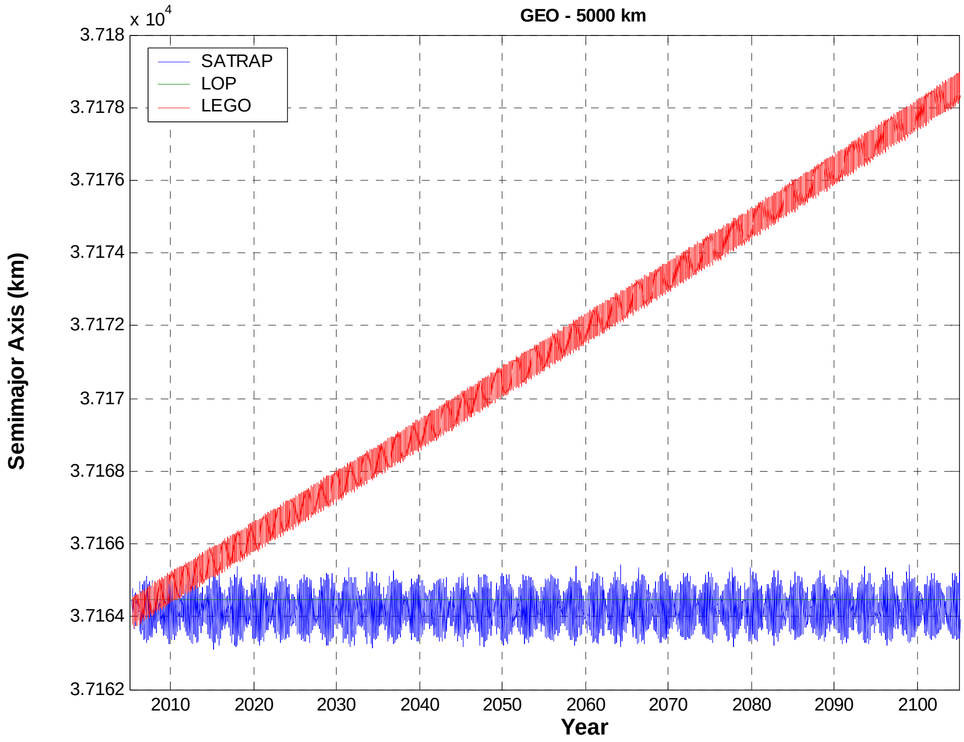

Fig. 2.35

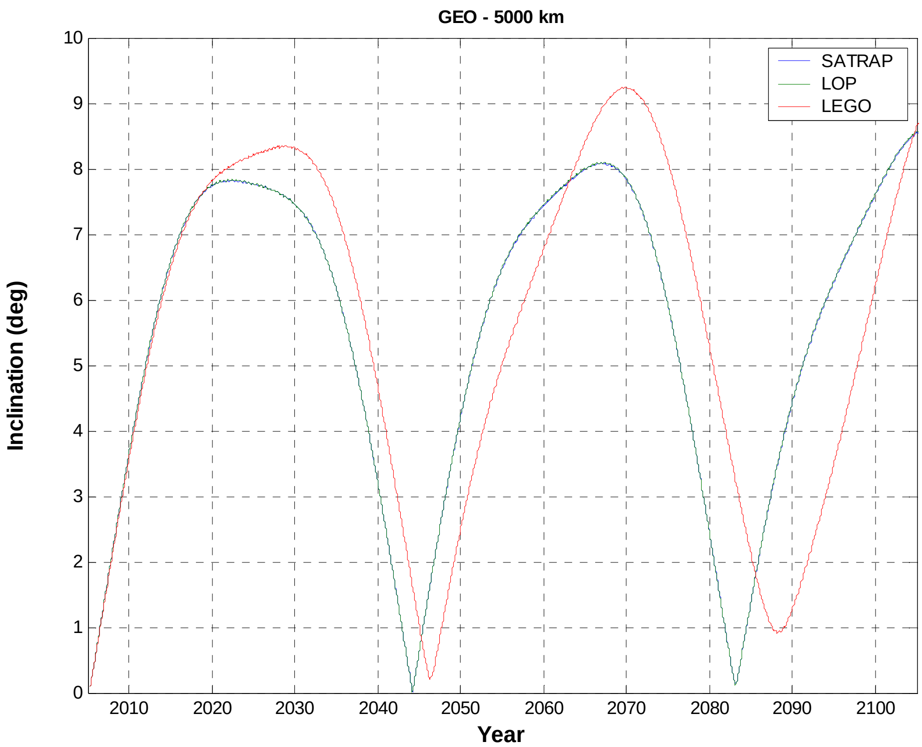

Fig. 2.36

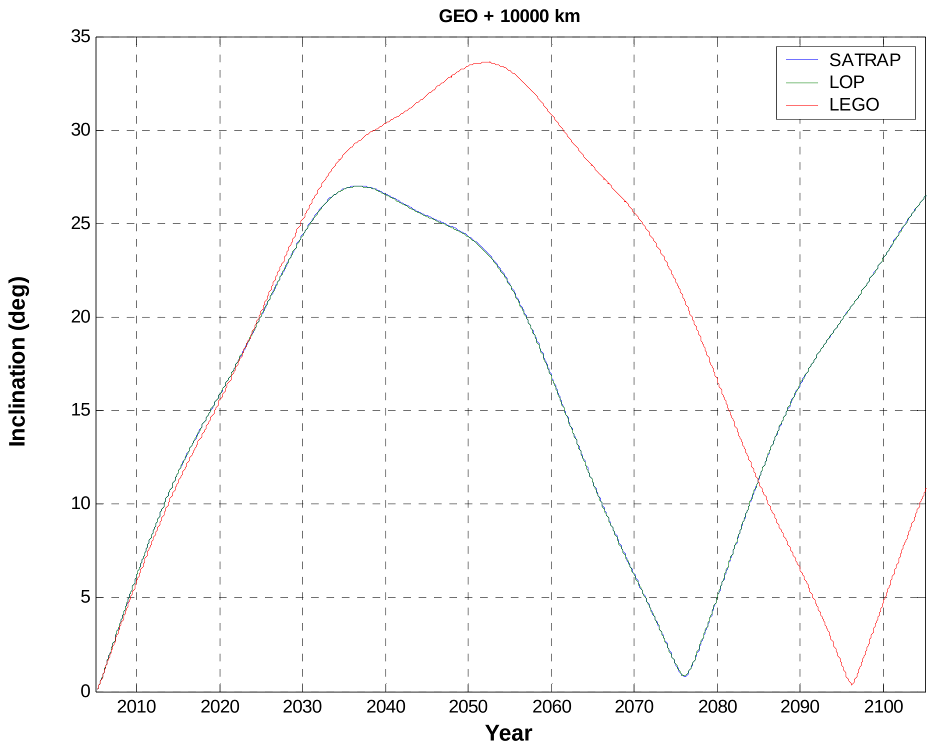

Fig. 2.37

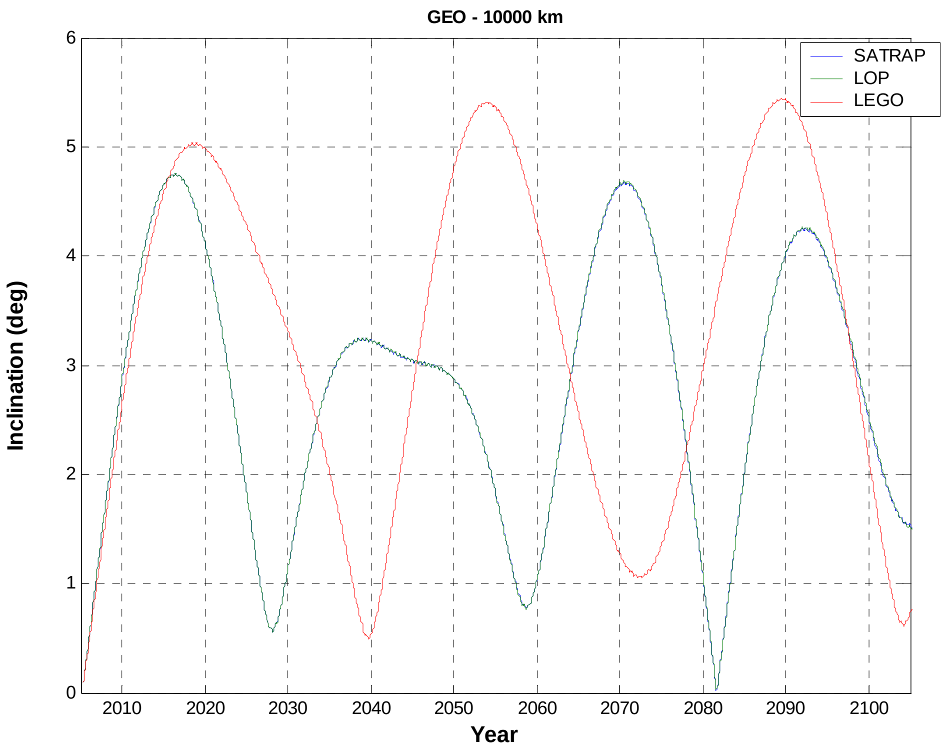

Fig. 2.38

In conclusion, the use of LEGO can be recommended up to 5000 km below or above the GEO altitude, while outside this region a LOP derivative, like FOP, should be preferred.

2.4 Summary

Considering the long-term propagation – in SDM 4.0 – of objects in the geosynchronous, or near-geosynchronous, regime, the following conclusions can be inferred from the extensive set of propagator runs carried out (63).

First of all, LOP can adequately cover all the considered intervals of semimajor axis (GEO ± 10000 km), eccentricity (up to 0.8) and area-to-mass ratio (up to 40 m^2/kg) with a considerable level of accuracy. Concerning the use of the ultra-fast LEGO analytical propagator, in general it can be recommended when all the three following conditions apply:

1. GEO – 5000 km ≤ SMA ≤ GEO + 5000 km;
2. ECC ≤ 0.2;
3. A/M ≤ 1 m^2/kg.

However, the use of LEGO may be inappropriate even at low eccentricities (below 0.2), and close to GEO, for specific studies requiring a high fidelity modeling of the eccentricity vector evolution.

3. NAVIGATIONAL SPACECRAFT ORBITS

3.1 Long-Term Evolution of Objects Abandoned in a GPS Orbit

The aim of the analysis was to compare the long-term trajectory evolution predicted by LOP[3] and SATRAP for objects abandoned in a GPS orbit. The reference orbit adopted as initial conditions for the runs is given in Table 3.1. The time span of the simulations was 100 years and area-to-mass ratios of 0.05, 1 and 10 m^2/kg were considered, in order to include both satellites with large solar arrays and high A/M fragments.

Table 3.1

Reference GPS Orbit (Initial Conditions)

Epoch	2005.07.12 07:06:39.28 UTC
Orbital Elements	Mean Keplerian
Earth Centered Reference Frame	True of Date
Semimajor Axis	26559.357 km
Eccentricity	0.0091107
Inclination	54.6752 deg
Right Ascension of Ascending Node	275.8354 deg
Argument of Perigee	107.7453 deg
Mean Anomaly	253.3161 deg

The results of the propagations are summarized in Table 3.2 and in Figures 3.1-3.17. In most situations the agreement between LOP and SATRAP is excellent, and in any case it is more than adequate for the applications and purposes of SDM 4.0.

Table 3.2

GPS Orbit Evolution: LOP vs. SATRAP

Area-to-Mass Ratio (m^2/kg)	Orbital Elements				
	SMA	ECC	INC	RAAN	AP
0.05	≈	=	=	=	=
1	=	=	≈	=	=
10	~	=	≈	≈	=

= excellent agreement *≈ satisfactory agreement* *~ approximate agreement*

[3] In the LOP runs described in this section, ABSERR = RELERR = 10^{-4}.

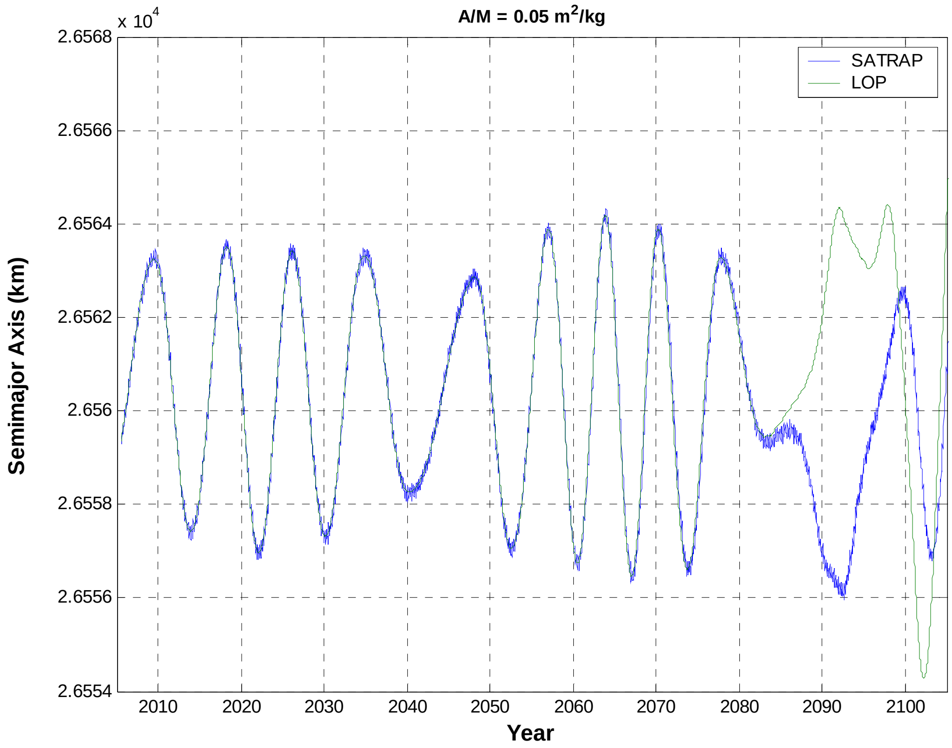
A/M = 0.05 m2/kg
x 10^4
2.6568
2.6566
2.6564
2.6562
2.656
2.6558
2.6556
2.6554
Semimajor Axis (km)
2010
2020
2030
2040
2050
2060
2070
2080
2090
2100
Year
SATRAP
LOP

Fig. 3.1

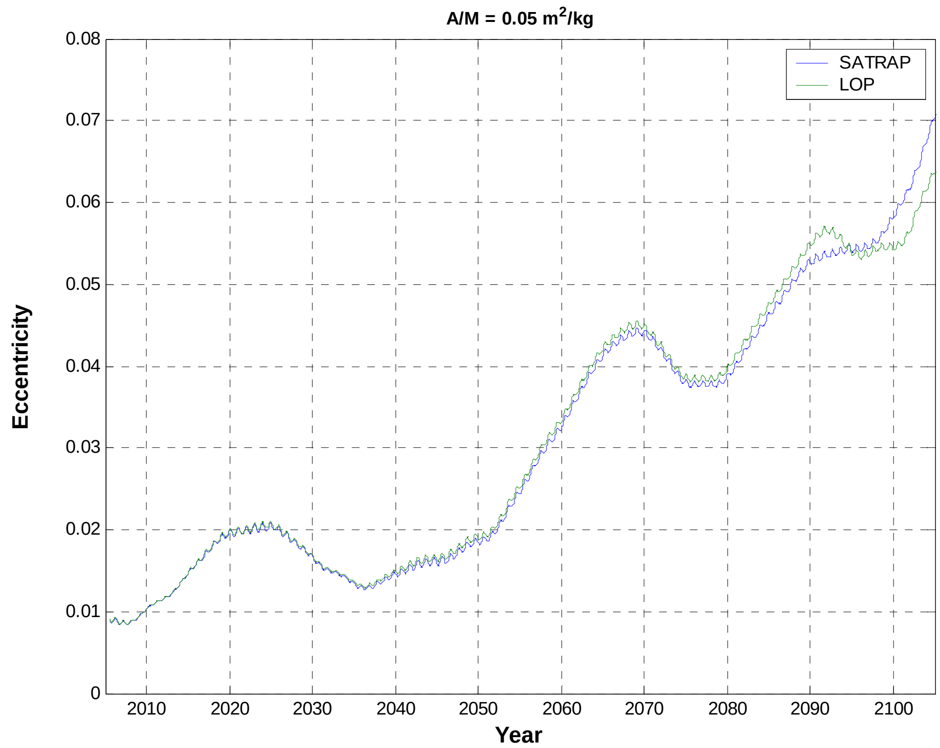
A/M = 0.05 m2/kg
0.08
0.07
0.06
0.05
0.04
0.03
0.02
0.01
0
Eccentricity
2010
2020
2030
2040
2050
2060
2070
2080
2090
2100
Year
SATRAP
LOP

Fig. 3.2

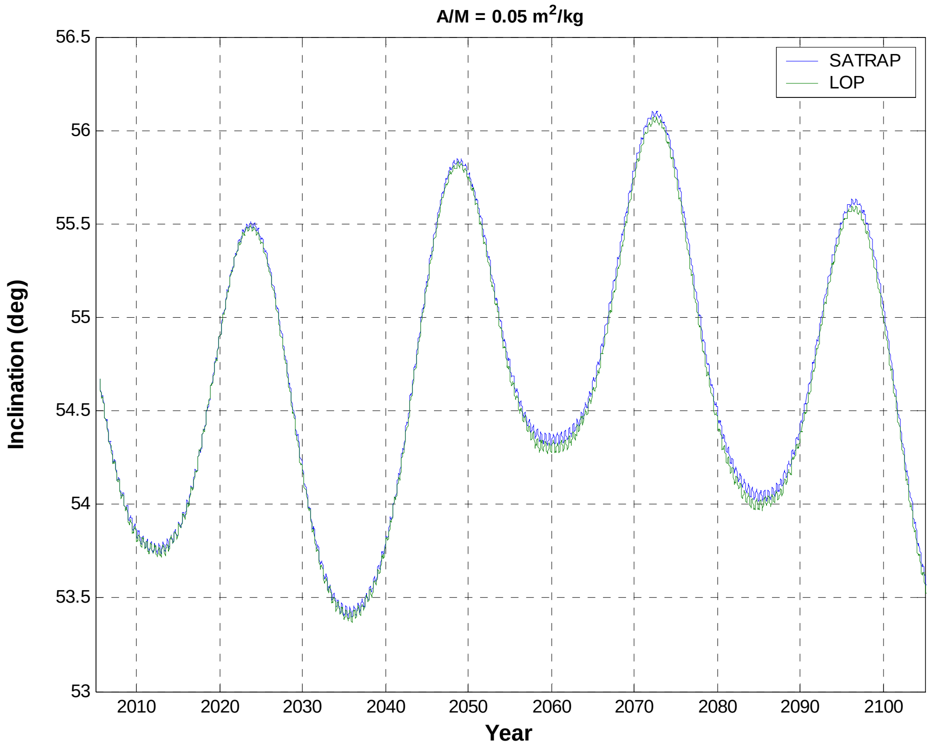
A/M = 0.05 m²/kg
SATRAP
LOP
Inclination (deg)
Year
56.5
56
55.5
55
54.5
54
53.5
53
2010
2020
2030
2040
2050
2060
2070
2080
2090
2100

Fig. 3.3

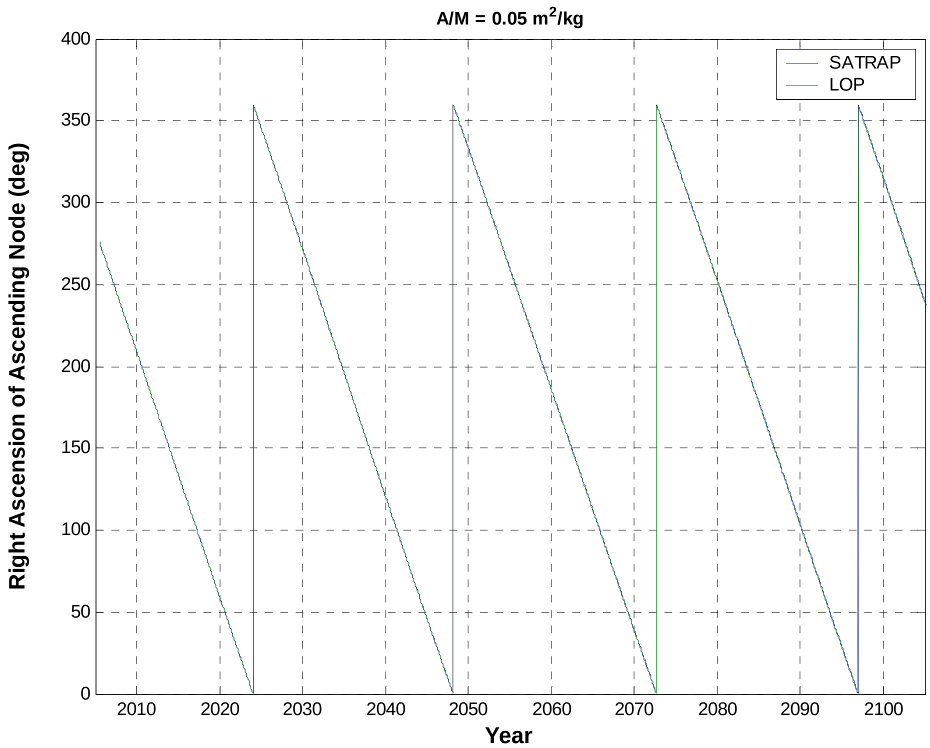
A/M = 0.05 m²/kg
SATRAP
LOP
Right Ascension of Ascending Node (deg)
Year
400
350
300
250
200
150
100
50
0
2010
2020
2030
2040
2050
2060
2070
2080
2090
2100

Fig. 3.4

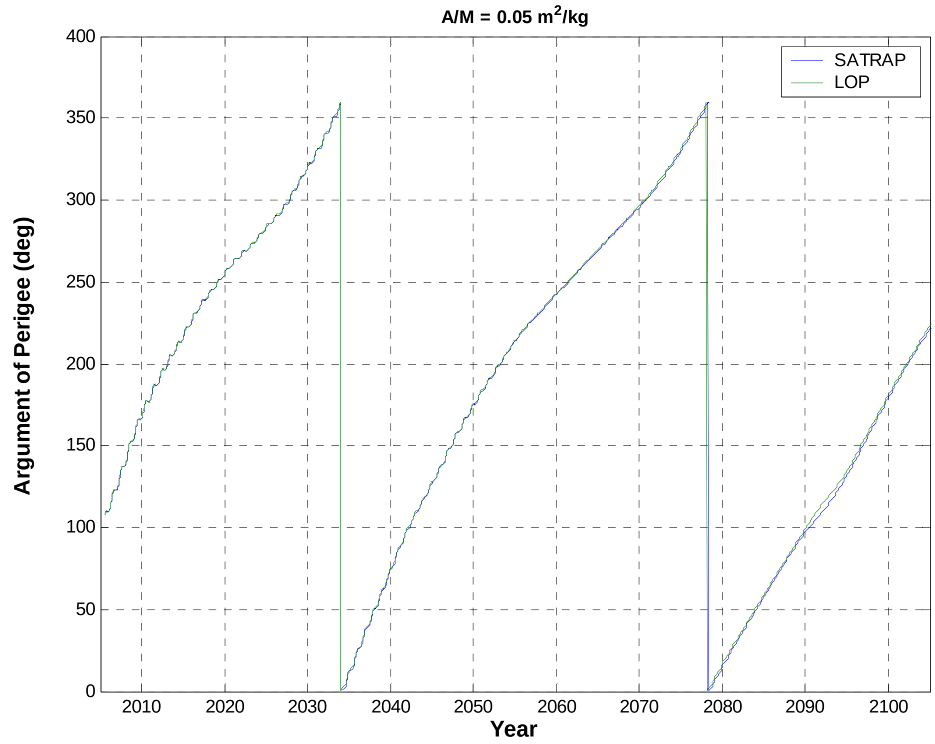
A/M = 0.05 m2/kg
Argument of Perigee (deg)
400
350
300
250
200
150
100
50
0
2010
2020
2030
2040
2050
2060
2070
2080
2090
2100
Year
SATRAP
LOP

Fig. 3.5

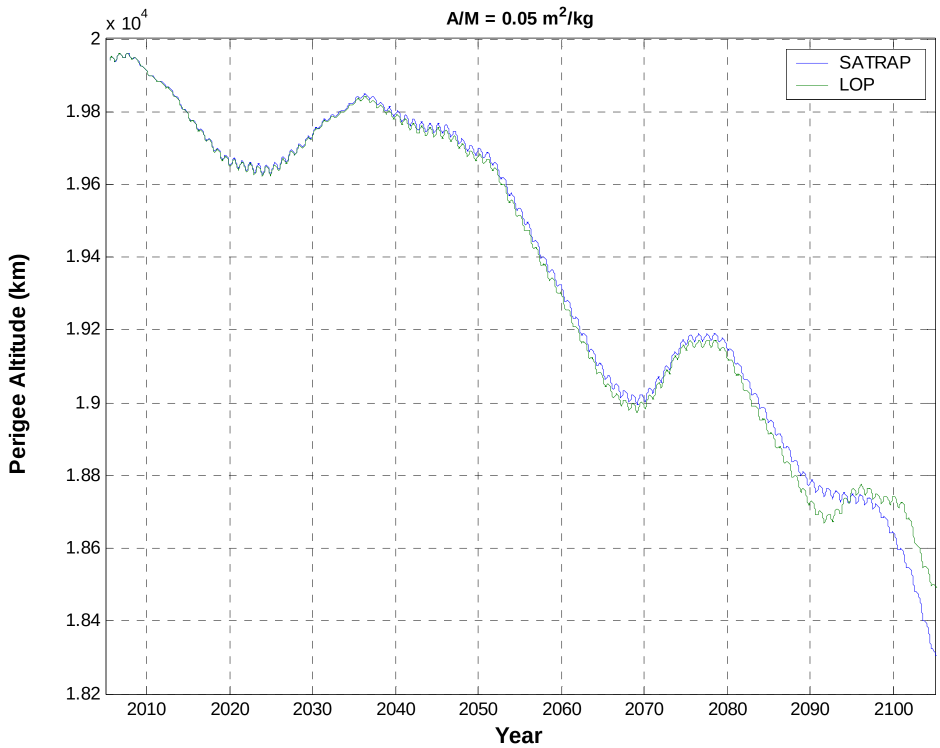
A/M = 0.05 m2/kg
x 10^4
Perigee Altitude (km)
2
1.98
1.96
1.94
1.92
1.9
1.88
1.86
1.84
1.82
2010
2020
2030
2040
2050
2060
2070
2080
2090
2100
Year
SATRAP
LOP

Fig. 3.6

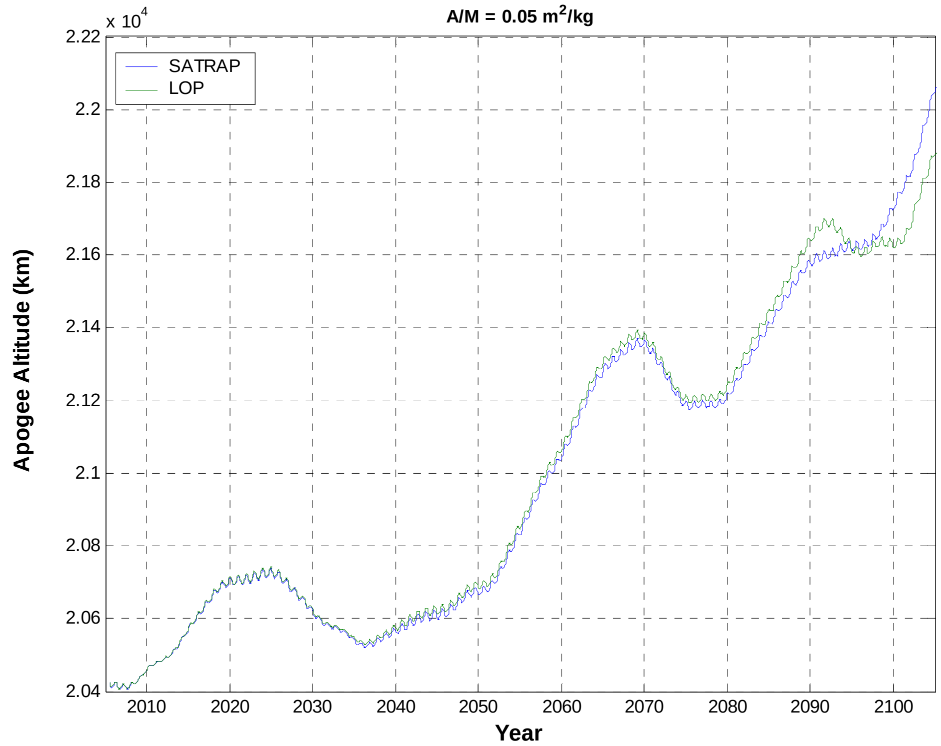
A/M = 0.05 m2/kg
x 10^4
2.22
2.2
2.18
2.16
2.14
2.12
2.1
2.08
2.06
2.04
Apogee Altitude (km)
SATRAP
LOP
2010
2020
2030
2040
2050
2060
2070
2080
2090
2100
Year

Fig. 3.7

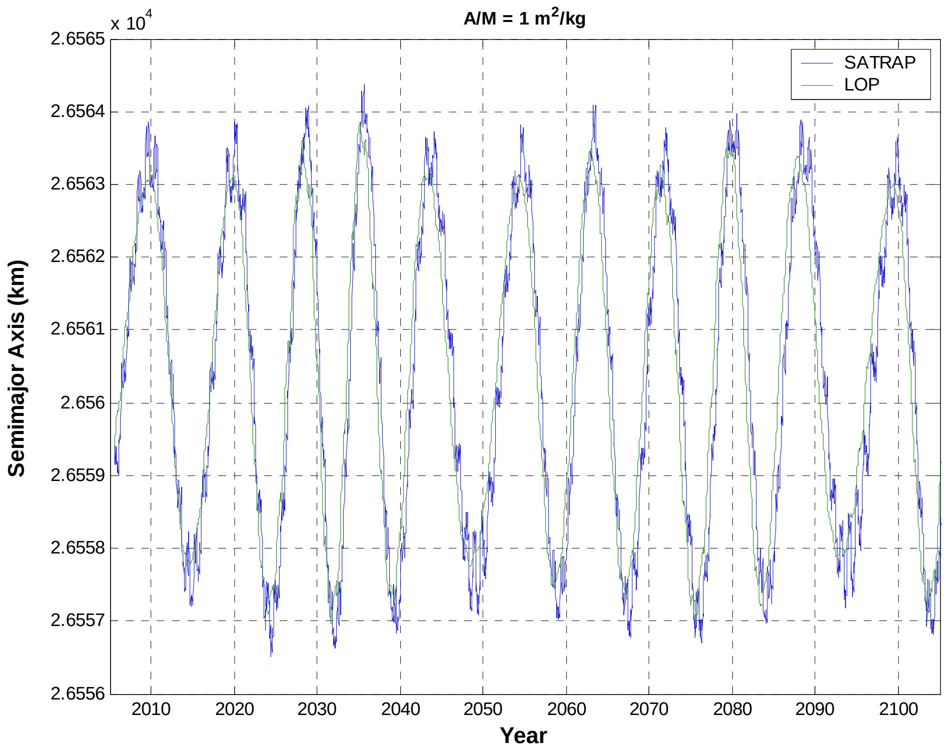
A/M = 1 m2/kg
x 10^4
2.6565
2.6564
2.6563
2.6562
2.6561
2.656
2.6559
2.6558
2.6557
2.6556
Semimajor Axis (km)
SATRAP
LOP
2010
2020
2030
2040
2050
2060
2070
2080
2090
2100
Year

Fig. 3.8

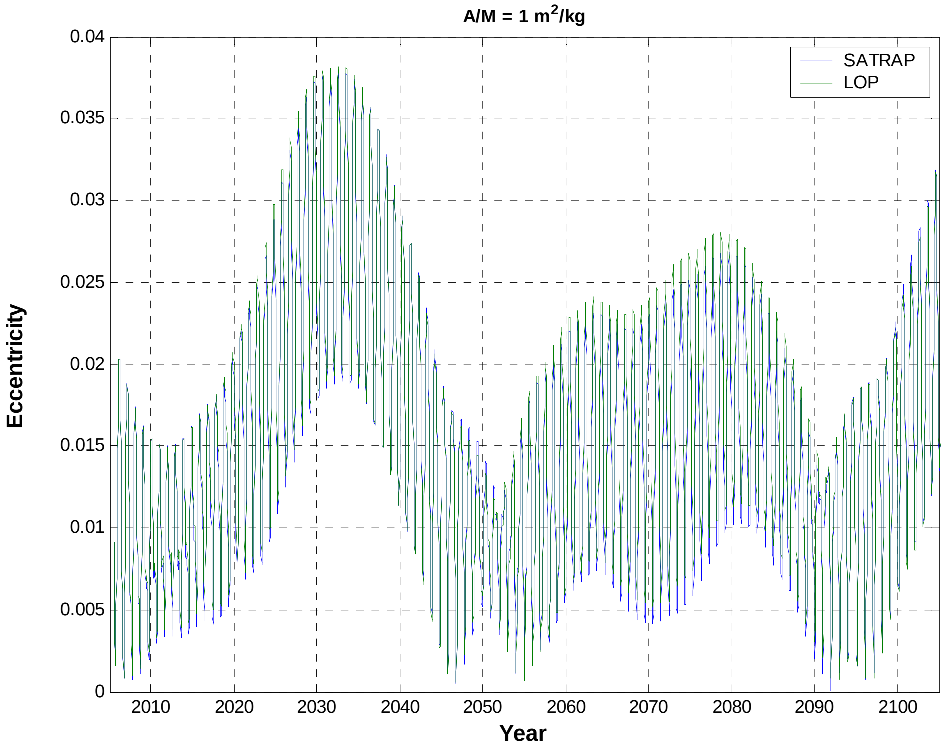

Fig. 3.9

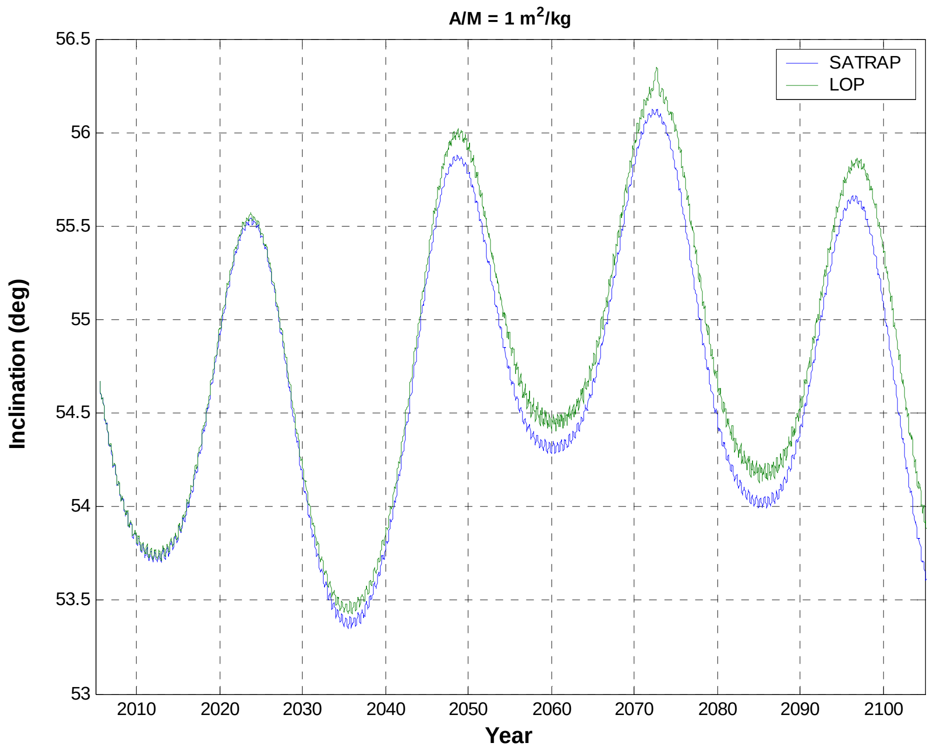

Fig. 3.10

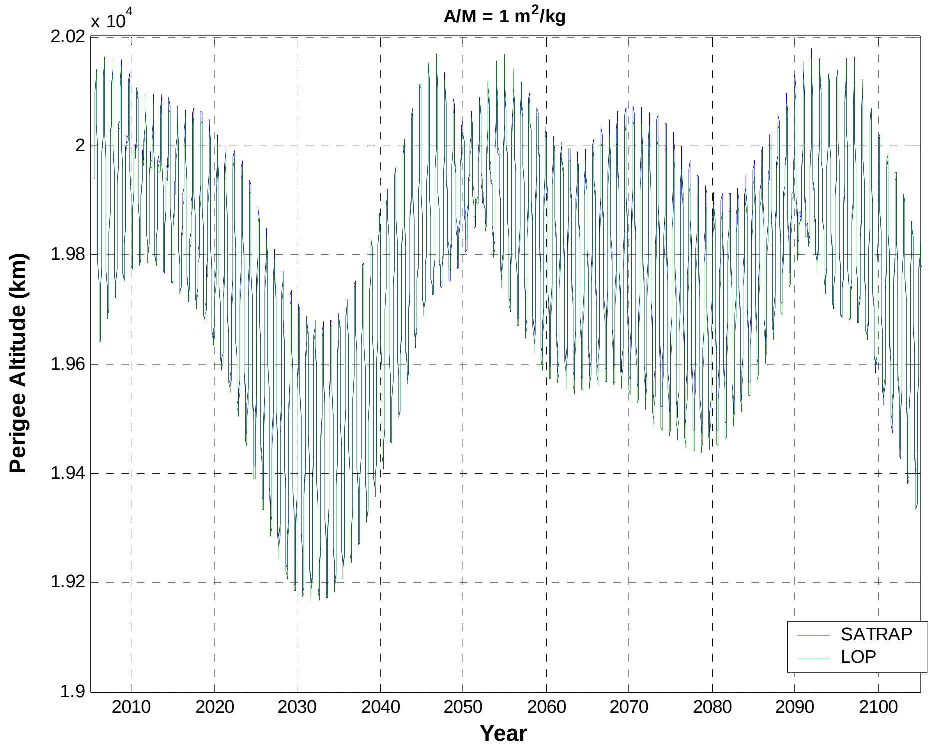

Fig. 3.11

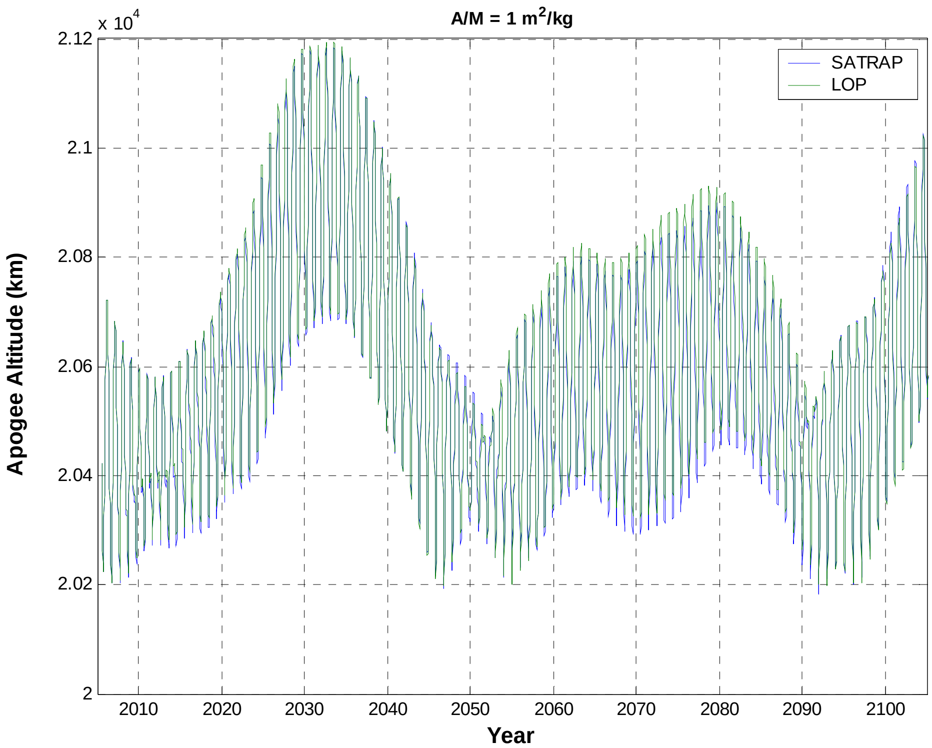

Fig. 3.12

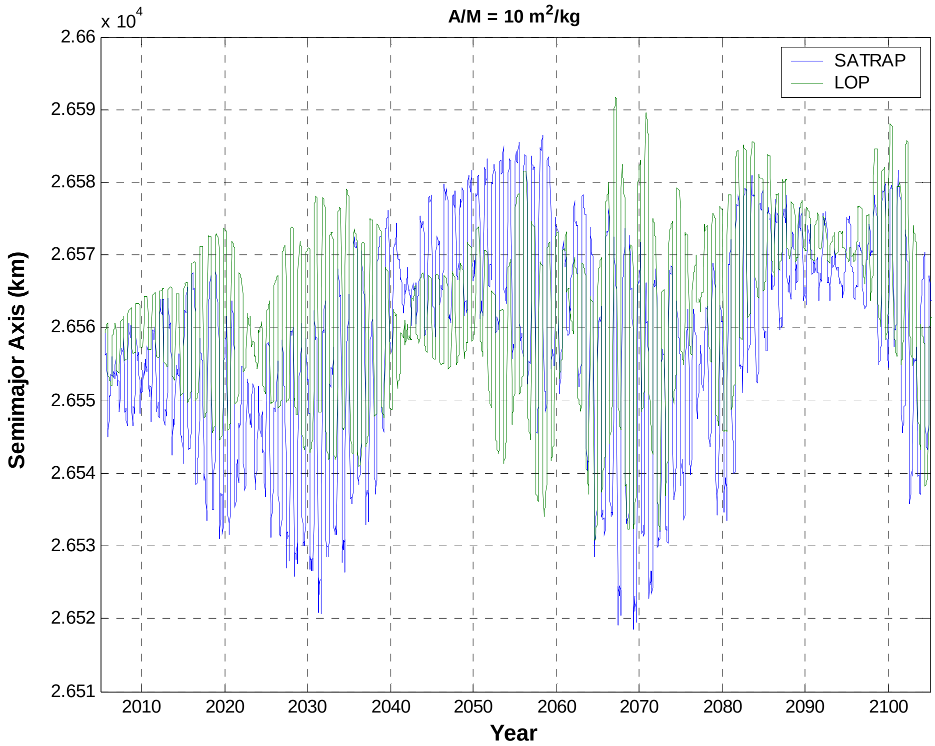

Fig. 3.13

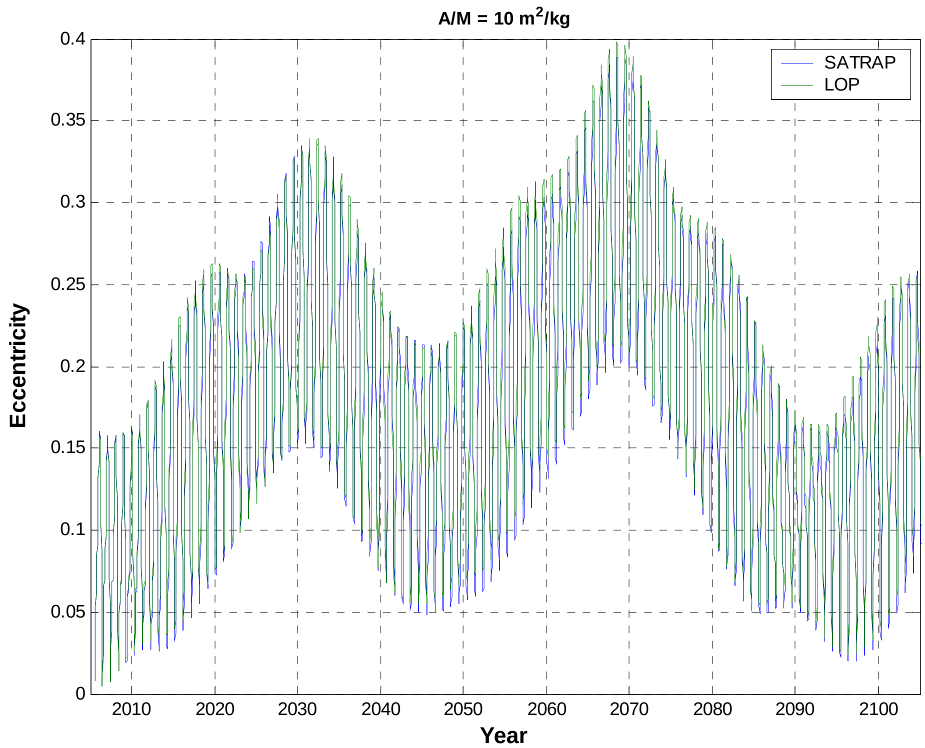

Fig. 3.14

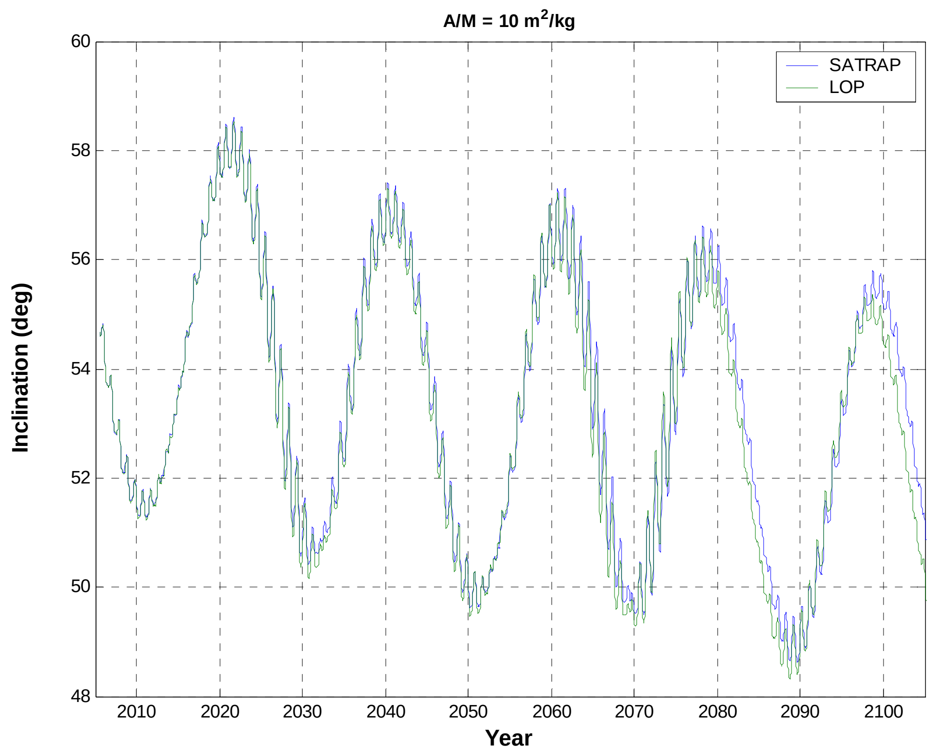

Fig. 3.15

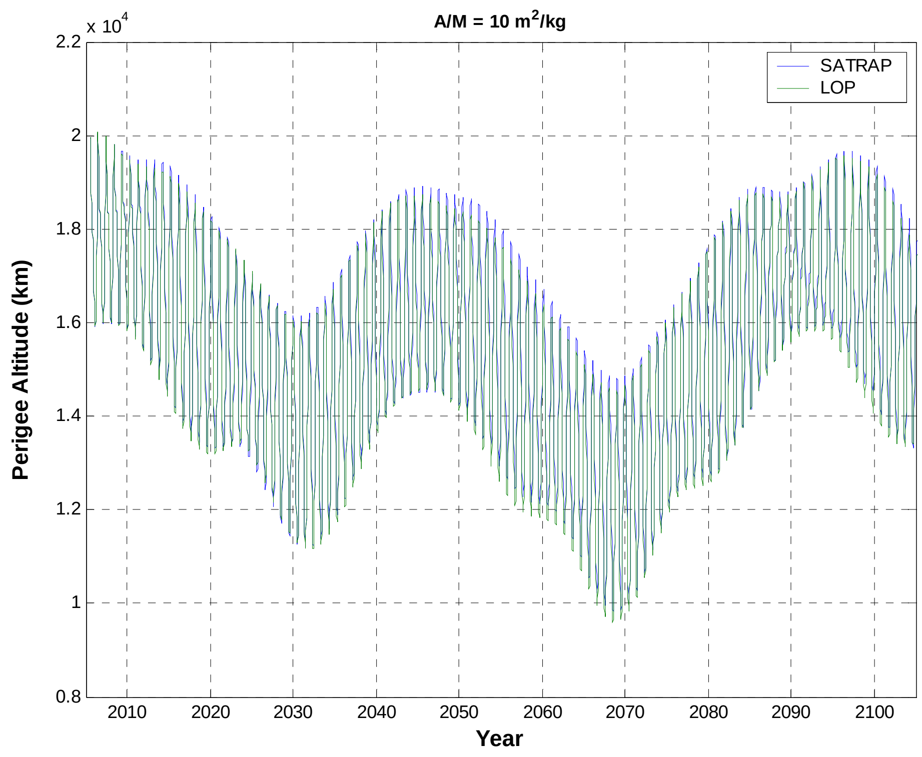

Fig. 3.16

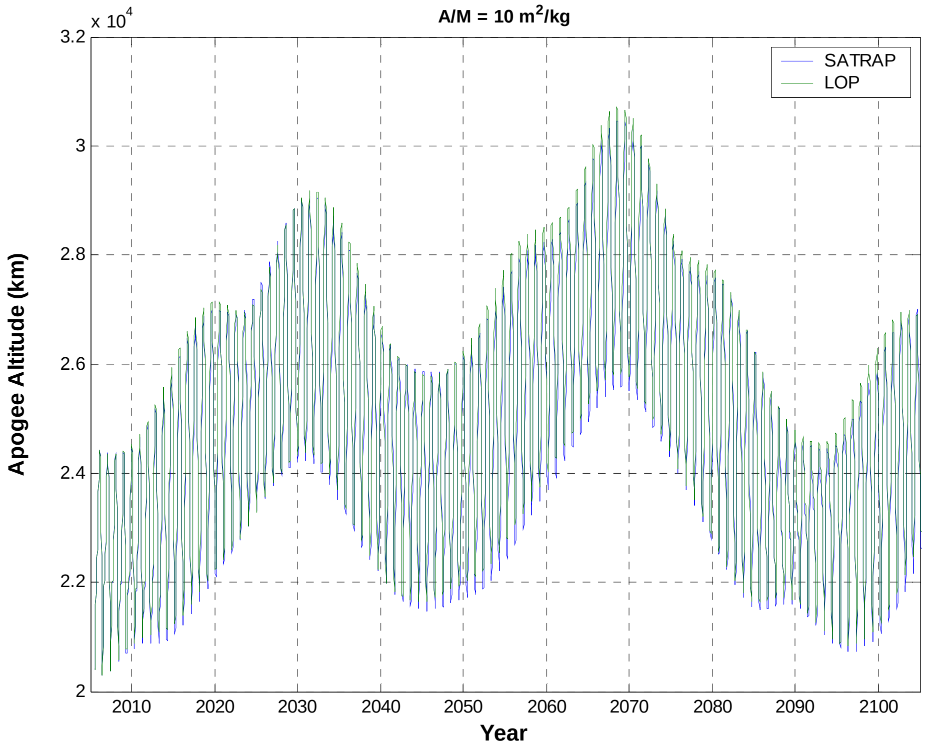
A/M = 10 m2/kg
x 10^4
3.2
3
2.8
2.6
2.4
2.2
2
Apogee Altitude (km)
2010
2020
2030
2040
2050
2060
2070
2080
2090
2100
Year
SATRAP
LOP

Fig. 3.17

4. MOLNIYA ORBITS

4.1 Long-Term Evolution of Objects Abandoned in a Molniya Orbit

The aim of the analysis was to compare the long-term trajectory evolution predicted by LOP[4] and SATRAP for objects abandoned in a Molniya orbit. The reference orbit adopted as initial conditions for the runs is given in Table 4.1. The time span of the simulations was 100 years, or until orbital decay, when applicable, and area-to-mass ratios of 0.05, 1 and 10 m^2/kg were considered, in order to include both satellites with large solar arrays and high A/M fragments.

Table 4.1

Reference Molniya Orbit (Initial Conditions)

Epoch	2005.07.12 18:29:20.47 UTC
Orbital Elements	Mean Keplerian
Earth Centered Reference Frame	True of Date
Semimajor Axis	26558.929 km
Eccentricity	0.6982377
Inclination	63.6525 deg
Right Ascension of Ascending Node	96.6475 deg
Argument of Perigee	273.7710 deg
Mean Anomaly	15.7838 deg

The results of the propagations are summarized in Table 4.2 and in Figures 4.1-4.15. For A/M = 0.05 and 10 m^2/kg, the latter case being characterized by an orbital lifetime of about 200 days, the agreement between LOP and SATRAP is more than satisfactory.

Table 4.2

Molniya Orbit Evolution: LOP vs. SATRAP

Area-to-Mass Ratio (m^2/kg)	**Orbital Elements**				
	SMA	**ECC**	**INC**	**RAAN**	**AP**
0.05	≈/~	=/≈	=/≈	=/≈	=/≈
1	=/≈/~/≠	=/≈	=/≈	=/≈/~	=/≈
10	=	=	≈	=	=

= excellent agreement *≈ satisfactory agreement* *~ approximate agreement*
≠ disagreement

[4] In the LOP runs described in this section, ABSERR = RELERR = 10^{-4}.

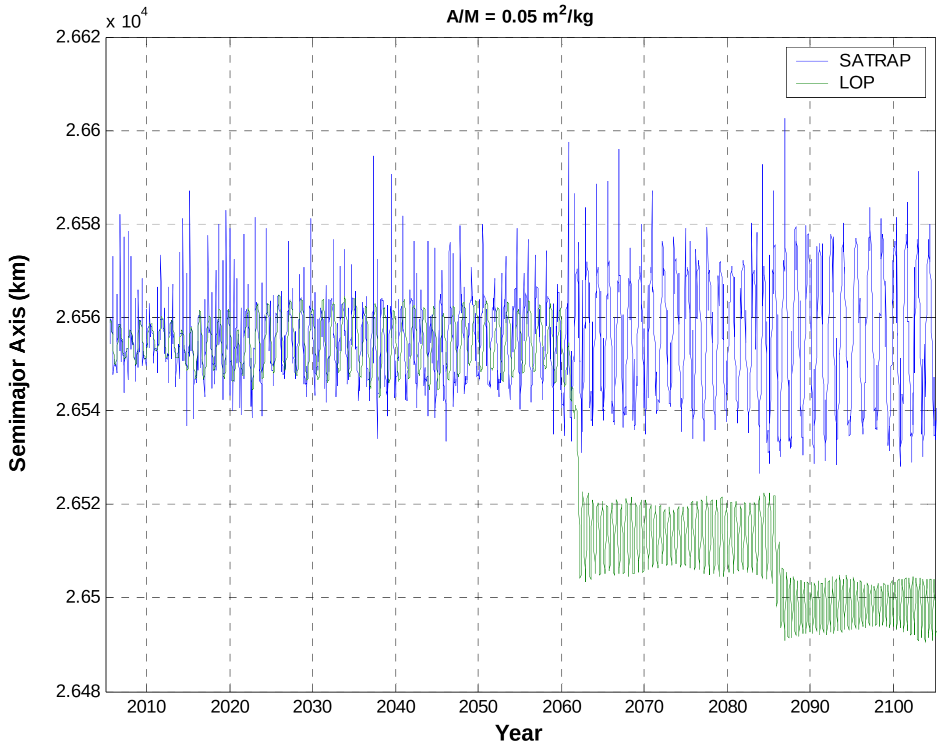
A/M = 0.05 m²/kg
x 10⁴
2.662
2.66
2.658
2.656
2.654
2.652
2.65
2.648
Semimajor Axis (km)
SATRAP
LOP
2010
2020
2030
2040
2050
2060
2070
2080
2090
2100
Year

Fig. 4.1

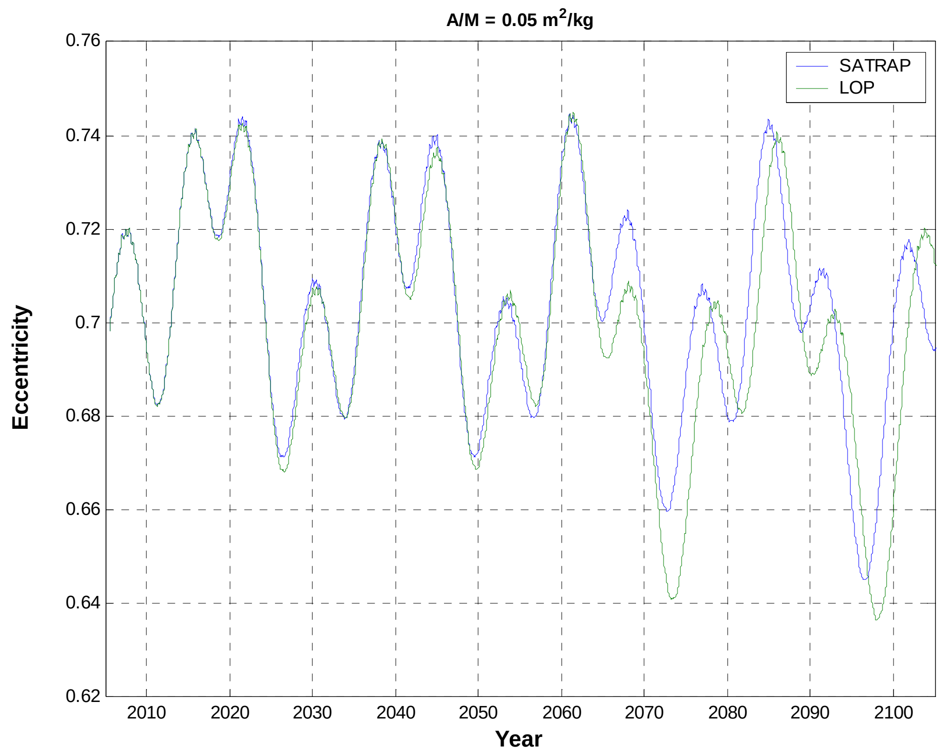
A/M = 0.05 m²/kg
0.76
0.74
0.72
0.7
0.68
0.66
0.64
0.62
Eccentricity
SATRAP
LOP
2010
2020
2030
2040
2050
2060
2070
2080
2090
2100
Year

Fig. 4.2

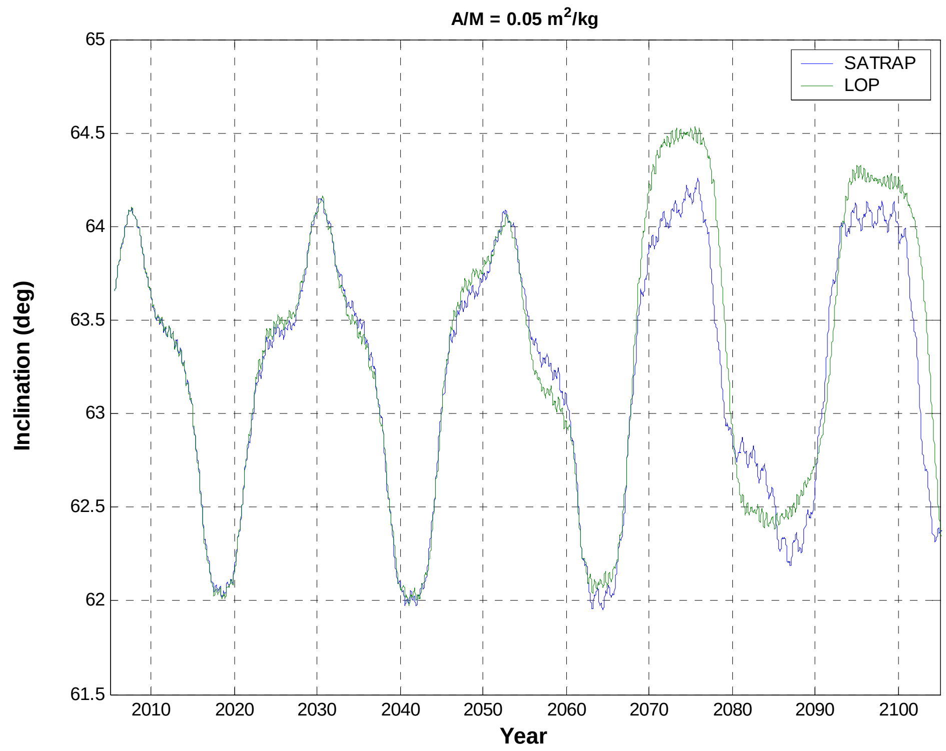
A/M = 0.05 m2/kg
SATRAP
LOP
Inclination (deg)
Year
65
64.5
64
63.5
63
62.5
62
61.5
2010
2020
2030
2040
2050
2060
2070
2080
2090
2100

Fig. 4.3

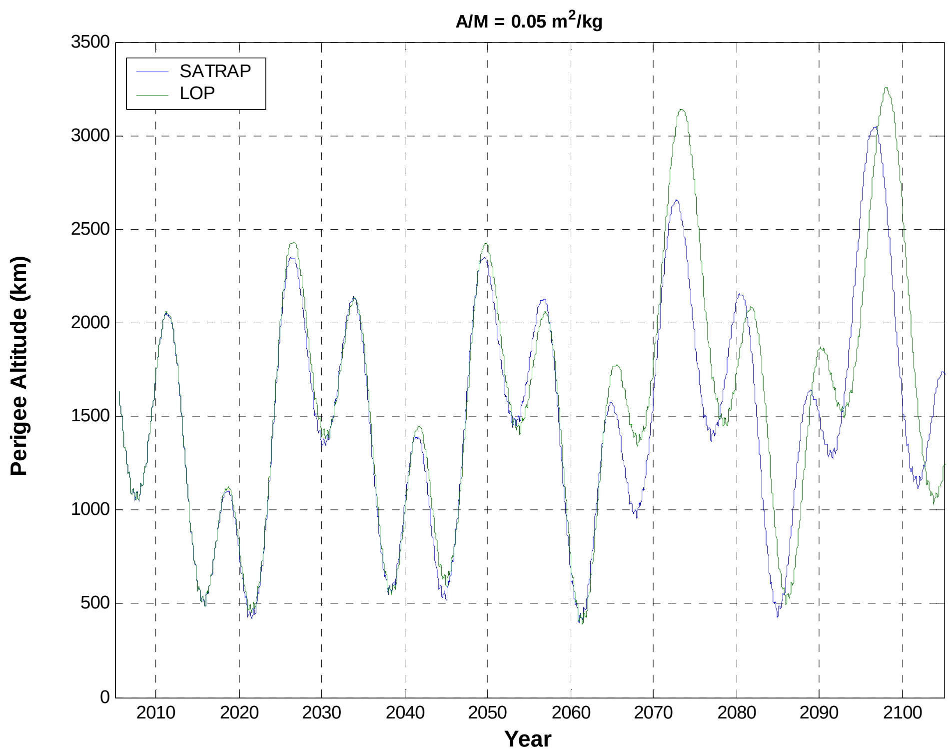
A/M = 0.05 m2/kg
SATRAP
LOP
Perigee Altitude (km)
Year
3500
3000
2500
2000
1500
1000
500
0
2010
2020
2030
2040
2050
2060
2070
2080
2090
2100

Fig. 4.4

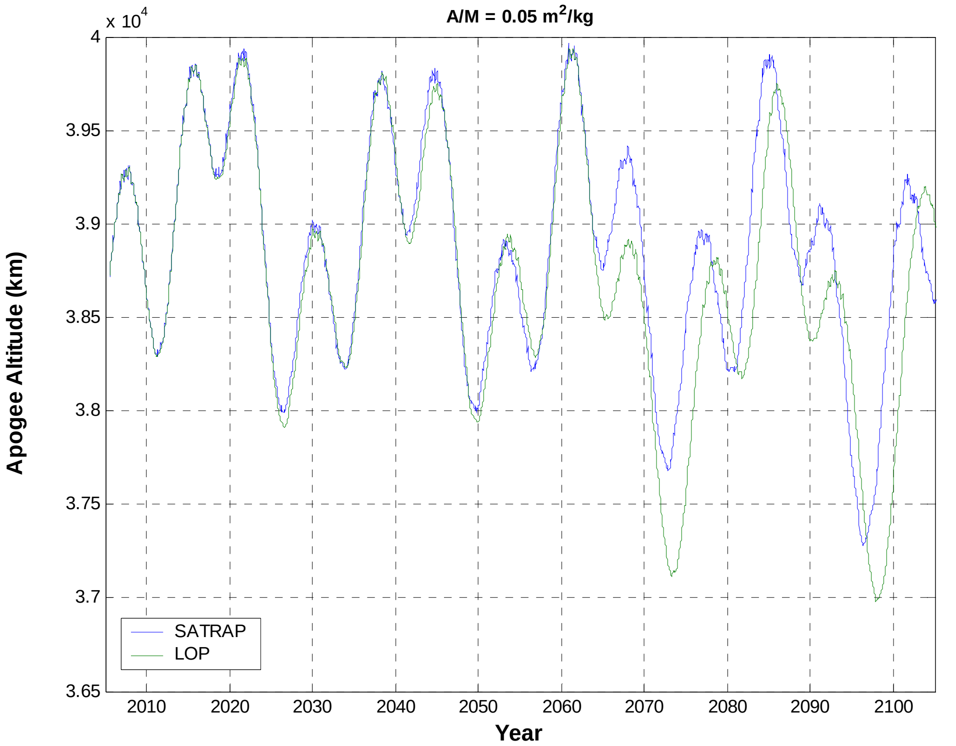
A/M = 0.05 m²/kg
x 10⁴
4
3.95
3.9
3.85
3.8
3.75
3.7
3.65
Apogee Altitude (km)
2010
2020
2030
2040
2050
2060
2070
2080
2090
2100
Year
SATRAP
LOP

Fig. 4.5

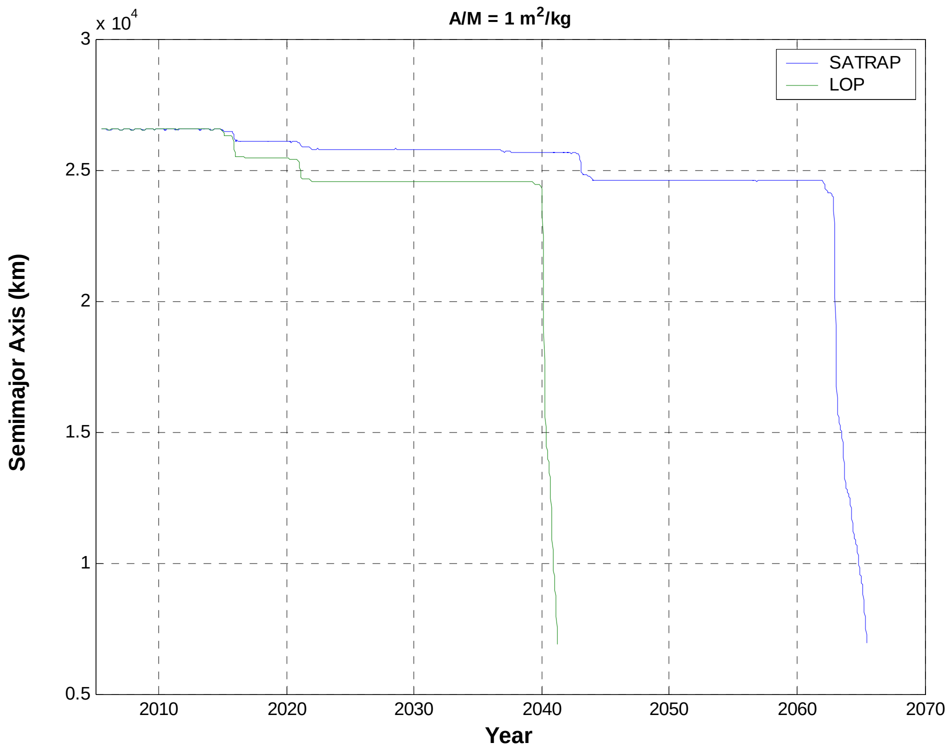
A/M = 1 m²/kg
x 10⁴
3
2.5
2
1.5
1
0.5
Semimajor Axis (km)
2010
2020
2030
2040
2050
2060
2070
Year
SATRAP
LOP

Fig. 4.6

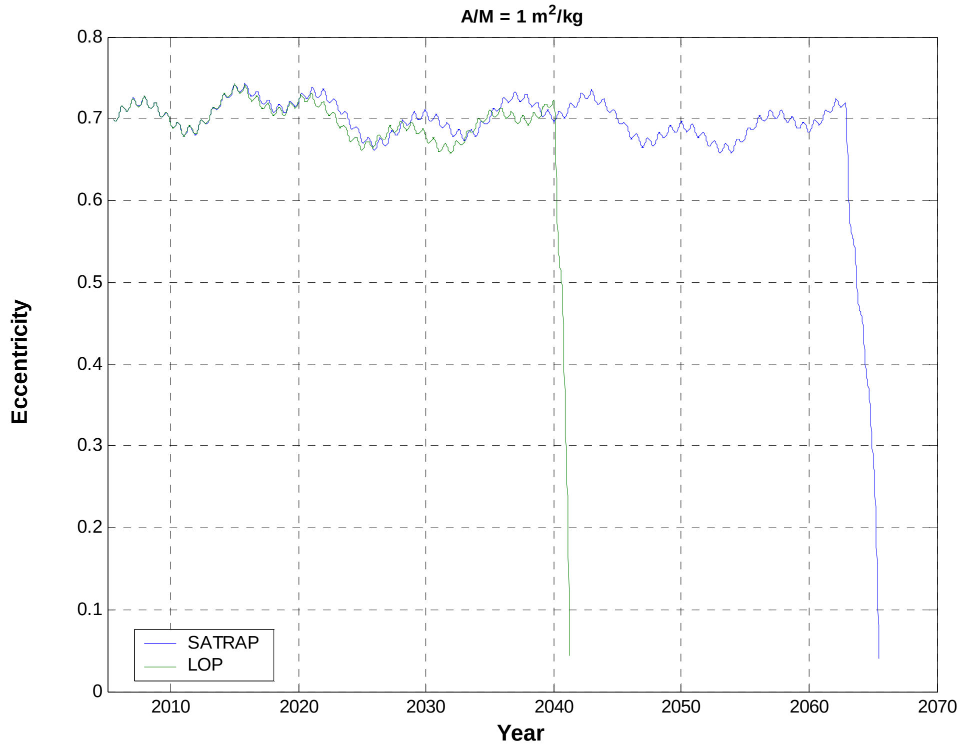
A/M = 1 m2/kg
Eccentricity
0.8
0.7
0.6
0.5
0.4
0.3
0.2
0.1
0
SATRAP
LOP
2010
2020
2030
2040
2050
2060
2070
Year

Fig. 4.7

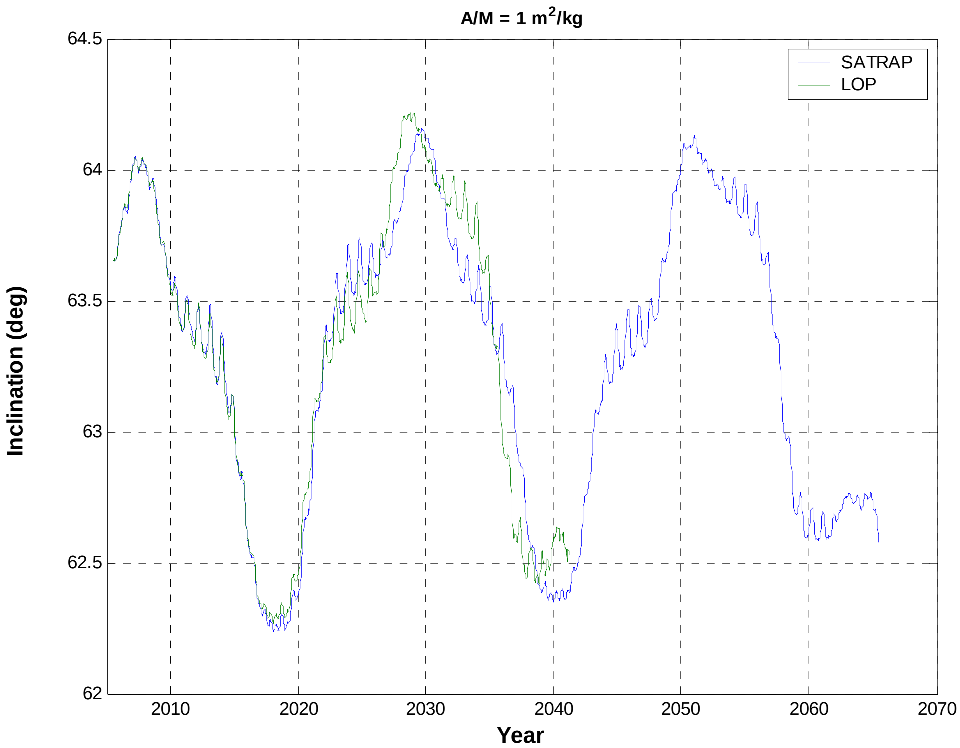
A/M = 1 m2/kg
Inclination (deg)
64.5
64
63.5
63
62.5
62
SATRAP
LOP
2010
2020
2030
2040
2050
2060
2070
Year

Fig. 4.8

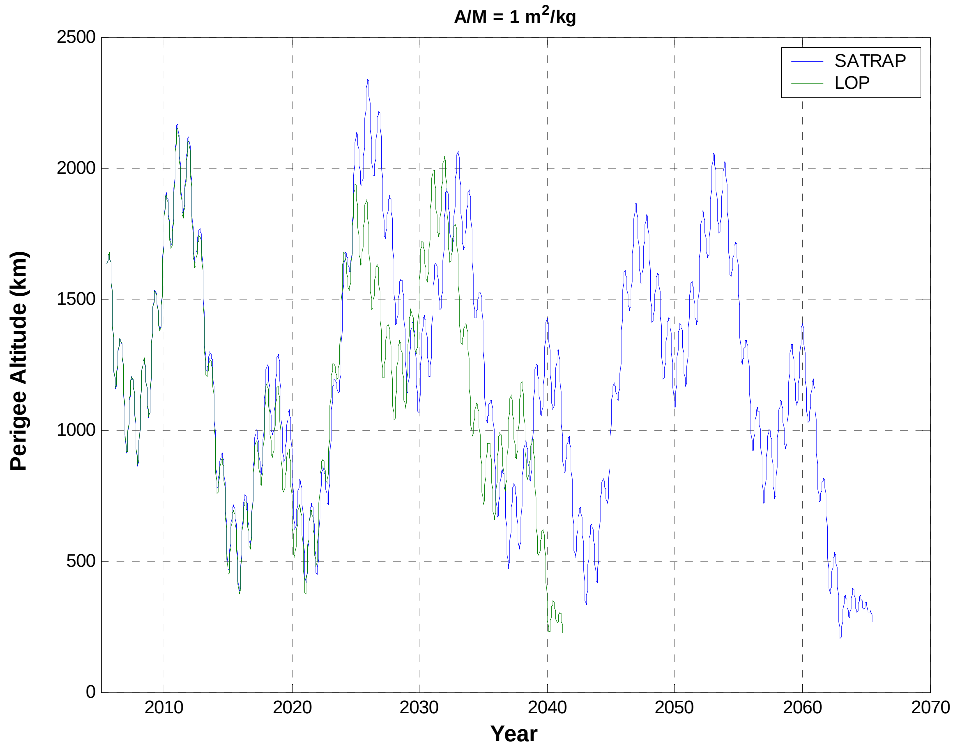

Fig. 4.9

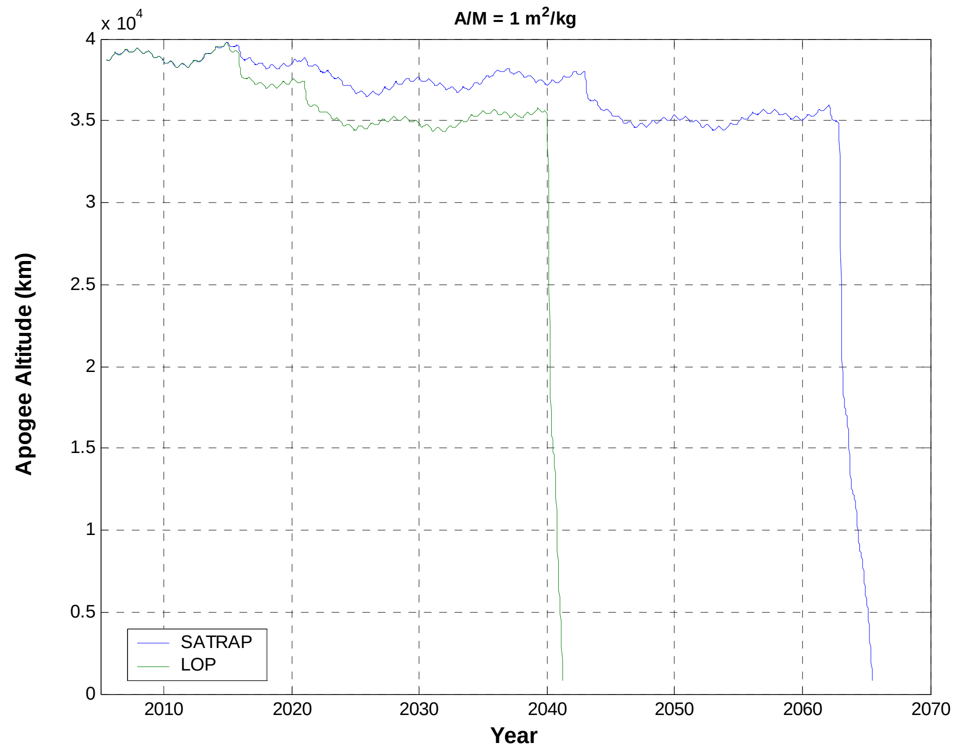

Fig. 4.10

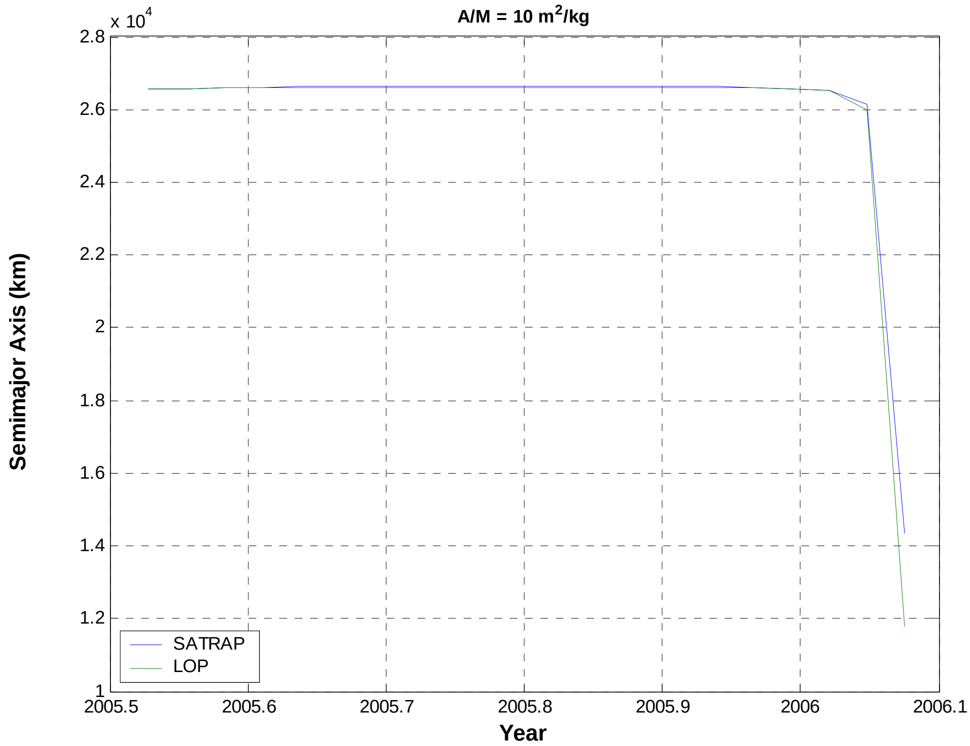

Fig. 4.11

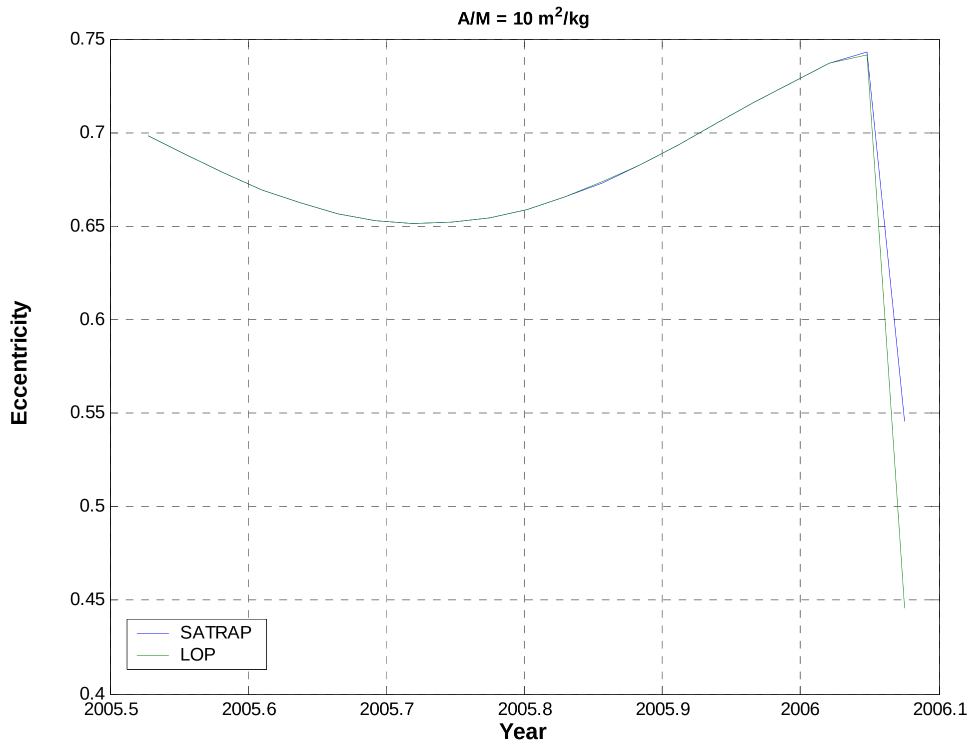

Fig. 4.12

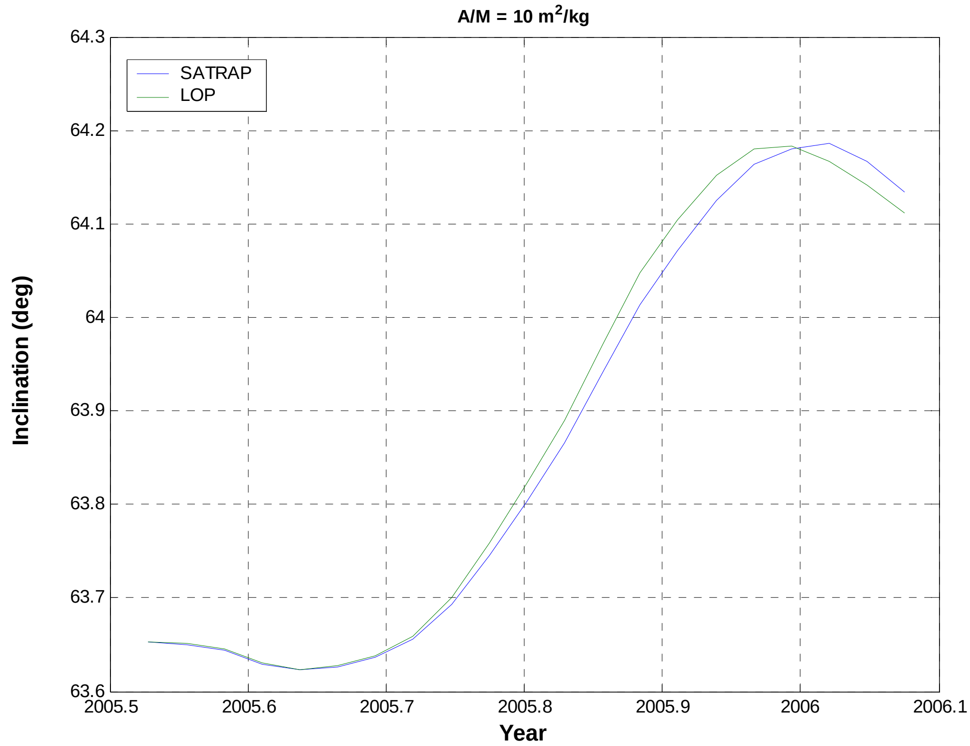

Fig. 4.13

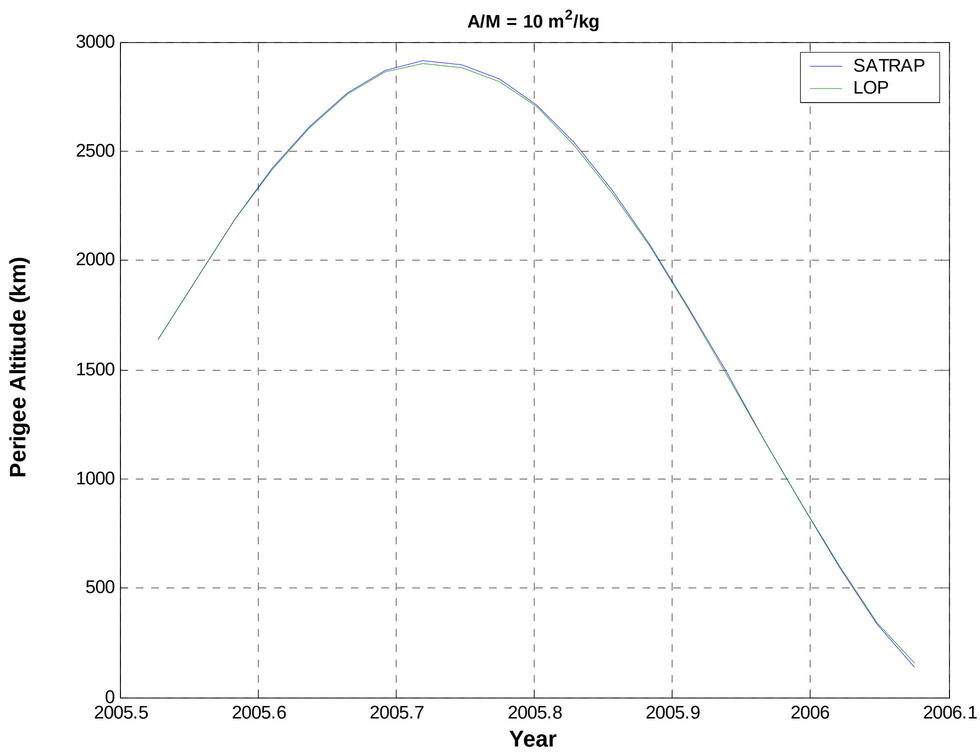

Fig. 4.14

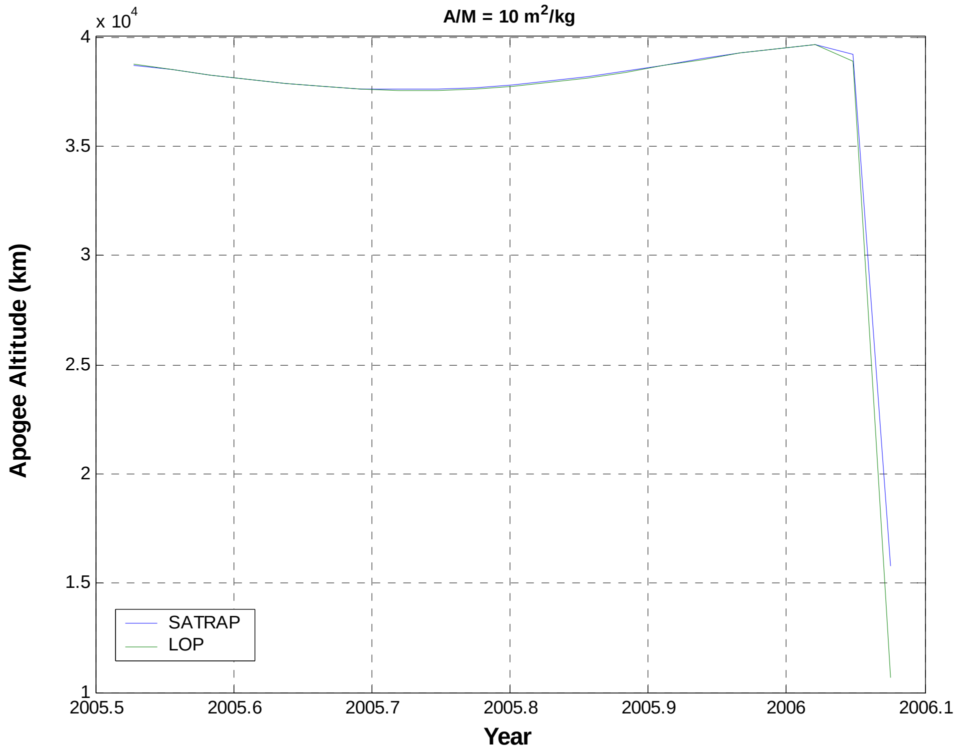

Fig. 4.15

For A/M = 1 m^2/kg, this is true during the first 35 years. There is, in fact, a significant orbital lifetime difference, with object decay after 35 years with LOP and after 60 years with SATRAP. Until the first decay, the two propagators are in reasonable agreement. However, around 2040, the perigee predicted by LOP becomes sufficiently lower in the atmosphere, by just the right amount needed to induce a rapid decrease of the apogee and the consequent orbital decay. Again, a relatively small difference in the orbital elements is amplified by the perturbations, resulting in a macroscopic discrepancy.

5. ARIANE 5 GEO TRANSFER ORBITS

5.1 Long-Term Evolution of Objects Abandoned in an Ariane 5 GTO

The aim of the analysis was to compare the long-term trajectory evolution predicted by LOP[5] and SATRAP for objects abandoned in an Ariane 5 GTO. The reference orbit adopted as initial conditions for the runs is given in Table 5.1. The time span of the simulations was 100 years, or until orbital decay, when applicable, and area-to-mass ratios of 0.05, 1 and 10 m^2/kg were considered.

Table 5.1

Reference Ariane 5 GTO (Initial Conditions)

Epoch	2005.07.13 19:28:41.06 UTC
Orbital Elements	Mean Keplerian
Earth Centered Reference Frame	True of Date
Semimajor Axis	25932.231 km
Eccentricity	0.7289232
Inclination	7.5452 deg
Right Ascension of Ascending Node	3.9417 deg
Argument of Perigee	53.1657 deg
Mean Anomaly	353.7054 deg

The results of the propagations are summarized in Table 5.2 and in Figures 5.1-5.15. For A/M = 0.05 and 10 m^2/kg, the latter case being characterized by an orbital lifetime of about 11 months, the agreement between LOP and SATRAP is more than satisfactory.

Table 5.2

Ariane 5 GTO Evolution: LOP vs. SATRAP

Area-to-Mass Ratio (m^2/kg)	**Orbital Elements**				
	SMA	**ECC**	**INC**	**RAAN**	**AP**
0.05	≈	≈	≈	≈	≈
1	≈/≠	≈	≈	≈	≈
10	≈	=	≈	=	=

= *excellent agreement* ≈ *satisfactory agreement* ~ *approximate agreement*
≠ *disagreement*

[5] In the LOP runs described in this section, ABSERR = RELERR = 10^{-4}.

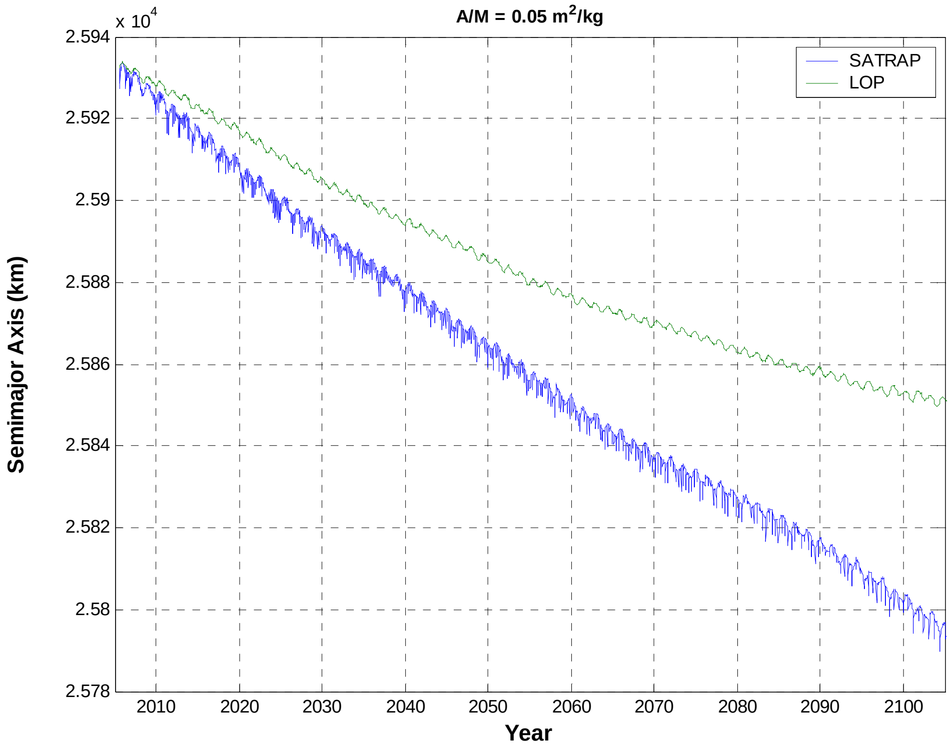
A/M = 0.05 m²/kg
x 10⁴
2.594
2.592
2.59
2.588
2.586
2.584
2.582
2.58
2.578
Semimajor Axis (km)
SATRAP
LOP
2010
2020
2030
2040
2050
2060
2070
2080
2090
2100
Year

Fig. 5.1

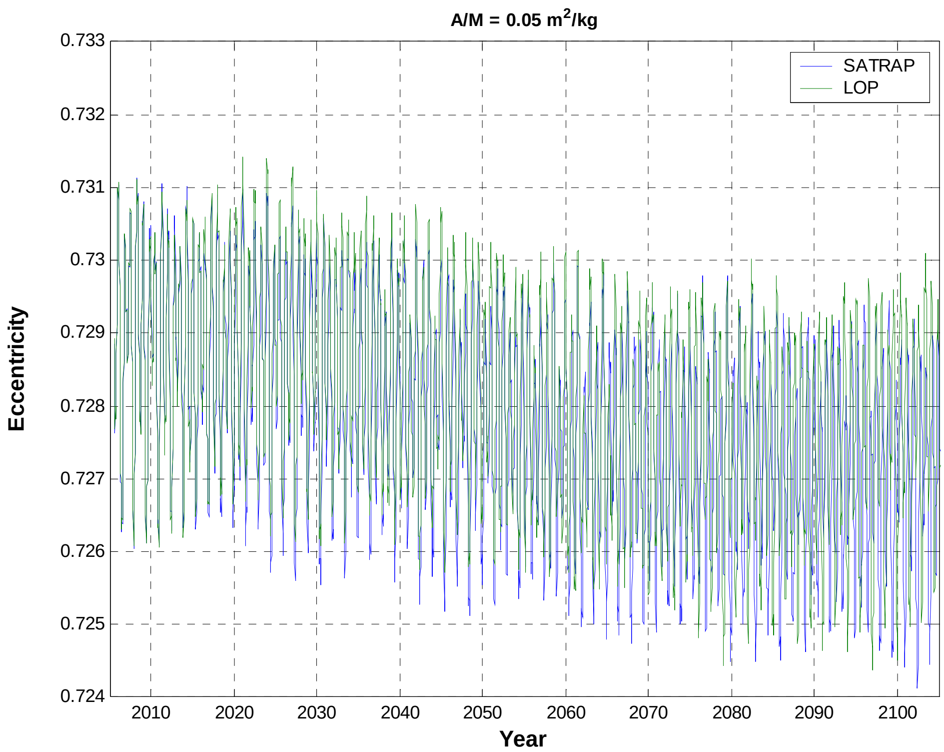
A/M = 0.05 m²/kg
0.733
0.732
0.731
0.73
0.729
0.728
0.727
0.726
0.725
0.724
Eccentricity
SATRAP
LOP
2010
2020
2030
2040
2050
2060
2070
2080
2090
2100
Year

Fig. 5.2

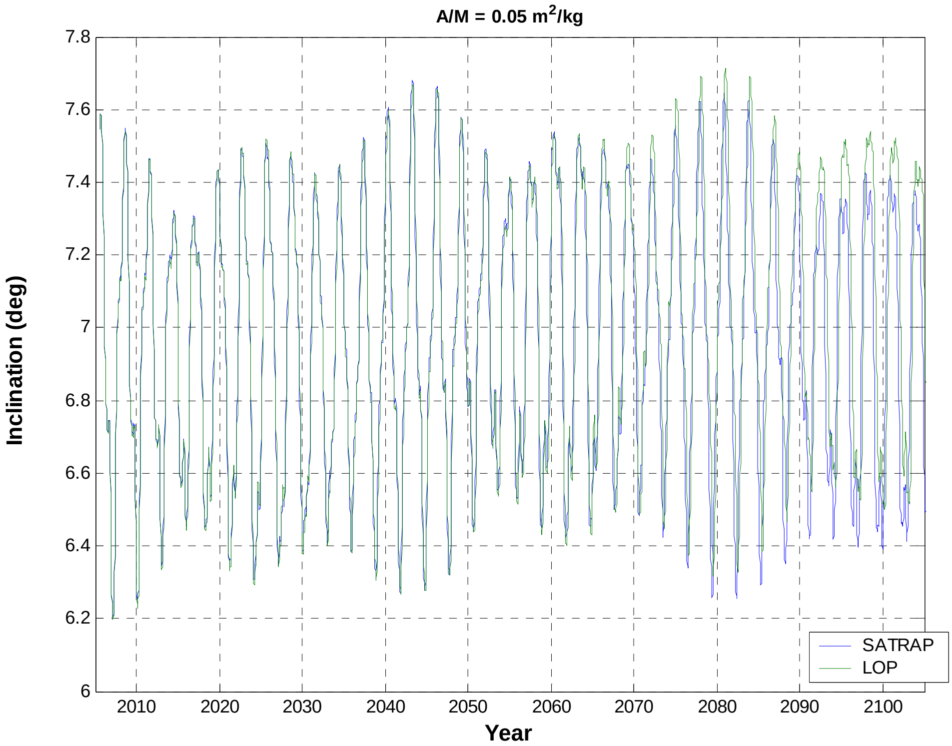
A/M = 0.05 m2/kg
Inclination (deg)
Year
7.8
7.6
7.4
7.2
7
6.8
6.6
6.4
6.2
6
2010
2020
2030
2040
2050
2060
2070
2080
2090
2100
SATRAP
LOP

Fig. 5.3

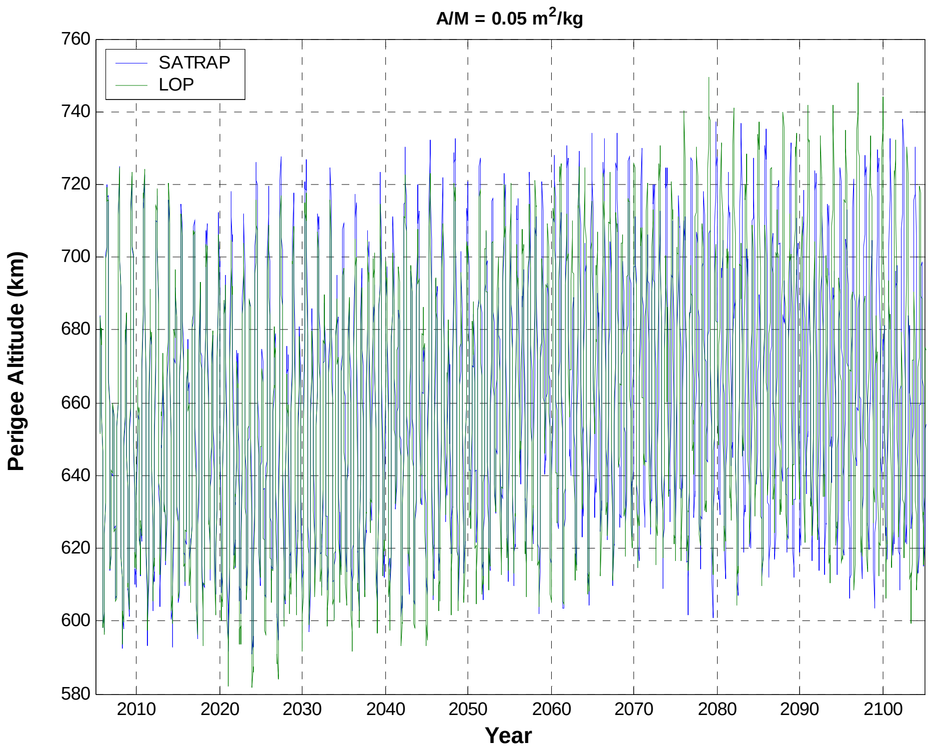
A/M = 0.05 m2/kg
Perigee Altitude (km)
Year
760
740
720
700
680
660
640
620
600
580
2010
2020
2030
2040
2050
2060
2070
2080
2090
2100
SATRAP
LOP

Fig. 5.4

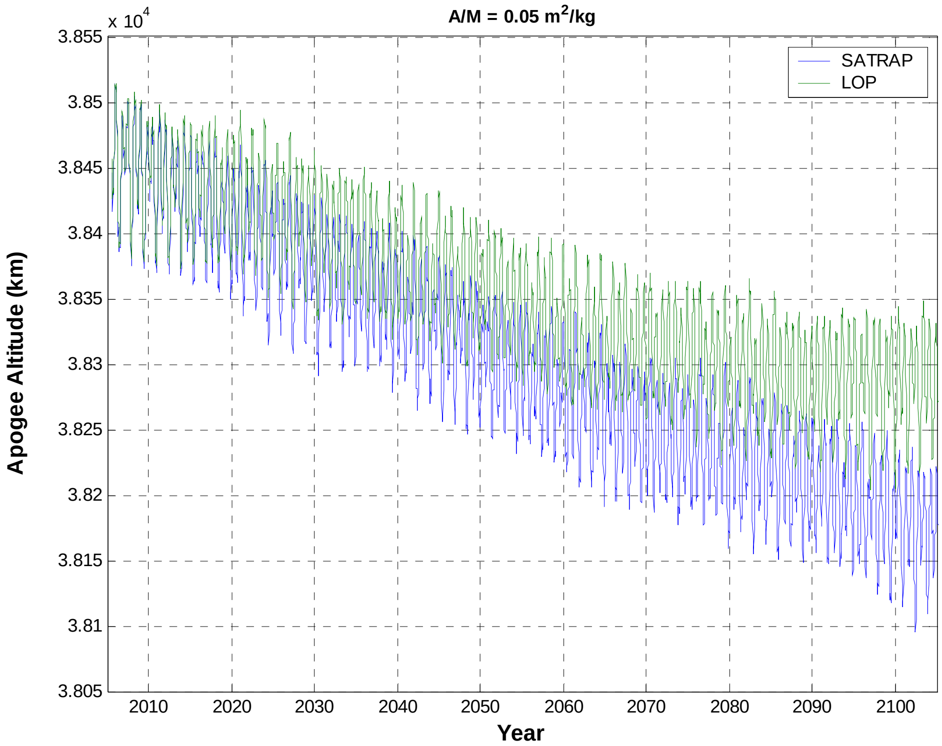
A/M = 0.05 m2/kg
x 10^4
3.855
3.85
3.845
3.84
3.835
3.83
3.825
3.82
3.815
3.81
3.805
Apogee Altitude (km)
2010
2020
2030
2040
2050
2060
2070
2080
2090
2100
Year
SATRAP
LOP

Fig. 5.5

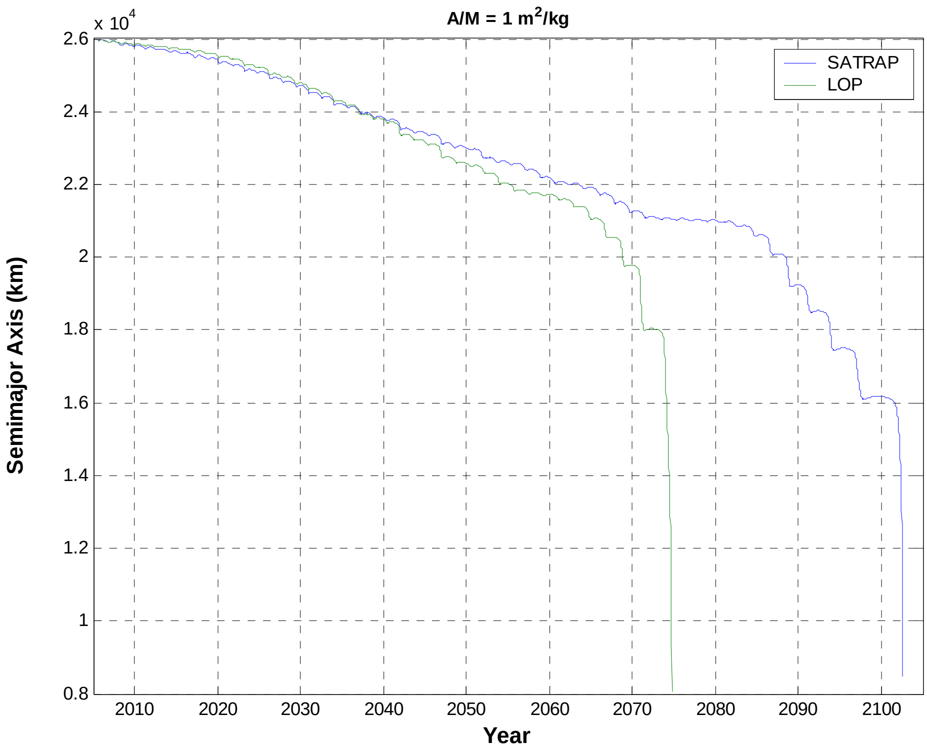
A/M = 1 m2/kg
x 10^4
2.6
2.4
2.2
2
1.8
1.6
1.4
1.2
1
0.8
Semimajor Axis (km)
2010
2020
2030
2040
2050
2060
2070
2080
2090
2100
Year
SATRAP
LOP

Fig. 5.6

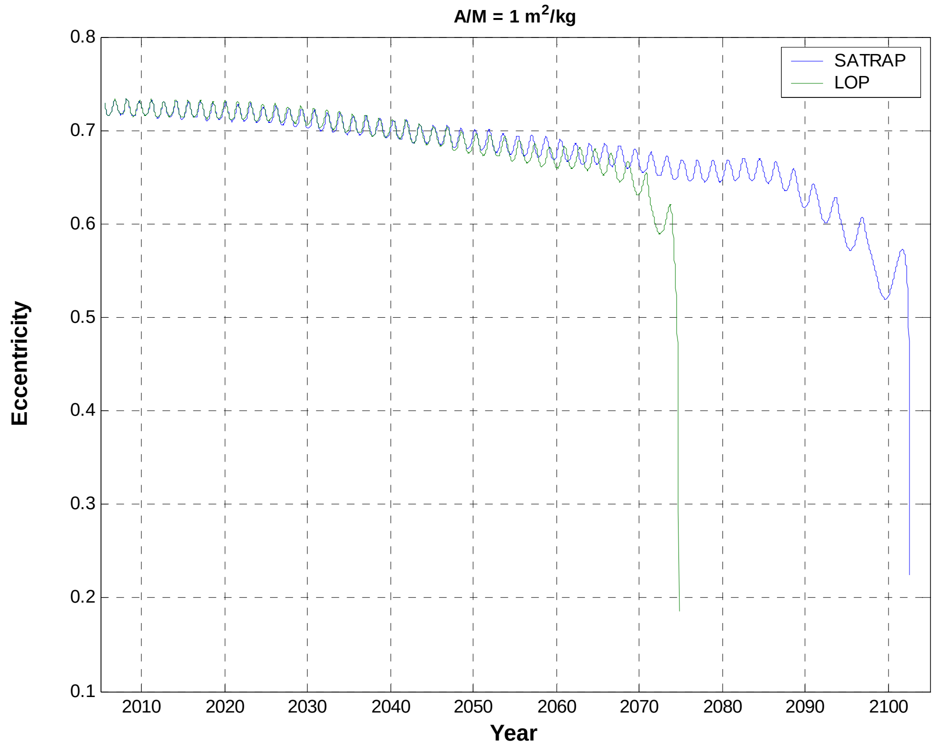
A/M = 1 m²/kg
Eccentricity
Year
SATRAP
LOP
0.8
0.7
0.6
0.5
0.4
0.3
0.2
0.1
2010
2020
2030
2040
2050
2060
2070
2080
2090
2100

Fig. 5.7

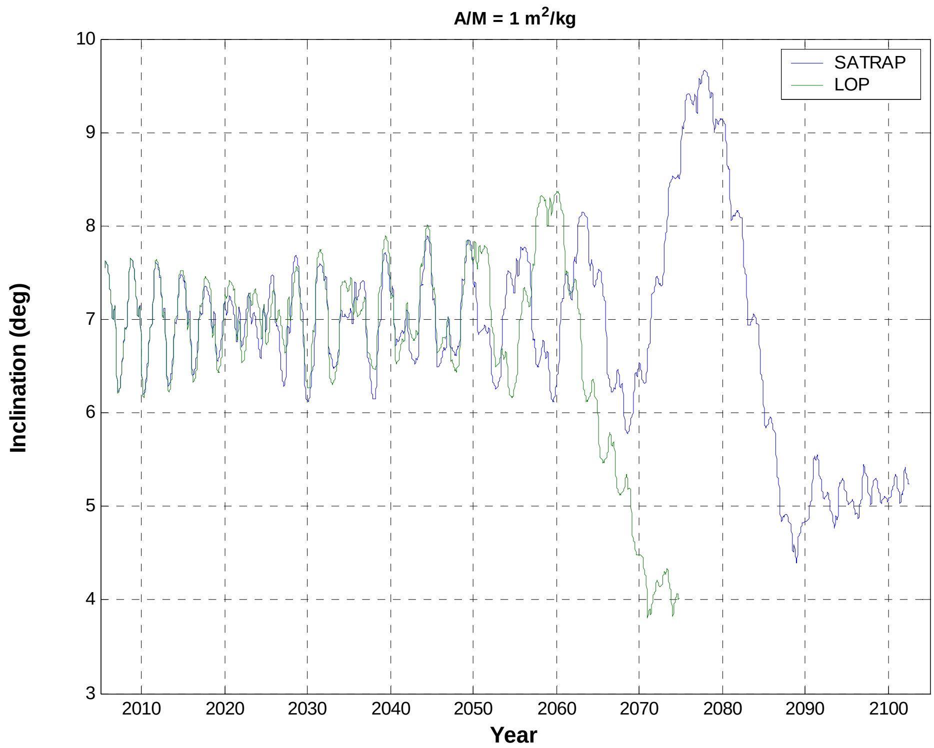
A/M = 1 m²/kg
Inclination (deg)
Year
SATRAP
LOP
10
9
8
7
6
5
4
3
2010
2020
2030
2040
2050
2060
2070
2080
2090
2100

Fig. 5.8

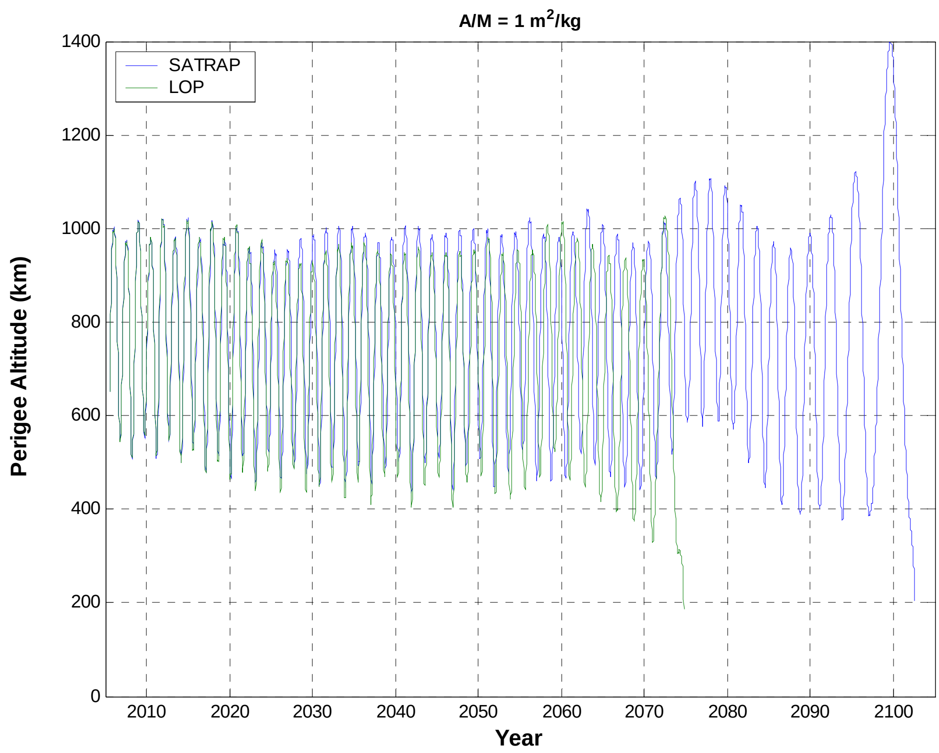

Fig. 5.9

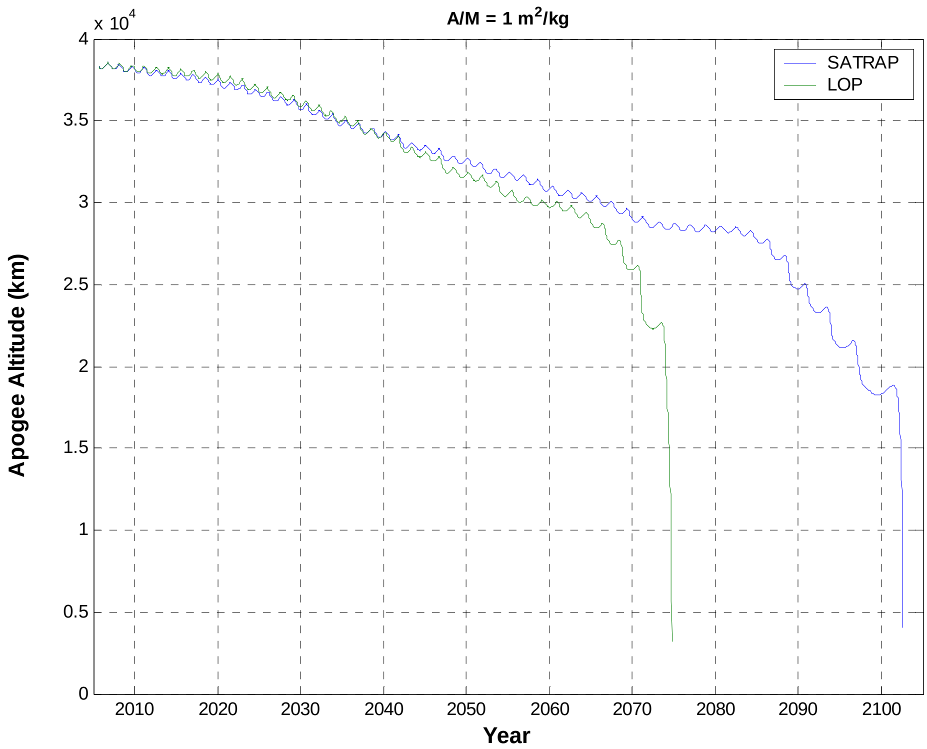

Fig. 5.10

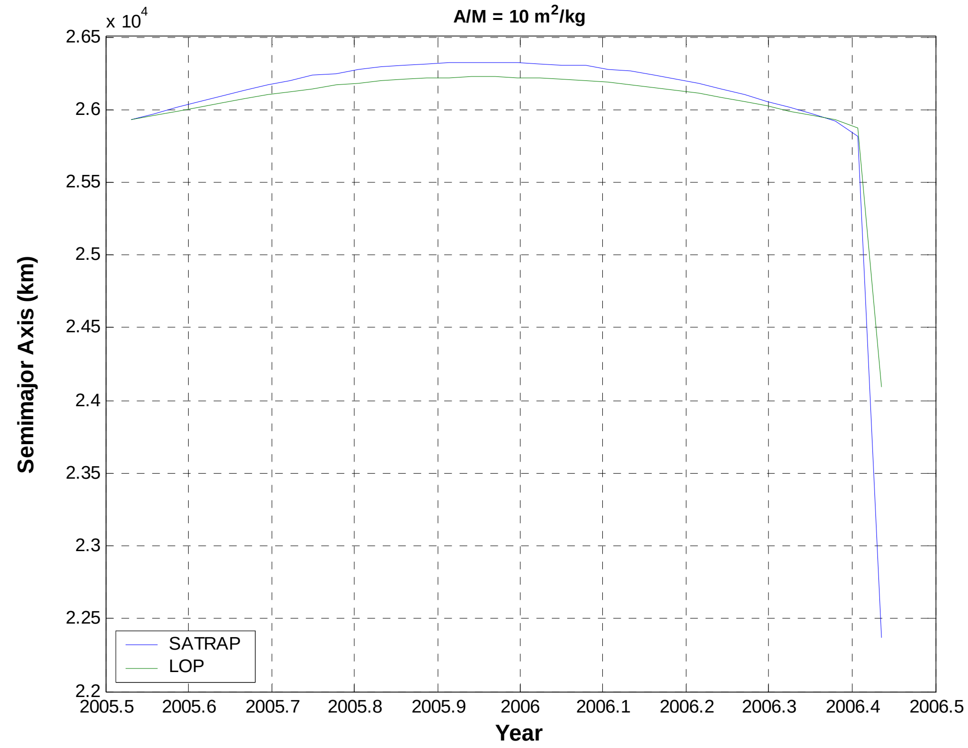

Fig. 5.11

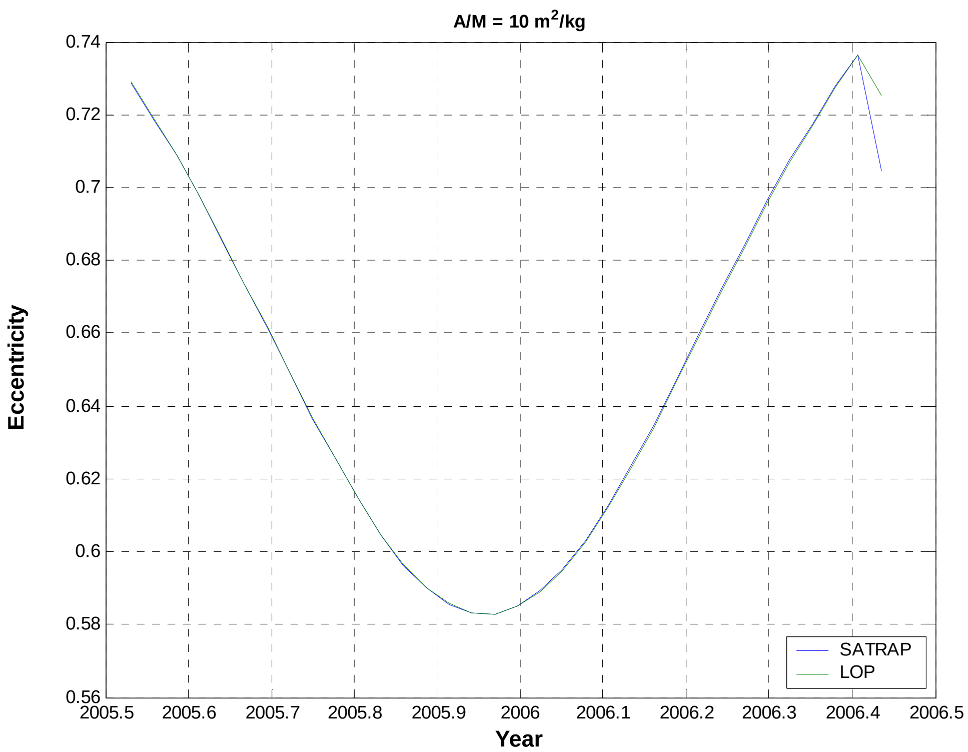

Fig. 5.12

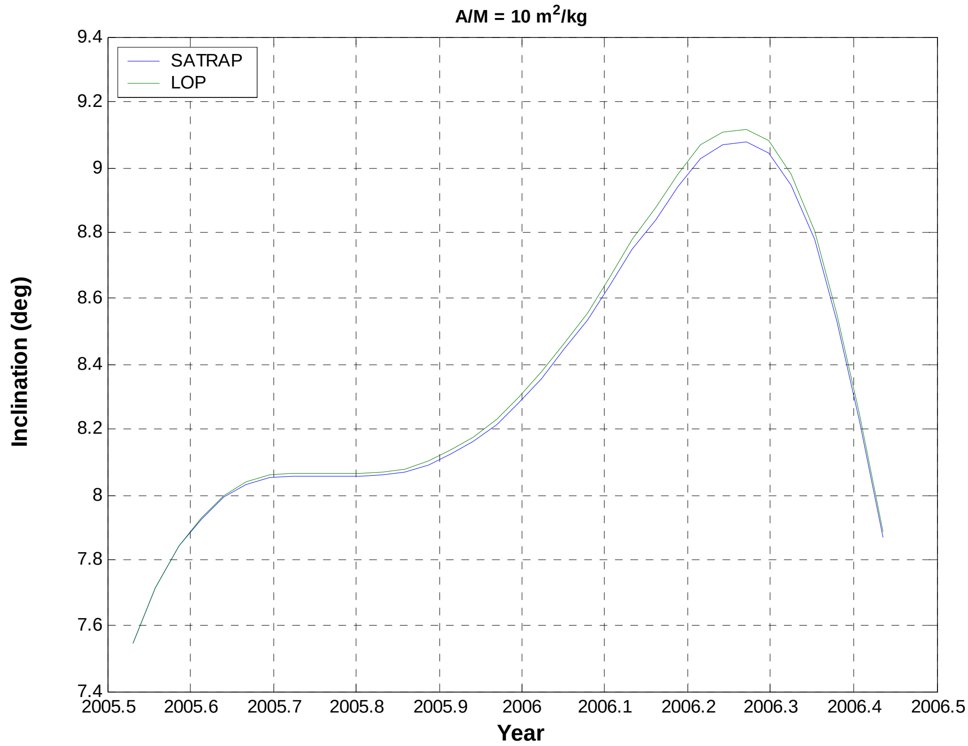

Fig. 5.13

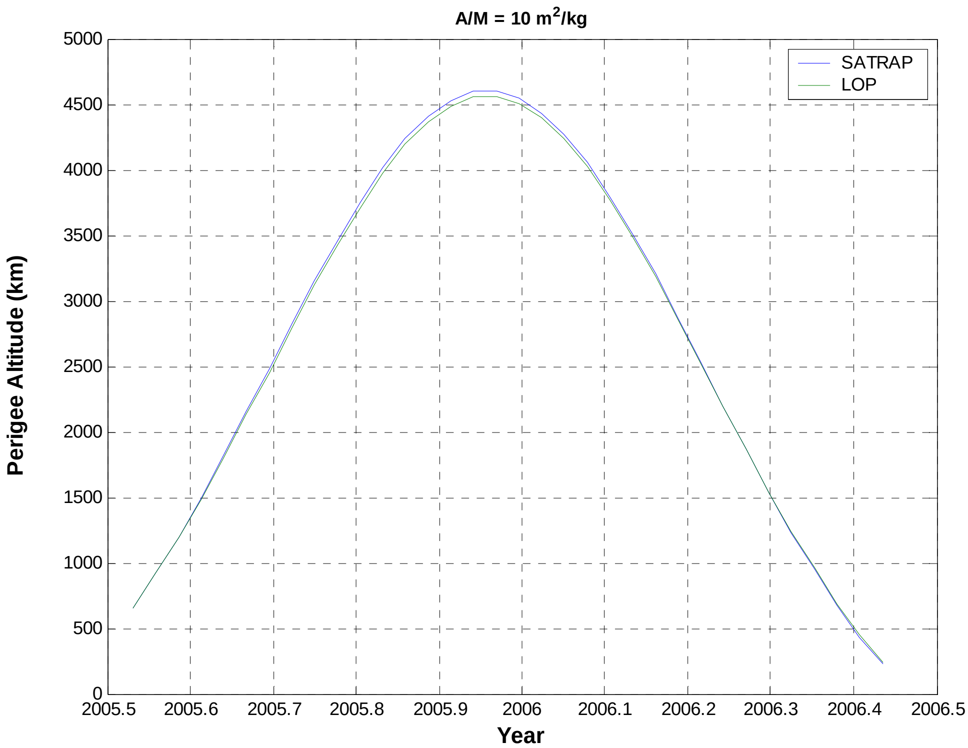

Fig. 5.14

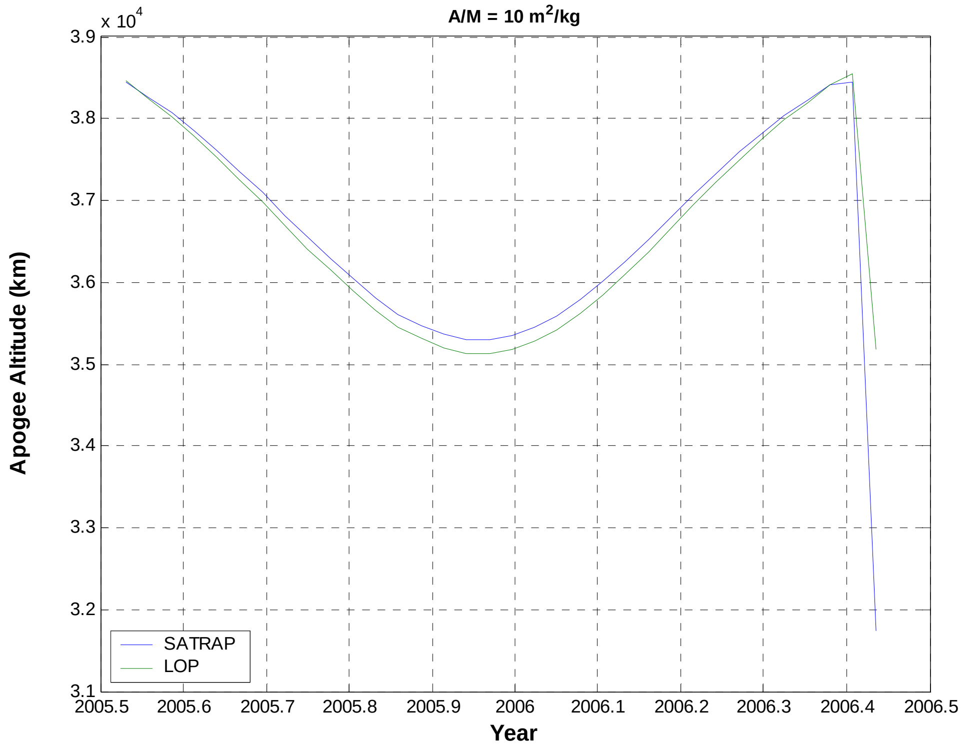

Fig. 5.15

For the intermediate area-to-mass ratio (A/M = 1 m^2/kg), this is true during the first 60-70 years. There is, in fact, a significant orbital lifetime difference, with object decay in 2075 with LOP and 2103 with SATRAP. Until the first decay, the two propagators are in reasonable agreement. However, around 2075, the perigee predicted by LOP becomes sufficiently lower in the atmosphere, by just the right amount needed to induce a rapid decrease of the apogee and the consequent orbital decay. As in the corresponding Molniya orbit case, discussed in Chapter 4, a relatively small difference in the orbital elements is amplified by the perturbations, resulting, at the end, in a macroscopic discrepancy.

6. ACCURACY VS. COMPUTATIONAL SPEED

6.1 Introduction

The results presented in Chapters 2-5 show that a propagator based on the LOP approach can more than adequately describe the long-term behavior of MEO, GEO and super-GEO mean orbital elements, with accuracies comparable, in most cases, with those of a numerical code. This is also true for very high A/M objects, characterized by significant non-gravitational perturbations. The advantage of the LOP approach is the substantially reduced execution time with respect to a special perturbations method and its general applicability to any type of orbit (circular and eccentric, low and high, resonant and non-resonant), even though much faster analytical propagators can be found for very specific orbital regimes (as LEGO for GEO).

The computational speed of LOP depends on the relative (RELERR) and absolute (ABSERR) accuracy of the integrator. Based on general numerical arguments, a value of at least 10^{-6} is recommended for both parameters [2]. However, practical experience has shown that this requirement can be significantly relaxed in many situations, guaranteeing an adequate level of accuracy. And because an increase of a factor of 10 in the values of RELERR and ABSERR translates into a gain of approximately one order of magnitude in computational speed, a specific analysis was carried out to identify the maximum values compatible with the SDM 4.0 requirements, as a function of orbital regime and satellite area-to-mass ratio.

6.2 Geostationary Orbit

Assuming the initial conditions specified in Table 2.1, objects with area-to-mass ratios of 0.05, 1, 5, 10, 20, 30 and 40 m^2/kg were propagated for one century with LOP, assuming RELERR = ABSERR = 10^{-8}, 10^{-6}, 10^{-4}, 10^{-3} and 10^{-2}, respectively. Some of the results obtained are summarized in Figures 6.1-6.5 for A/M = 1 m^2/kg and in Figures 6.6-6.10 for A/M = 40 m^2/kg.

Quite surprisingly, for A/M ≤ 5 m^2/kg, a good accuracy is obtained also with RELERR = ABSERR = 10^{-2}, while, for A/M > 5 m^2/kg, the maximum value acceptable is 10^{-3}, because 10^{-2} induces a too rapid orbital decay.

6.3 MEO and LEO Orbits

The analysis was extended to the following MEO orbits: GPS (Table 3.1), Molniya (Table 4.1) and Ariane 5 GTO (Table 5.1). In addition, the LEO orbit given in Table 6.1 was considered as well. Objects with area-to-mass ratios in between 0.05 and 10 m^2/kg were

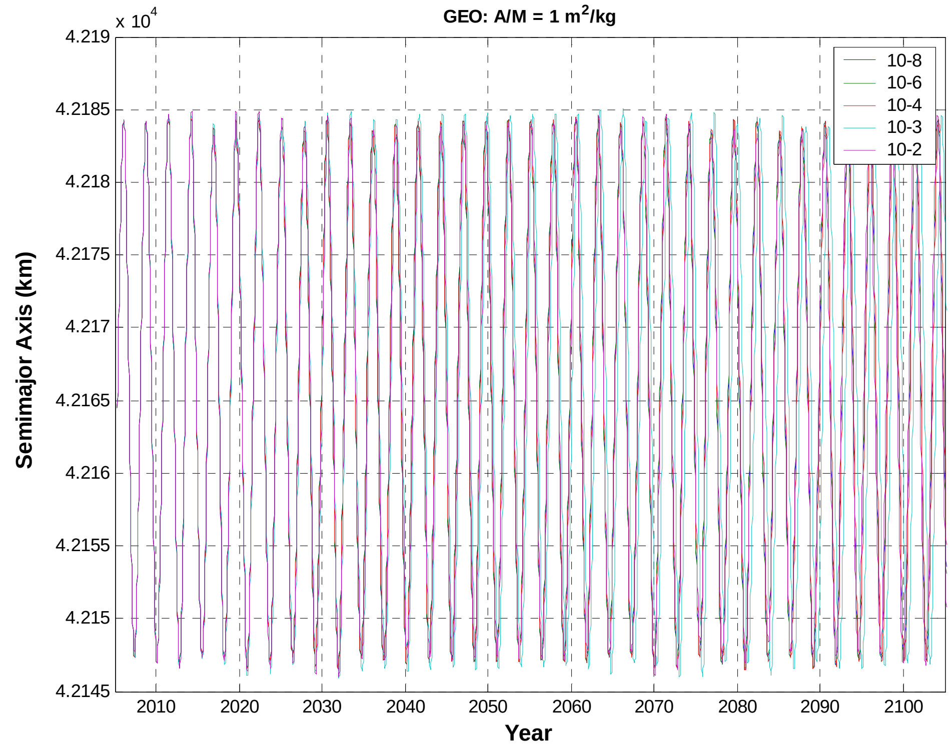
GEO: A/M = 1 m²/kg
x 10⁴
Semimajor Axis (km)
4.219
4.2185
4.218
4.2175
4.217
4.2165
4.216
4.2155
4.215
4.2145
2010
2020
2030
2040
2050
2060
2070
2080
2090
2100
Year
10-8
10-6
10-4
10-3
10-2

Fig. 6.1

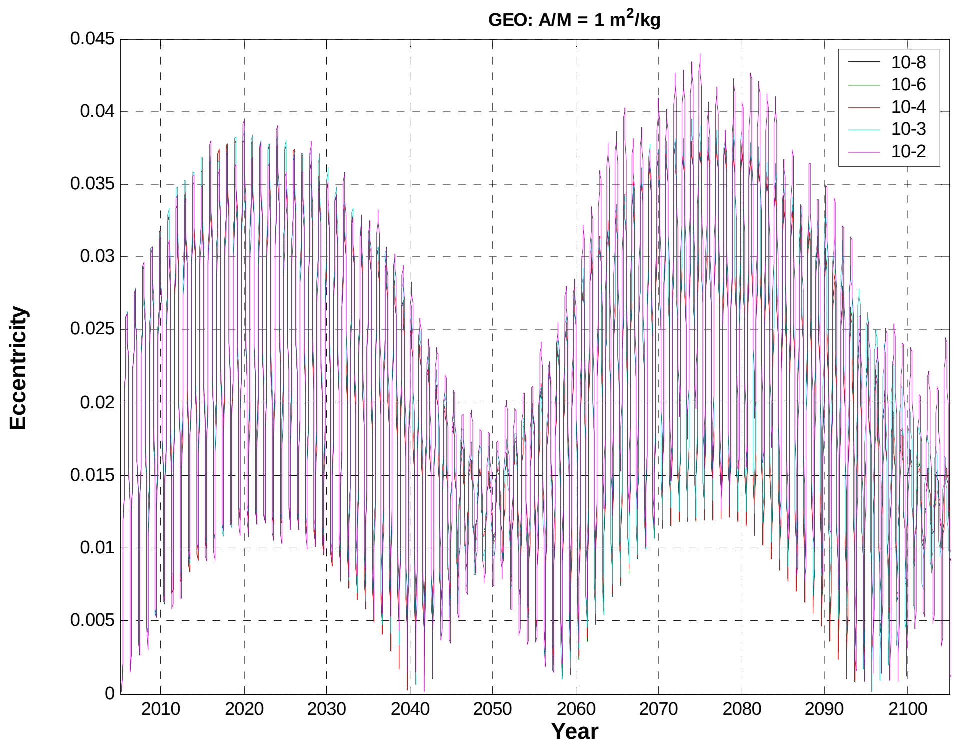
GEO: A/M = 1 m²/kg
Eccentricity
0.045
0.04
0.035
0.03
0.025
0.02
0.015
0.01
0.005
0
2010
2020
2030
2040
2050
2060
2070
2080
2090
2100
Year
10-8
10-6
10-4
10-3
10-2

Fig. 6.2

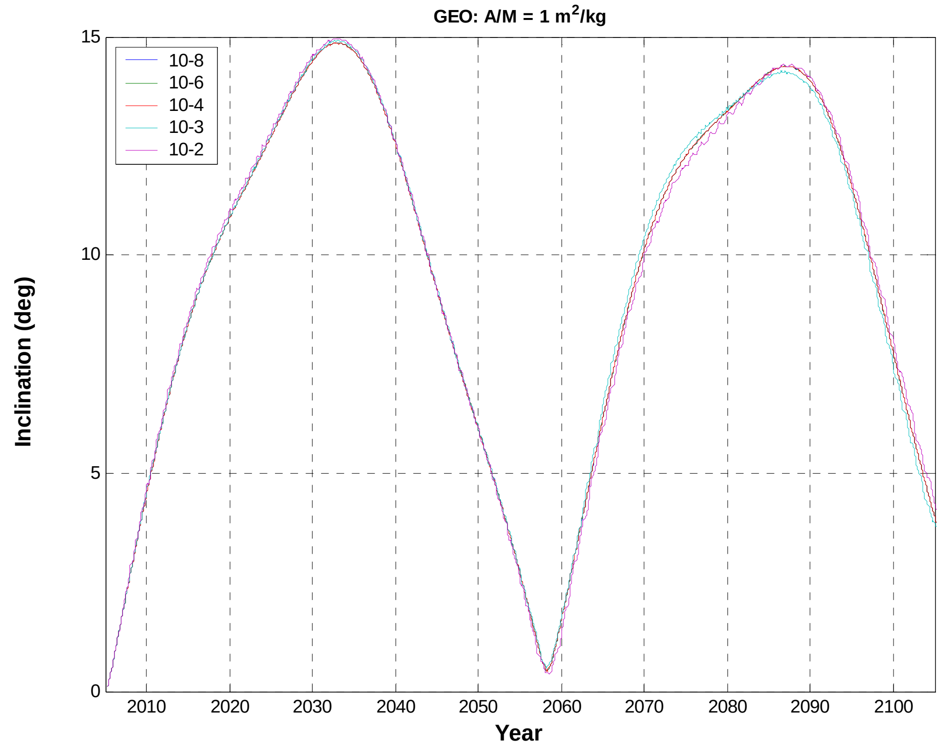
GEO: A/M = 1 m2/kg
10-8
10-6
10-4
10-3
10-2
Inclination (deg)
0
5
10
15
2010
2020
2030
2040
2050
2060
2070
2080
2090
2100
Year

Fig. 6.3

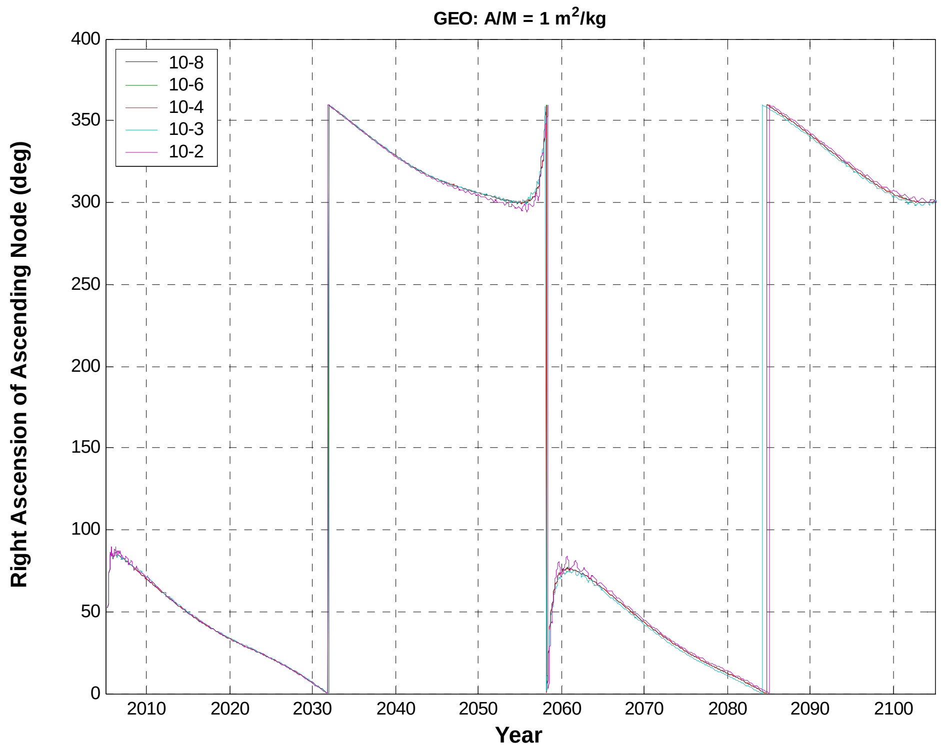
GEO: A/M = 1 m2/kg
10-8
10-6
10-4
10-3
10-2
Right Ascension of Ascending Node (deg)
0
50
100
150
200
250
300
350
400
2010
2020
2030
2040
2050
2060
2070
2080
2090
2100
Year

Fig. 6.4

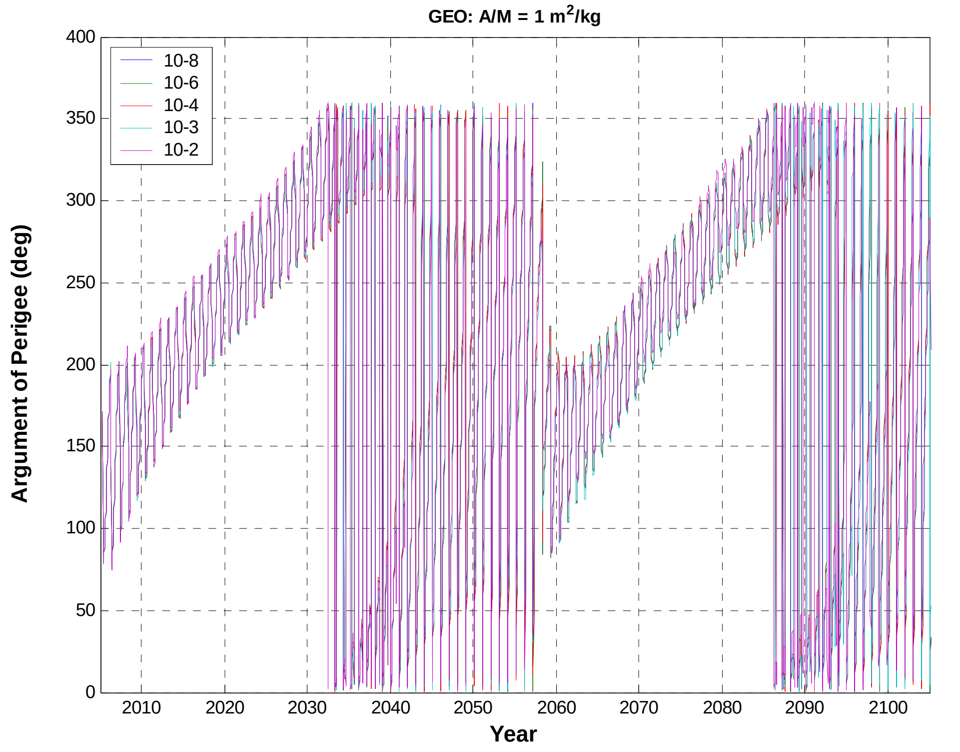
GEO: A/M = 1 m²/kg
Argument of Perigee (deg)
Year
10-8
10-6
10-4
10-3
10-2
0
50
100
150
200
250
300
350
400
2010
2020
2030
2040
2050
2060
2070
2080
2090
2100

Fig. 6.5

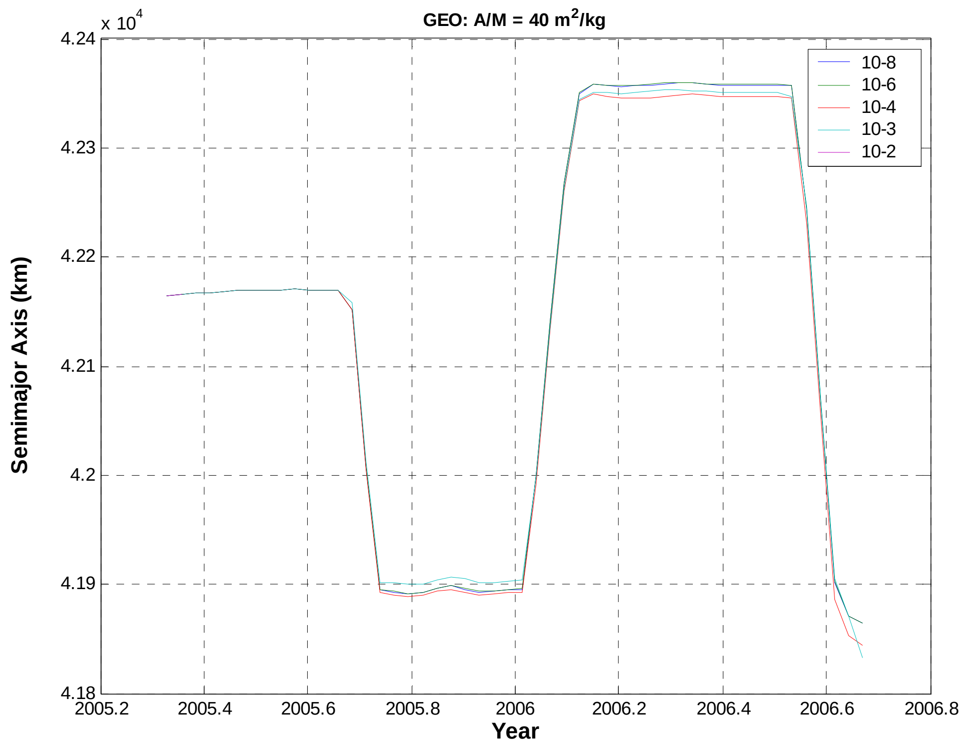
GEO: A/M = 40 m²/kg
x 10⁴
Semimajor Axis (km)
Year
10-8
10-6
10-4
10-3
10-2
4.18
4.19
4.2
4.21
4.22
4.23
4.24
2005.2
2005.4
2005.6
2005.8
2006
2006.2
2006.4
2006.6
2006.8

Fig. 6.6

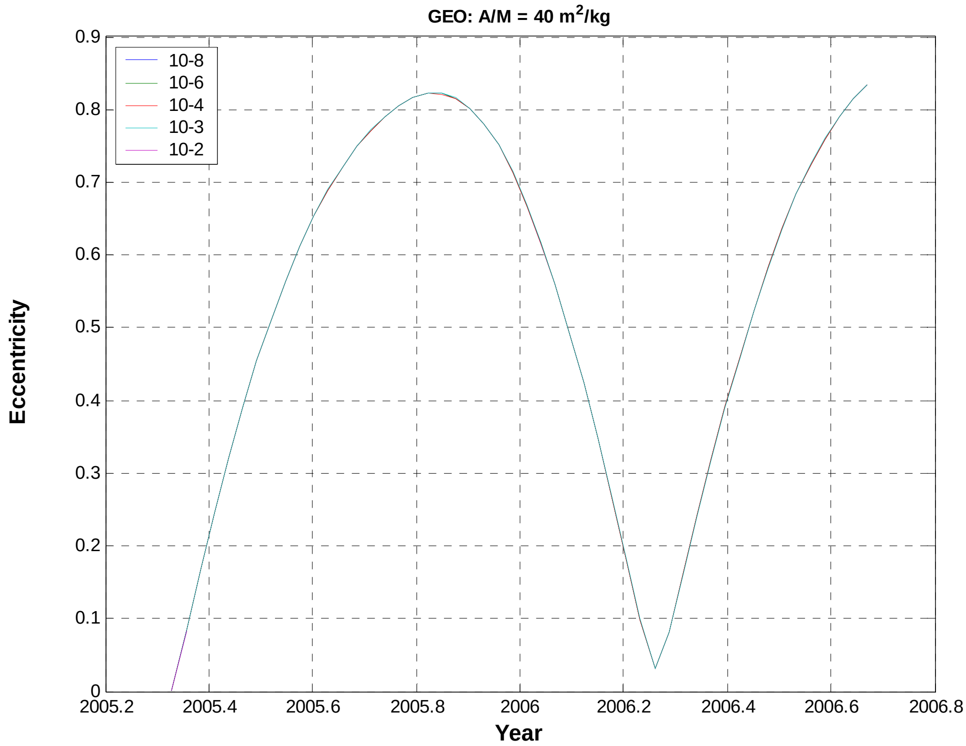
GEO: A/M = 40 m²/kg
10-8
10-6
10-4
10-3
10-2
Eccentricity
0.9
0.8
0.7
0.6
0.5
0.4
0.3
0.2
0.1
0
2005.2
2005.4
2005.6
2005.8
2006
2006.2
2006.4
2006.6
2006.8
Year

Fig. 6.7

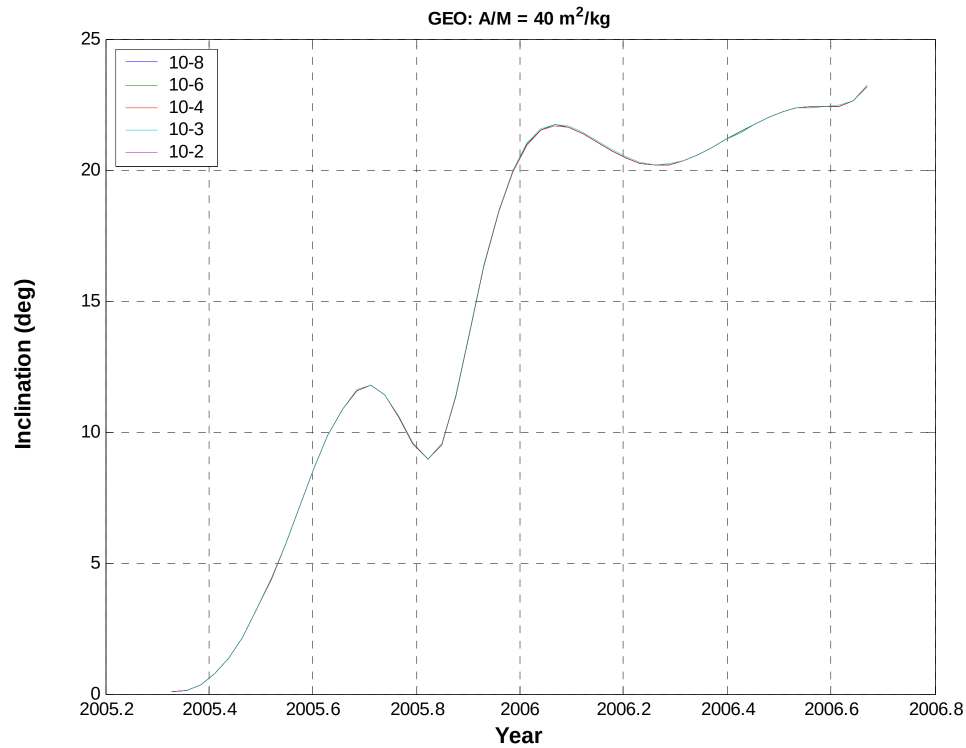
GEO: A/M = 40 m²/kg
10-8
10-6
10-4
10-3
10-2
Inclination (deg)
25
20
15
10
5
0
2005.2
2005.4
2005.6
2005.8
2006
2006.2
2006.4
2006.6
2006.8
Year

Fig. 6.8

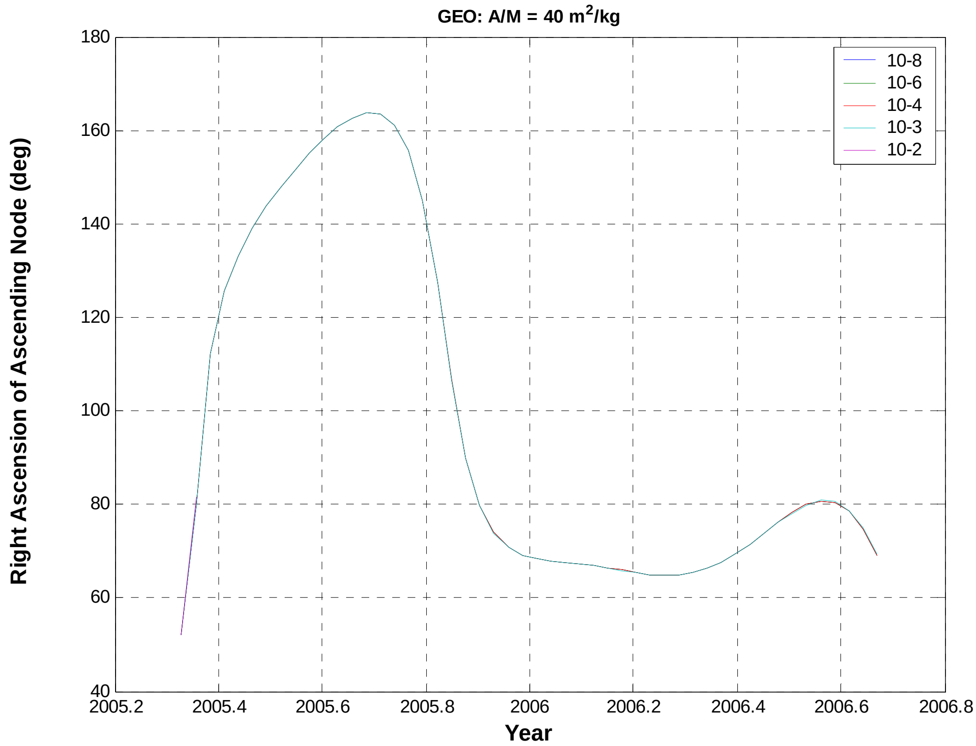

Fig. 6.9

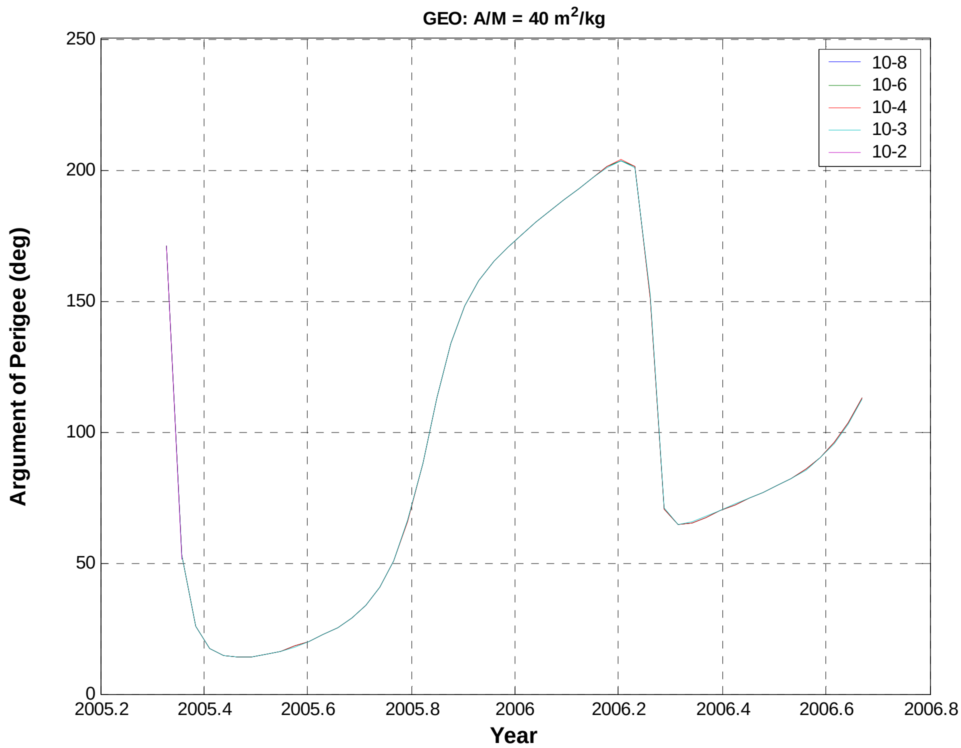

Fig. 6.10

propagated for one century with LOP, assuming RELERR = ABSERR = 10^{-4}, 10^{-3} and 10^{-2}. The results of a comparison with SATRAP are summarized in Table 6.2, for objects with area-to-mass ratios of 0.05, 1 and 10 m^2/kg.

Table 6.1

Reference LEO (Initial Conditions)

Epoch	2005.07.12 18:29:20.47 UTC
Orbital Elements	Mean Keplerian
Earth Centered Reference Frame	True of Date
Semimajor Axis	7200 km
Eccentricity	0.0
Inclination	63 deg
Right Ascension of Ascending Node	96.6475 deg
Argument of Perigee	273.7710 deg
Mean Anomaly	15.7838 deg

Table 6.2

LOP-SATRAP Comparison
LOP Accuracy vs. Orbit, A / M and RELERR / ABSERR

ORBIT	A / M (m^2 / kg)	LOP RELERR / ABSERR		
		10^{-2}	10^{-3}	10^{-4}
GPS	0.05	≈	~	=
	1	~	=	=
	10	≈	=	=
Ariane 5 GTO	0.05	≠	≈	≈
	1	≠	≠	~
	10	≈	=	=
Molniya	0.05	≠	≈	≈
	1	≠	≠	~
	10	≈	=	=
LEO	0.05	≈	~	=
	1	≠	≈	≈
	10	~	=	=

= excellent *≈ satisfactory* *~ approximate* *≠ inadequate*

In general, a relative and absolute error of 10^{-4} can guarantee very good results, but often it is possible to obtain adequate accuracies with appreciably higher values, like 10^{-2} for GPS orbits and 10^{-3} for objects in LEO.

6.4 Conclusions

The main conclusion of the analysis presented in this chapter is that a relative and absolute error of 10^{-4} is more than adequate to guarantee a sufficient level of accuracy for any orbit and application envisaged for SDM 4.0. However, in many cases, even this value can be furthermore relaxed, as summarized in Table 6.3.

Table 6.3

LOP: Maximum Acceptable Value of RELERR / ABSERR

ORBIT	A / M (m^2 / kg)	RELERR / ABSERR
LEO	A/M < 0.15	10^{-2}
	A/M ≥ 0.15	10^{-3}
Molniya	A/M < 0.1	10^{-3}
	0.1 ≤ A/M < 5	10^{-4}
	5 ≤ A/M < 10	10^{-3}
	A/M ≥ 10	10^{-2}
Ariane 5 GTO	A/M < 0.05	10^{-3}
	0.05 ≤ A/M < 5	10^{-4}
	A/M ≥ 5	10^{-3}
GPS	A/M ≤ 0.5	10^{-2}
	0.5 < A/M < 5	10^{-3}
	A/M ≥ 5	10^{-2}
GEO	A/M ≤ 5	10^{-2}
	A/M > 5	10^{-3}

7. APPLICATION TO THE IADC AI 22.1

7.1 The IADC Action Item 22.1

In order to preserve the geostationary orbit for future use, the Inter-Agency Space Debris Coordination Committee (IADC) has proposed a re-orbiting strategy for the geostationary spacecraft at the end-of-life [9]. They should be disposed to a region above the geostationary altitude and passivated, in order to reduce the risk of inadvertent explosions. The recommended perigee of the disposal orbit should be higher of the geostationary altitude by an amount ΔH (km) given by

$$\Delta H = 235 + C_r \times 1000 \times A / M \qquad (1)$$

where A is the satellite average cross-sectional area (m^2), M is the satellite mass (kg) and C_r is a radiation pressure coefficient, typically between 1 and 2, specifying the amount of solar radiation transmitted, absorbed and reflected by the spacecraft.

The aim of this recommendation is to prevent, in the long-term, the return of the re-orbited satellites in the GEO protected region, whose upper altitude limit is at GEO + 200 km [9]. However, depending on the initial conditions, an end-of-life re-orbiting according to Eq. (1) alone may not be sufficient to guarantee such long-term result, if the eccentricity vector of the new orbit is left unconstrained. On the other hand, by a careful choice of the eccentricity vector, even a smaller ΔH increase may – sometimes – prevent the long-term return of the re-orbited spacecraft in the GEO protected region, meeting the spirit, if not the letter, of the IADC recommendation.

Just to further investigate these aspects, during the 22^{nd} IADC Plenary Meeting, a specific Action Item (AI 22.1) was approved to clarify the consequences of the “GEO disposal orbit eccentricity”.

7.2 Study Parameters

In order to explore the long-term evolution of GEO disposal orbits as a function of the initial orientation of the eccentricity vector, a specific set of study parameters was endorsed by IADC for the analysis. Together with some derived quantities, they are summarized in Table 7.1. The aim of the analysis was to quantify, for a given end-of-life re-orbiting epoch (January 1, 2005), the effect of the initial eccentricity and perigee orientation of the graveyard orbit on the possibility of a long-term spacecraft return in the GEO protected region. For this purpose, three perigee altitudes, eccentricities and perigee orientations with respect to the Sun were considered, for a total of 27 independent simulations.

Table 7.1

IADC AI 22.1 (GEO Disposal Orbit Eccentricity) Study Parameters

Initial angle between Sun and perigee direction	0 deg, +45 deg, +90 deg
Initial eccentricity	0.005, 0.05, 0.1
Initial inclination	0.1 deg
Initial right ascension of ascending node	90 deg
Initial mean anomaly	0 deg
Initial perigee altitude above GEO	ΔH, 2 × ΔH, 3 × ΔH
Spacecraft area-to-mass ratio	0.02 m^2/kg
Spacecraft radiation pressure coefficient (C_r)	1.2
ΔH, 2 × ΔH, 3 × ΔH	259 km, 518 km, 777 km
Initial argument of perigee: 0 deg w.r.t. the Sun	191.6 deg
Initial argument of perigee: +45 deg w.r.t. the Sun	236.6 deg
Initial argument of perigee: +90 deg w.r.t. the Sun	281.6 deg
Reference epoch for the propagations	1 January 2005, 00:00 UTC
Propagation time span	100 years

7.3 Results

Figures 7.1-7.3 show the results obtained, as a function of the initial eccentricity vector of the graveyard orbit, for a re-orbiting according to the IADC recommendation. An initial eccentricity of 0.005 (Figure 7.1) is able to guarantee the preservation of the GEO protected region during the time span considered, irrespective of the perigee orientation with respect the Sun. This is not true for higher eccentricities (Figures 7.2 and 7.3), where the simple application of Eq. (1) is not sufficient to meet the mitigation requirement. However, if the initial perigee of the graveyard orbit is oriented toward the Sun, even an initial eccentricity as high as 0.1 does not result in a long-term crossing of the GEO protected region.

Increasing the altitude of the graveyard orbit perigee substantially above the IADC recommendation (Figures 7.4-7.9), the trends observed are basically the same, progressively relaxing the requirements on the eccentricity vector magnitude and orientation in order to preserve the GEO protected region.

7.4 Conclusions

From a propellant consumption point of view, a good strategy to preserve the GEO protected region is obtained by combining Eq. (1) with constraints on the initial eccentricity vector of the graveyard orbit. A sufficiently small eccentricity, a Sun-pointing perigee, or a suitable combination of eccentricity and argument of perigee, are all able to avoid, in the long-term, the crossing of the GEO protected region. Depending on the initial epoch and conditions, in certain cases such a result may also be obtained with a perigee altitude above GEO a little bit lower than ΔH.

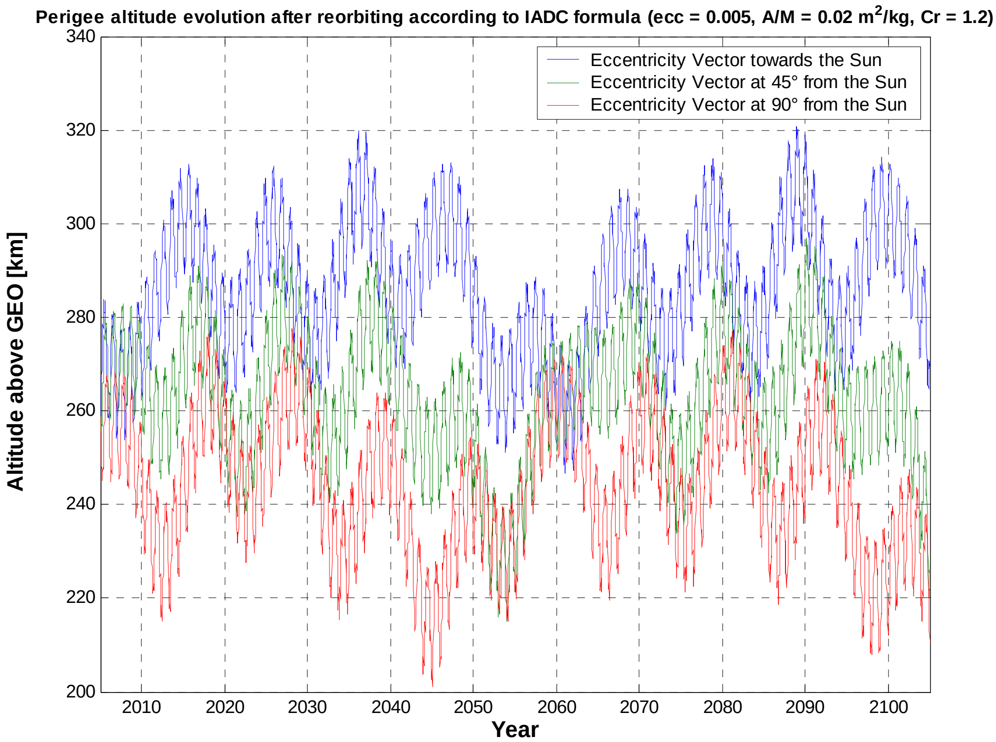
Perigee altitude evolution after reorbiting according to IADC formula (ecc = 0.005, A/M = 0.02 m2/kg, Cr = 1.2)
Eccentricity Vector towards the Sun
Eccentricity Vector at 45° from the Sun
Eccentricity Vector at 90° from the Sun
Altitude above GEO [km]
340
320
300
280
260
240
220
200
2010
2020
2030
2040
2050
2060
2070
2080
2090
2100
Year

Fig. 7.1

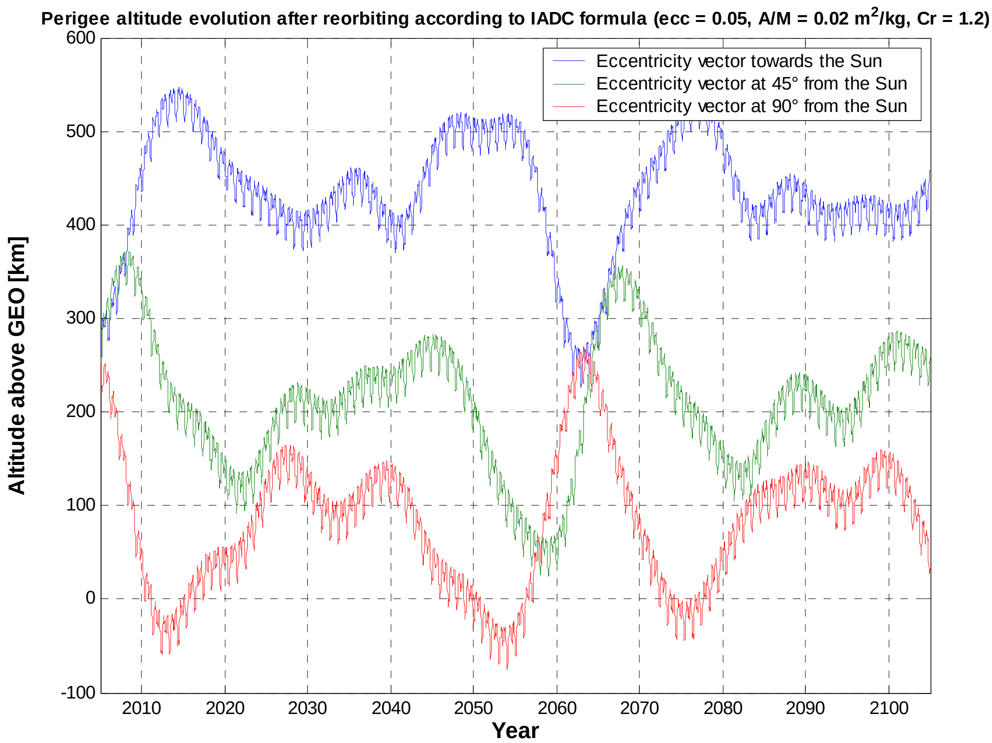
Perigee altitude evolution after reorbiting according to IADC formula (ecc = 0.05, A/M = 0.02 m2/kg, Cr = 1.2)
Eccentricity vector towards the Sun
Eccentricity vector at 45° from the Sun
Eccentricity vector at 90° from the Sun
Altitude above GEO [km]
600
500
400
300
200
100
0
-100
2010
2020
2030
2040
2050
2060
2070
2080
2090
2100
Year

Fig. 7.2

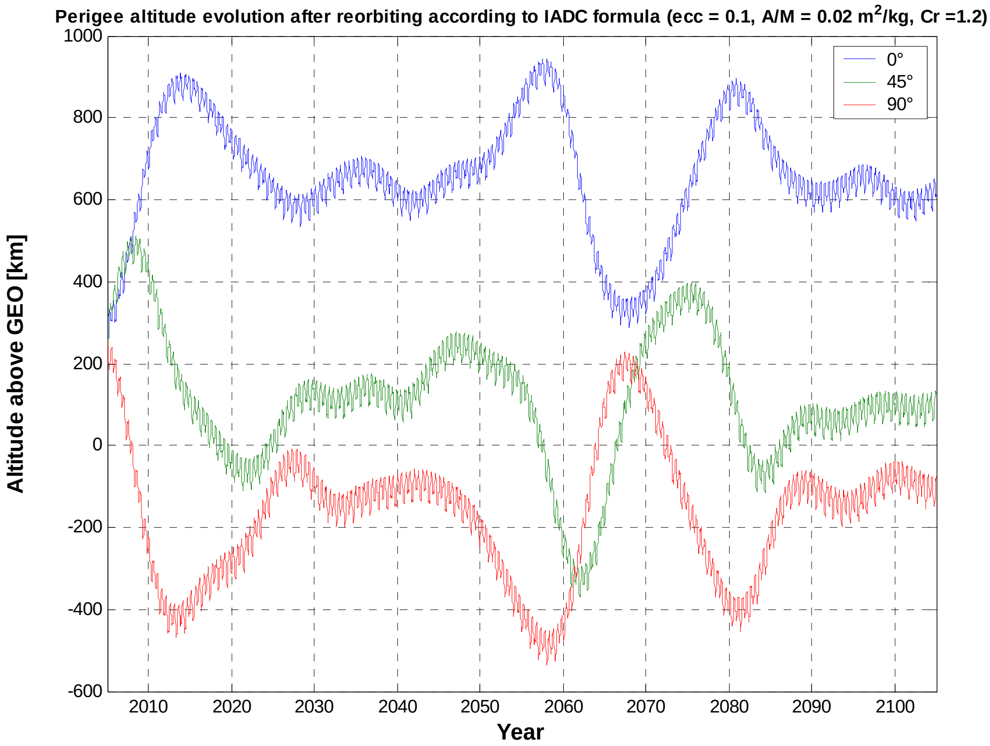
Perigee altitude evolution after reorbiting according to IADC formula (ecc = 0.1, A/M = 0.02 m2/kg, Cr =1.2)
Altitude above GEO [km]
Year
0°
45°
90°
1000
800
600
400
200
0
-200
-400
-600
2010
2020
2030
2040
2050
2060
2070
2080
2090
2100

Fig. 7.3

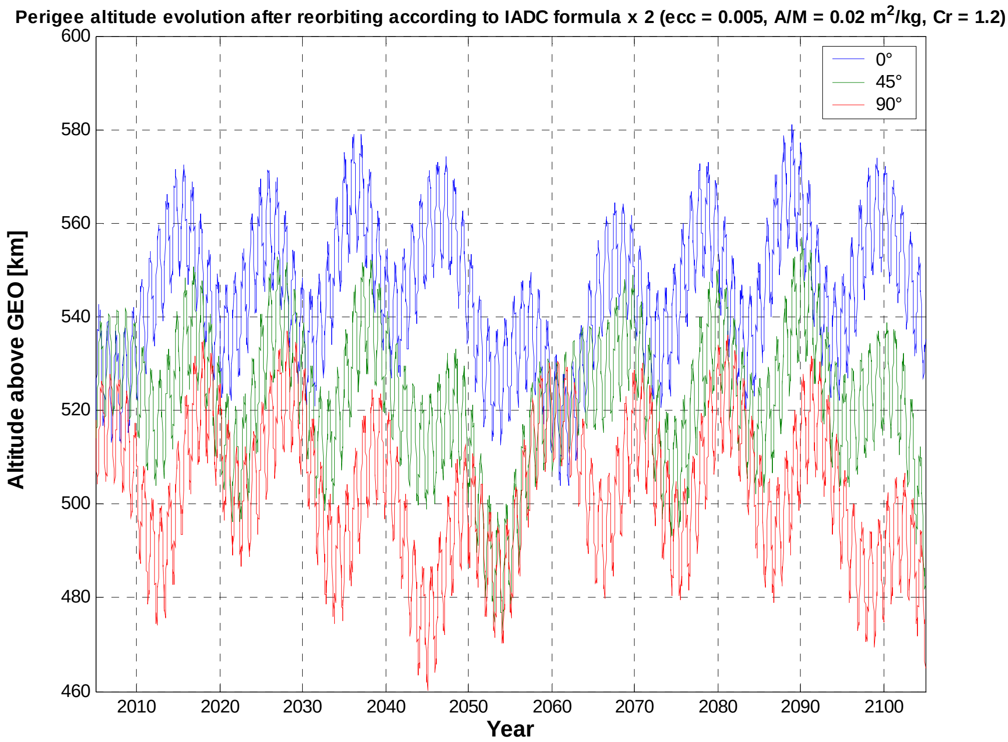
Perigee altitude evolution after reorbiting according to IADC formula x 2 (ecc = 0.005, A/M = 0.02 m2/kg, Cr = 1.2)
Altitude above GEO [km]
Year
0°
45°
90°
600
580
560
540
520
500
480
460
2010
2020
2030
2040
2050
2060
2070
2080
2090
2100

Fig. 7.4

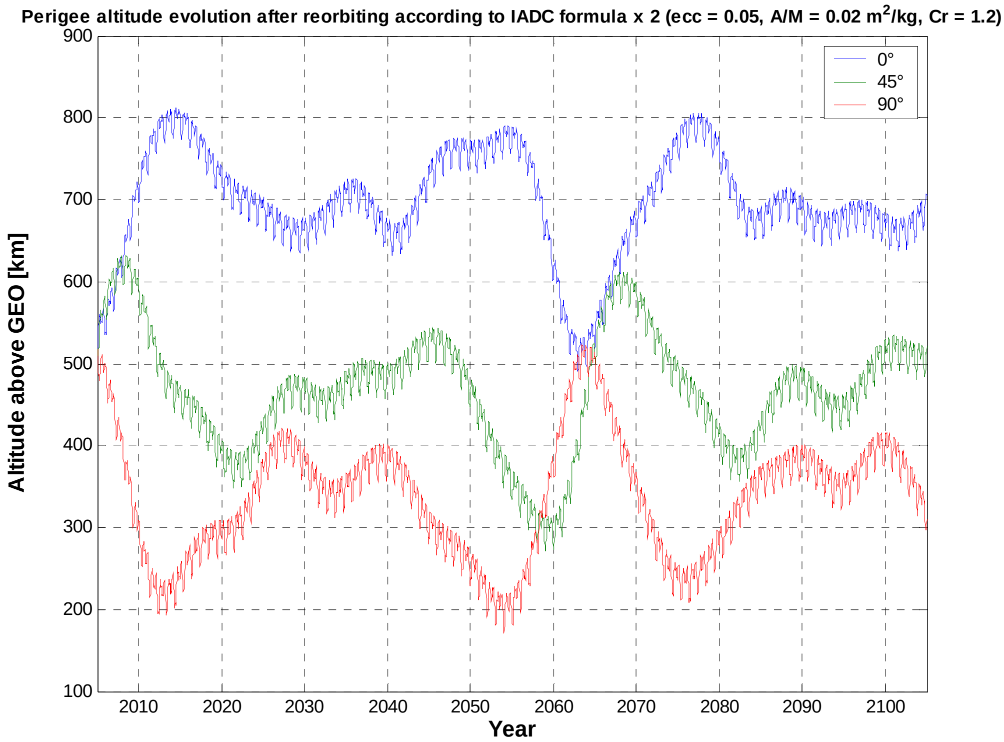
Perigee altitude evolution after reorbiting according to IADC formula x 2 (ecc = 0.05, A/M = 0.02 m2/kg, Cr = 1.2)
Altitude above GEO [km]
Year
0°
45°
90°
900
800
700
600
500
400
300
200
100
2010
2020
2030
2040
2050
2060
2070
2080
2090
2100

Fig. 7.5

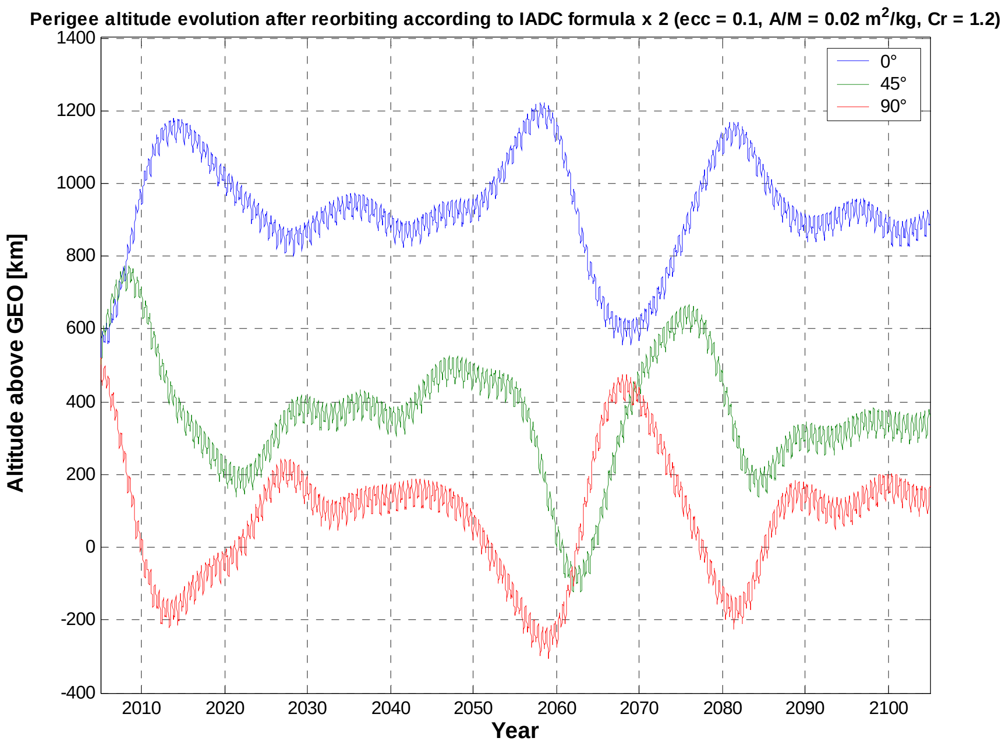
Perigee altitude evolution after reorbiting according to IADC formula x 2 (ecc = 0.1, A/M = 0.02 m2/kg, Cr = 1.2)
Altitude above GEO [km]
Year
0°
45°
90°
1400
1200
1000
800
600
400
200
0
-200
-400
2010
2020
2030
2040
2050
2060
2070
2080
2090
2100

Fig. 7.6

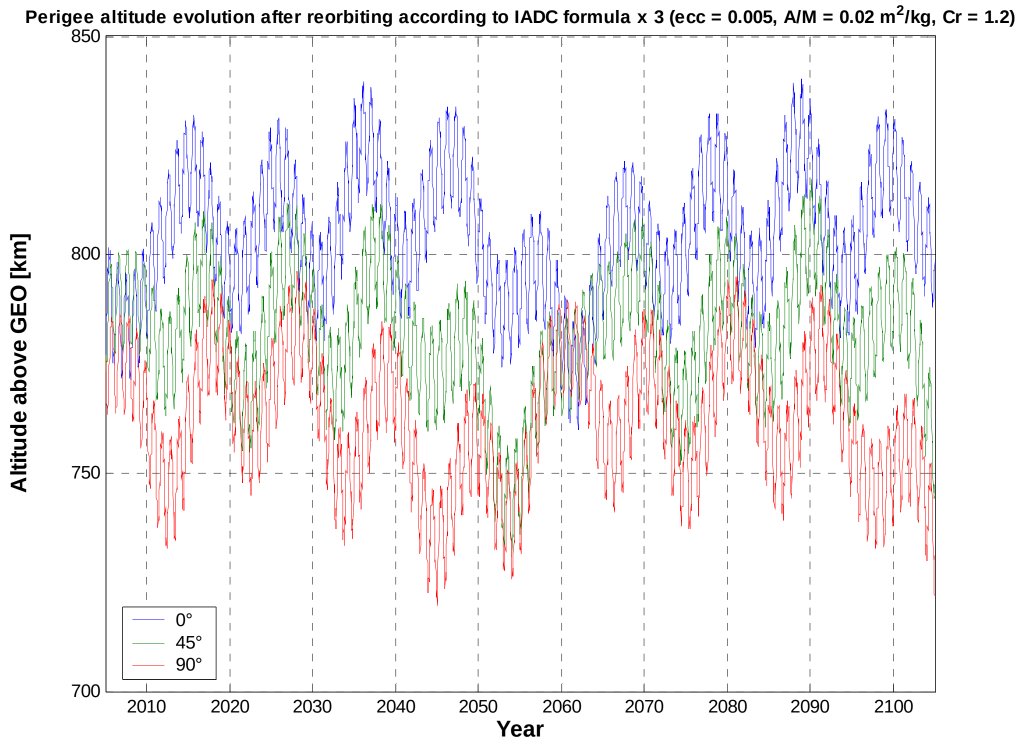
Perigee altitude evolution after reorbiting according to IADC formula x 3 (ecc = 0.005, A/M = 0.02 m2/kg, Cr = 1.2)
Altitude above GEO [km]
850
800
750
700
2010
2020
2030
2040
2050
2060
2070
2080
2090
2100
Year
0°
45°
90°

Fig. 7.7

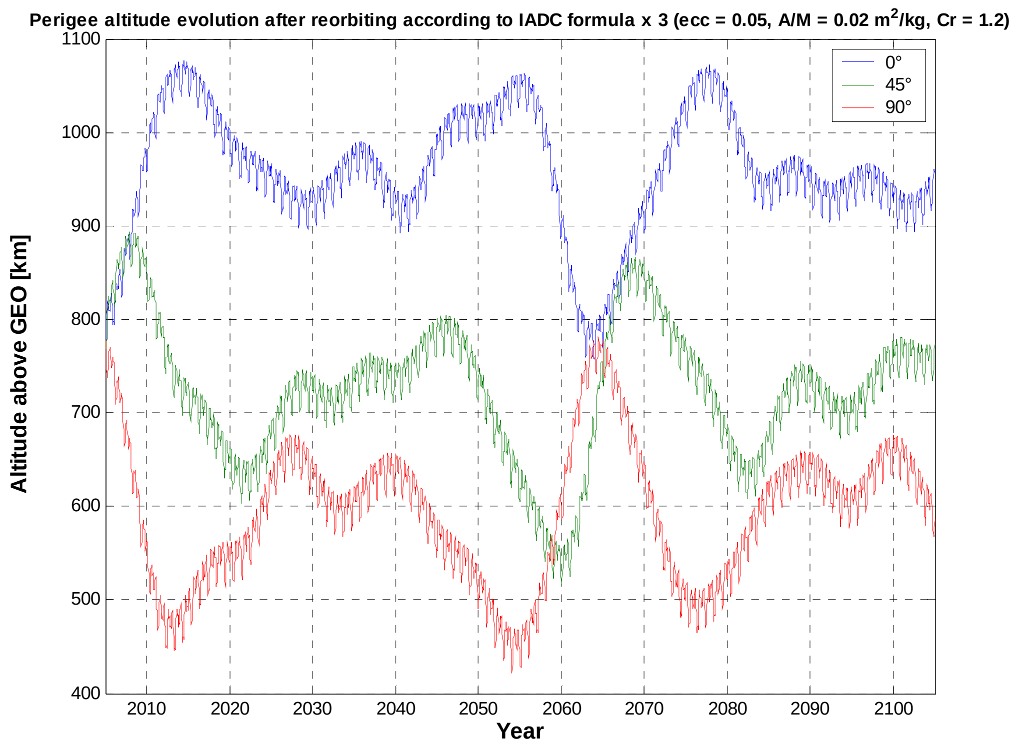
Perigee altitude evolution after reorbiting according to IADC formula x 3 (ecc = 0.05, A/M = 0.02 m2/kg, Cr = 1.2)
Altitude above GEO [km]
1100
1000
900
800
700
600
500
400
2010
2020
2030
2040
2050
2060
2070
2080
2090
2100
Year
0°
45°
90°

Fig. 7.8

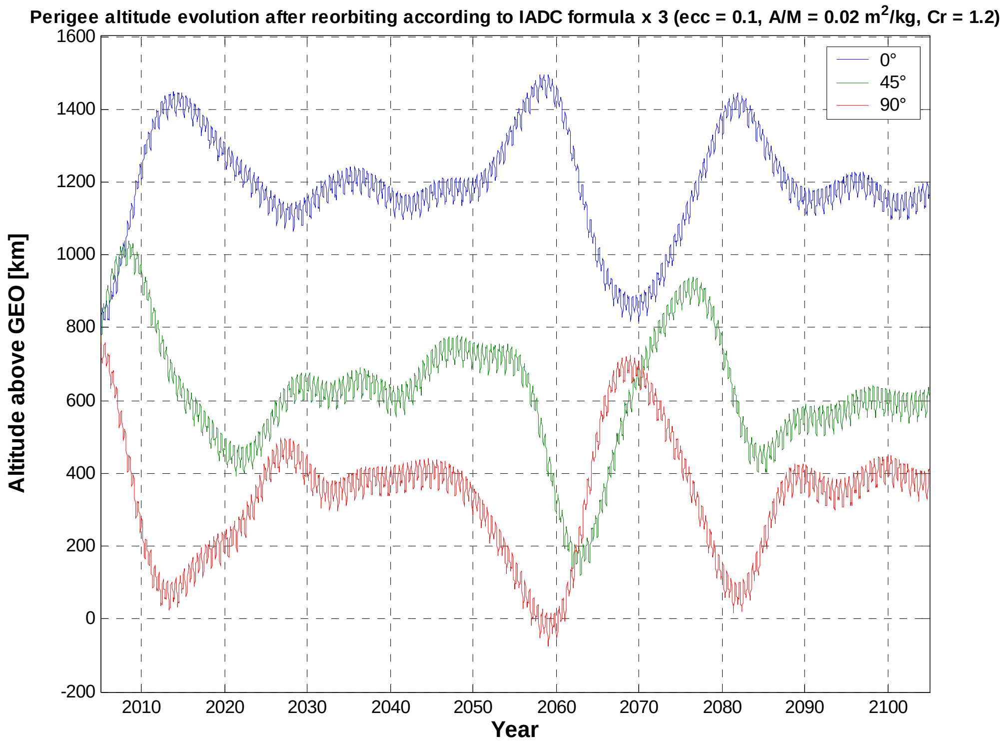
Perigee altitude evolution after reorbiting according to IADC formula x 3 (ecc = 0.1, A/M = 0.02 m2/kg, Cr = 1.2)
Altitude above GEO [km]
Year
0°
45°
90°
1600
1400
1200
1000
800
600
400
200
0
-200
2010
2020
2030
2040
2050
2060
2070
2080
2090
2100

Fig. 7.9

GLOSSARY

ABSERR	Absolute accuracy of the LOP/FOP integrator
AI	Action Item
AP	Argument of Perigee
A/M	Area-to-Mass ratio
CNR	Consiglio Nazionale delle Ricerche (Italian National Research Council)
ECC	ECCentricity
ESA	European Space Agency
ESOC	European Space Operations Centre
FOP	Fast Orbit Propagator
GEO	GEostationary Orbit
GLONASS	Russian GLObal NAvigation Satellite System
GPS	Global Positioning System
GTO	Geosynchronous Transfer Orbit
IADC	Inter-Agency Space Debris Coordination Committee
INC	INClination
ISTI	Istituto di Scienza e Tecnologie dell'Informazione "Alessandro Faedo"
LEGO	Long-term Evolution of Geostationary and near-geostationary Orbit propagator
LEO	Low Earth Orbit (orbital region below the altitude of 2000 km)
LOP	Long-term Orbit Predictor
MEO	Medium Earth Orbit, i.e. intermediate in altitude between LEO and GEO
RAAN	Right Ascension of Ascending Node
RELERR	Relative accuracy of the LOP/FOP integrator
SATRAP	SATellite Reentry Analysis Program
SDM	Semi-Deterministic Model for space debris mitigation analysis
SMA	Semi-Major Axis

REFERENCES

1. Analysis of Mitigation Measures Based on the Semi-Deterministic Model, Proposal presented in response to the ESA Request for Quotation RFQ/3-10961/04/D/HK, ISTI/CNR, Pisa, Italy, 13 September 2004
2. Kwok J.H., The Long-Term Orbit Predictor (LOP), Version 2.0, NPO-17052, Jet Propulsion Laboratory, Pasadena, California, USA, June 1986
3. Pardini C., Rossi A., Farinella P. and Cordelli A., Modelling of Sources and Sinks, Study Note of Work Package 2300, ESA/ESOC Contract No.10034/92/D/IM(SC) "Study on Long-Term Evolution of Earth Orbiting Debris, Consorzio Pisa Ricerche, Pisa, Italy, March 1993
4. Pardini C., Development of a Fast Orbit Propagator, Study Note of Work Package 3100, ESA/ESOC Contract No.10034/92/D/IM(SC) "Study on Long-Term Evolution of Earth Orbiting Debris, Consorzio Pisa Ricerche, Pisa, Italy, September 1993
5. Pardini C., Fast Orbit Propagator User's Guide, Version 2.00, Annex to the Study Note of Work Package 3100, ESA/ESOC Contract No.10034/92/D/IM(SC) "Study on Long-Term Evolution of Earth Orbiting Debris, Consorzio Pisa Ricerche, Pisa, Italy, February 1994
6. Van Der Ha J.C., Very Long Term Orbit Evolution of a Geostationary Satellite, MAO Working Paper No. 122, ESA/ESOC, Darmstadt, Germany, March 1980
7. Pardini C. and Anselmo L., SATRAP: Satellite Reentry Analysis Program, Internal Report C94-17, CNUCE Institute, CNR, Pisa, Italy, August 1994
8. Kwok J.H., The Artificial Satellite Analysis Program (ASAP), Version 2.0, NPO-17522, Jet Propulsion Laboratory, Pasadena, California, USA, April 1987
9. Inter-Agency Space Debris Coordination Committee (IADC), IADC Space Debris Mitigation Guidelines, IADC-02-01, 12 April 2002